

**A MICROALGAL-BASED APPROACH TO CARBON CAPTURE AND  
REUSE: IMPACTS OF VARYING CULTURE CONDITIONS ON  
*SCENEDESMUS ACUTUS* PRODUCTIVITY AND BIOCHEMICAL  
COMPOSITION**

by

Jenna Young Schambach

A thesis submitted to the Faculty of the University of Delaware in partial fulfillment of the requirements for the degree of Master of Science in Marine Studies

Fall 2017

© 2017 Jenna Young Schambach  
All Rights Reserved

**A MICROALGAL-BASED APPROACH TO CARBON CAPTURE AND  
REUSE: IMPACTS OF VARYING CULTURE CONDITIONS ON  
*SCENEDESMUS ACUTUS* PRODUCTIVITY AND BIOCHEMICAL  
COMPOSITION**

by

Jenna Young Schambach

Approved: \_\_\_\_\_  
Mark E. Warner, Ph.D.  
Professor in charge of thesis on behalf of the Advisory Committee

Approved: \_\_\_\_\_  
Mark A. Moline, Ph.D.  
Director of the School of Marine Science and Policy

Approved: \_\_\_\_\_  
Estella Atekwana, Ph.D.  
Dean of the College of Earth, Ocean, and Environment

Approved: \_\_\_\_\_  
Ann L. Ardis, Ph.D.  
Senior Vice Provost for Graduate and Professional Education

## **ACKNOWLEDGMENTS**

I thank my advisors, Dr. Jennifer Stewart and Dr. Mark Warner, for their continuous guidance, support, and the all of the opportunities they have afforded me during my time here. I thank the University of Kentucky Center for Applied Energy Research for bringing me on to the project, all of their help and feedback, as well as providing me with the samples for DNA sequencing. I thank my lab mate Anna Schutschkow for teaching how to culture algae, providing instruction on numerous assays, and for being there to answer all of my questions. I thank all of the students, faculty, and staff at the Hugh R. Sharp Campus for the outpouring of support during my project. I also thank my friends and family for always giving me encouragement and driving me to always do my best. I dedicate this thesis to one of my biggest role models, my late grandmother, Mary Young Schambach, whose boundless energy and perseverance to finish everything she started is something I look to everyday as I begin my career as a scientist.

## TABLE OF CONTENTS

LIST OF TABLES.....	vii
LIST OF FIGURES .....	viii
ABSTRACT.....	xiii
Chapter	
1 INTRODUCTION .....	15
1.1 Overview of Microalgal-based CO <sub>2</sub> Capture and Reuse .....	15
1.2 Demonstration Facility.....	16
1.3 <i>Scenedesmus acutus</i> .....	17
1.4 Research Questions.....	18
REFERENCES .....	20
2 INFLUENCE OF FLUE GAS ON GROWTH AND BIOMASS COMPOSITION OF <i>SCENEDESMUS ACUTUS</i> .....	21
2.1 Abstract.....	21
2.2 Introduction.....	22
2.2.1 Influence of Flue Gas.....	22
2.2.2 Power Outage Mitigation.....	24
2.3 Methods.....	25
2.3.1 Cultivation Setup .....	25
2.3.2 Growth Measurements .....	26
2.3.3 Biomass Characterization .....	27
2.3.4 Photochemical Measurements .....	28
2.3.5 Power Outage Mitigation Experimental Design .....	29
2.3.6 Statistical analysis.....	30
2.4 Results.....	30
2.4.1 Influence of Flue Gas on Growth of <i>S. acutus</i> .....	30
2.4.2 Influence of Flue Gas on Biochemical Composition.....	31
2.4.3 Photochemical Measurements .....	33

2.4.4	Power Outage Mitigation.....	33
2.5	Discussion.....	35
2.5.1	Influence of Flue Gas on Growth and Biochemical Composition of <i>S. acutus</i> .....	35
2.5.2	Power Outage Mitigation.....	43
	REFERENCES .....	70
3	INFLUENCE OF NITROGEN SOURCE ON GROWTH AND BIOMASS COMPOSITION OF <i>SCENEDESMUS ACUTUS</i> .....	75
3.1	Abstract.....	75
3.2	Introduction.....	76
3.3	Methods.....	78
3.3.1	Cultivation setup.....	78
3.3.2	Growth measurements .....	79
3.3.3	Biomass Characterization .....	80
3.3.4	Photochemical Measurements .....	81
3.3.5	Statistical analysis.....	82
3.4	Results.....	82
3.4.1	Influence of N Source on Growth of <i>S. acutus</i> .....	82
3.4.2	Influence of N Source on Biochemical Composition of <i>S.</i> <i>acutus</i> .....	83
3.4.3	Photochemical Measurements .....	86
3.5	Discussion.....	87
	REFERENCES .....	105
4	SURVERY OF CONTAMINATION IN A PILOT-SCALE PBR SYSTEM	109
4.1	Abstract.....	109
4.2	Introduction.....	110
4.3	Methods.....	112
4.3.1	Overview of <i>S. acutus</i> Cultivation in Pilot-Scale PBR.....	112
4.3.2	Sample Collection, DNA Extraction, and Sequencing .....	112
4.4	Results.....	114
4.5	Discussion.....	117

REFERENCES .....	133
------------------	-----

Appendix

A	CHAPTER 2 SUPPLEMENTAL FIGURES .....	135
B	CHAPTER 3 SUPPLEMENTAL FIGURES .....	137

## LIST OF TABLES

Table 1. Biomass productivity and specific growth rates of <i>S. acutus</i> during log phase growth when grown under air (0.04% CO <sub>2</sub> ), 9% CO <sub>2</sub> , and simulated flue gas (9% CO <sub>2</sub> , 55 ppm NO, 25 ppm SO <sub>2</sub> ). Values are means ± SD. Letters denote significant differences between treatments (p<0.05). .....	47
Table 2. Concentrations of urea in <i>S. acutus</i> cultures when grown under air (0.04% CO <sub>2</sub> ), 9%CO <sub>2</sub> , and simulated flue gas (9% CO <sub>2</sub> , 50 ppm NO, 25 ppm SO <sub>2</sub> ). Values are means ± SD. ....	50
Table 3. Concentrations of phosphate in <i>S. acutus</i> cultures grown under air (0.04% CO <sub>2</sub> ), 9%CO <sub>2</sub> , and simulated flue gas (9% CO <sub>2</sub> , 50 ppm NO, 25 ppm SO <sub>2</sub> ). Values are means ± SD. ....	51
Table 4. Average cetane number for <i>S. acutus</i> FAME content grown under air, 9% CO <sub>2</sub> , and simulated flue gas (9% CO <sub>2</sub> , 55 ppm NO, 25 ppm SO <sub>2</sub> ). .....	55
Table 5. Productivity and specific growth rates of <i>S. acutus</i> cultures maintained on flue gas compared to those amended with bicarbonate or air from days 4 to 7. Letters denote significant differences between treatments (p<0.05). .....	60
Table 6. Media components and concentrations (g L <sup>-1</sup> ). .....	93
Table 7. Biomass productivity and specific growth rate of <i>S. acutus</i> cultures grown using sodium nitrate or urea in air, 9% CO <sub>2</sub> , and simulated flue gas flue gas (9% CO <sub>2</sub> , 50 ppm NO, 25 ppm SO <sub>2</sub> ). Values are means ± SD. Letters denote significant differences between N treatments (p<0.05). ..	94
Table 8. Average cetane number for <i>S. acutus</i> FAME content grown using sodium nitrate or urea in air, 9% CO <sub>2</sub> , and simulated flue gas flue gas (9% CO <sub>2</sub> , 50 ppm NO, 25 ppm SO <sub>2</sub> ). .....	102
Table 9. Productivity, specific growth rate, and final biomass yield of <i>S. acutus</i> grown using media amended with 0.94 mM sodium nitrate or 4.3 mM urea in 9% CO <sub>2</sub> . Values are means ± SD. ....	137

## LIST OF FIGURES

Figure 1. Growth of <i>S. acutus</i> cultures when grown under air (0.04% CO <sub>2</sub> ), 9%CO <sub>2</sub> , and simulated flue gas (9% CO <sub>2</sub> , 55 ppm NO, 25 ppm SO <sub>2</sub> ). Values are means ± SD.....	48
Figure 2. pH of <i>S. acutus</i> cultures when grown under air (0.04% CO <sub>2</sub> ), 9%CO <sub>2</sub> , and simulated flue gas (9% CO <sub>2</sub> , 50 ppm NO, 25 ppm SO <sub>2</sub> ). Values are means ± SD.....	49
Figure 3. Protein content as a percentage of the total biomass in <i>S. acutus</i> grown under air (0.04% CO <sub>2</sub> ), 9% CO <sub>2</sub> , and simulated flue gas (9% CO <sub>2</sub> , 55 ppm NO, 25 ppm SO <sub>2</sub> ). Values are means ± SD.....	52
Figure 4. Total lipid content as a percentage of the total biomass in <i>S. acutus</i> grown under air (0.04% CO <sub>2</sub> ), 9% CO <sub>2</sub> , and simulated flue gas (9% CO <sub>2</sub> , 55 ppm NO, 25 ppm SO <sub>2</sub> ). Values are means ± SD.....	53
Figure 5. Saturated (SAFA), monounsaturated (MUFA), and polyunsaturated (PUFA) fatty acid content for <i>S. acutus</i> grown under air (0.04% CO <sub>2</sub> ), 9% CO <sub>2</sub> , and simulated flue gas (9% CO <sub>2</sub> , 55 ppm NO, 25 ppm SO <sub>2</sub> ). Values are percent means ± SD of the total fatty acid methyl ester (FAME) content. Only fatty acids that contributed to 2% or more of the total FAME composition were included in the calculation of each fatty acid. ....	54
Figure 6. Total carbohydrate content as a percentage of the total biomass in <i>S. acutus</i> grown under air (0.04% CO <sub>2</sub> ), 9% CO <sub>2</sub> , and simulated flue gas (9% CO <sub>2</sub> , 55 ppm NO, 25 ppm SO <sub>2</sub> ). Values are means ± SD.....	56
Figure 7. Chlorophyll a content per gram of algal biomass of <i>S. acutus</i> when grown under air (0.04% CO <sub>2</sub> ), 9% CO <sub>2</sub> , and simulated flue gas (9% CO <sub>2</sub> , 55 ppm NO, 25 ppm SO <sub>2</sub> ). Values are means ± SD.....	57
Figure 8. Maximum quantum yield of PSII (single turnover) of <i>S. acutus</i> when grown under air (0.04% CO <sub>2</sub> ), 9% CO <sub>2</sub> , and simulated flue gas (9% CO <sub>2</sub> , 55 ppm NO, 25 ppm SO <sub>2</sub> ). Values are means ± SD.....	58

Figure 9. Gross photosynthesis to respiration ratios for <i>S. acutus</i> when grown under air (0.04% CO <sub>2</sub> ), 9% CO <sub>2</sub> , and simulated flue gas (9% CO <sub>2</sub> , 55 ppm NO, 25 ppm SO <sub>2</sub> ). Black solid line represents the 1:1 line. Values are means ± SD.....	59
Figure 10. Growth of <i>S. acutus</i> cultures before and after flue gas was shut off and cultures were supplemented with bicarbonate or air. Values are means ± SD. Arrow indicates when flue gas was shut off.....	61
Figure 11. pH in <i>S. acutus</i> cultures before and after flue gas was shut off and cultures were supplemented with bicarbonate or air. Values are means ± SD.....	62
Figure 12. Protein content (% of biomass) in <i>S. acutus</i> before (day 4) and after (day 7) flue gas was shut off and cultures were supplemented with bicarbonate or air. Values are means ± SD.....	63
Figure 13. Lipid content (% of biomass) in <i>S. acutus</i> before and after flue gas was shut off and cultures were supplemented with bicarbonate or air. Values are means ± SD.....	64
Figure 14. Saturated (SAFA), monounsaturated (MUFA), and polyunsaturated (PUFA) fatty acid content for <i>S. acutus</i> before and after flue gas was shut off and cultures were supplemented with bicarbonate or air. Values are percent means ± SD of the total fatty acid methyl ester (FAME) content. Only fatty acids that contributed to 2% or more of the total FAME composition were included in the calculation of each fatty acid .....	65
Figure 15. Carbohydrate content (% of biomass) in <i>S. acutus</i> before and after flue gas was shut off and cultures were supplemented with bicarbonate or air. Values are mean ± SD.....	66
Figure 16. Chlorophyll a content of <i>S. acutus</i> normalized to grams of algal biomass before and after flue gas was shut off and cultures were supplemented with bicarbonate or air. Values are mean ± SD.....	67
Figure 17. Maximum quantum yield of PSII (Fv/Fm) of <i>S. acutus</i> before and after flue gas was shut off and cultures were supplemented with bicarbonate or air. Values are mean ± SD.....	68

Figure 18. Gross photosynthesis to respiration ratios (P:R) for <i>S. acutus</i> before and after flue gas was shut off and cultures were supplemented with bicarbonate or air. Black solid line represents the 1:1 line. Values are means $\pm$ SD.....	69
Figure 19. Growth, and pH of <i>S. acutus</i> cultures grown using nitrate or urea in air (A, D), 9% CO <sub>2</sub> (B, E) and flue gas (C, F). Values are means $\pm$ SD.....	95
Figure 20. Media concentrations of nitrogen and phosphate in <i>S. acutus</i> cultures grown using sodium nitrate or urea in air (A, D), 9% CO <sub>2</sub> (B, E), and simulated flue gas flue gas (9% CO <sub>2</sub> , 50 ppm NO, 25 ppm SO <sub>2</sub> ) (C, F). Values are means $\pm$ SD. ....	96
Figure 21. Protein content (% of total biomass) in <i>S. acutus</i> cultures grown using sodium nitrate or urea in air, 9% CO <sub>2</sub> , and simulated flue gas flue gas (9% CO <sub>2</sub> , 50 ppm NO, 25 ppm SO <sub>2</sub> ). Values are means $\pm$ SD.....	97
Figure 22. Total lipid content (% of total biomass) in <i>S. acutus</i> cultures grown using sodium nitrate or urea in air, 9% CO <sub>2</sub> , and simulated flue gas flue gas (9% CO <sub>2</sub> , 50 ppm NO, 25 ppm SO <sub>2</sub> ). Values are means $\pm$ SD. .	98
Figure 23. Saturated (SAFA), monounsaturated (MUFA), and polyunsaturated (PUFA) fatty acid content for <i>S. acutus</i> grown using sodium nitrate or urea in air (0.04% CO <sub>2</sub> ). Values are percent means $\pm$ SD of the total fatty acid methyl ester (FAME) content. Only fatty acids that contributed to 2% or more of the total FAME composition were included in the calculation of each fatty acid. ....	99
Figure 24. Saturated (SAFA), monounsaturated (MUFA), and polyunsaturated (PUFA) fatty acid content for <i>S. acutus</i> grown using sodium nitrate or urea in 9% CO <sub>2</sub> . Values are percent means $\pm$ SD of the total fatty acid methyl ester (FAME) content. Only fatty acids that contributed to 2% or more of the total FAME composition were included in the calculation of each fatty acid. ....	100
Figure 25. Saturated (SAFA), monounsaturated (MUFA), and polyunsaturated (PUFA) fatty acid content for <i>S. acutus</i> grown using sodium nitrate or urea in simulated flue (9% CO <sub>2</sub> , 55pm NO, 25 ppm SO <sub>2</sub> ). Values are percent means $\pm$ SD of the total fatty acid methyl ester (FAME) content. Only fatty acids that contributed to 2% or more of the total FAME composition were included in the calculation of each fatty acid.....	101

Figure 26. Total carbohydrate content (% of total biomass) in <i>S. acutus</i> cultures grown using sodium nitrate or urea in air, 9% CO <sub>2</sub> , and simulated flue gas (9% CO <sub>2</sub> , 50 ppm NO, 25 ppm SO <sub>2</sub> ). Values are means ± SD. ....	103
Figure 27. Chlorophyll a content, Fv/Fm value, and gross photosynthesis to respiration ratios for <i>S. acutus</i> cultures grown using sodium nitrate or urea in air (A, D, G), 9% CO <sub>2</sub> (B, E, H), and simulated flue gas (9% CO <sub>2</sub> , 50 ppm NO, 25 ppm SO <sub>2</sub> ) (C, F, I). Values are means ± SD. ....	104
Figure 28. Dry weights for <i>S. acutus</i> grown on flue gas emissions in a 1200 L outdoor PBR from June to October 2016. Seed cultures are represented by the red points and biomass harvests are indicated with asterisks.....	123
Figure 29. Composition of eukaryotic organisms in the outdoor PBR from June to October 2016, identified by sequencing the 18S rRNA gene.....	125
Figure 30. Composition of bacteria in the outdoor PBR from June to October 2016, identified by sequencing the 16S rRNA gene.....	127
Figure 31. Composition of fungi in the outdoor PBR from June to October 2016, identified by sequencing the ITS region in the rRNA opero .....	129
Figure 32. Composition of eukaryotes in a stock culture of <i>S. acutus</i> compared to the five seed cultures used to inoculate the PBR.....	130
Figure 33. Composition of bacteria in a stock culture of <i>S. acutus</i> compared to the five seed cultures used to inoculate the PBR.....	131
Figure 34. Composition of fungi in a stock culture of <i>S. acutus</i> compared to the five seed cultures used to inoculate the PBR. ....	132
Figure 35. Fatty acid methyl ester (FAME) profiles of <i>S. acutus</i> when grown under air (0.04% CO <sub>2</sub> ), 9% CO <sub>2</sub> , and simulated flue gas (9% CO <sub>2</sub> , 55 ppm NO, 25 ppm SO <sub>2</sub> ). Values are means ± SD. ....	135
Figure 36. Fatty acid methyl ester (FAME) profiles of <i>S. acutus</i> before and after flue gas was shut off and cultures were supplemented with bicarbonate or air. Values are mean ± SD. ....	136
Figure 37. Growth of <i>S. acutus</i> grown using media amended with 0.94 mM sodium nitrate or 4.3 mM urea in 9% CO <sub>2</sub> . Values are means ± SD .....	138

Figure 38. Fatty acid methyl ester (FAME) profile of *S. acutus* cultures grown using sodium nitrate or urea in air. Values are means  $\pm$  SD..... 140

Figure 39. Fatty acid methyl ester (FAME) profile of *S. acutus* cultures grown using sodium nitrate or urea in 9% CO<sub>2</sub>. Values are means  $\pm$  SD..... 142

Figure 40. Fatty acid methyl ester (FAME) profile of *S. acutus* cultures grown using sodium nitrate or urea in simulated flue gas flue gas (9% CO<sub>2</sub>, 50 ppm NO, 25 ppm SO<sub>2</sub>). Values are means  $\pm$  SD. .... 144

## ABSTRACT

Various mitigation systems have been proposed to reduce point-source emissions of carbon dioxide. Microalgae-based carbon capture and reuse capitalizes on the organisms' natural ability to biologically fix carbon and accumulate metabolites in high quantities that could make the entire process profitable. In order further optimize the freshwater chlorophyte *Scenedesmus acutus* (*S. acutus*) for carbon capture at a coal-fired power plant, laboratory studies were conducted to investigate the influence of flue gas, switching from flue gas to bicarbonate supplementation, and nitrogen source on the growth and biochemical composition of the alga. A survey using next generation DNA sequencing was also conducted to identify invading organisms that potentially cause the death of *S. acutus* in a pilot-scale photobioreactor at the demonstration facility in Boone County, Kentucky. Results showed that the high CO<sub>2</sub> concentration was responsible for the increased productivity in cultures exposed to simulated flue gas, despite a considerable decrease in pH. Protein content was also enhanced in these cultures, which is promising as a future application of *S. acutus* is to make plastic from the protein-containing fraction. Sodium bicarbonate supplementation proved to be an appropriate option to maintain the health and biochemical composition of the algae in the event of a power outage. Using urea as a nitrogen source is more cost-effective than sodium nitrate, and it supported greater productivity and protein content in *S. acutus* cultures grown under air, 9% CO<sub>2</sub>, and simulated flue gas. Lastly, several contaminants, including other chlorophyte microalgae, and parasitic fungi, as well as two potential sources of contamination were

identified in the outdoor cultivation of *S. acutus* growing on flue gas in a closed photobioreactor system. These results indicated that *S. acutus* is a good candidate for carbon capture and reuse at a coal-fired power plant and highlighted directions of future study to continue optimization of this alga.

## Chapter 1

### INTRODUCTION

#### 1.1 Overview of Microalgal-based CO<sub>2</sub> Capture and Reuse

Increasing atmospheric concentrations of greenhouse gases, particularly carbon dioxide (CO<sub>2</sub>), due to the anthropogenic combustion of fossil fuels and other activities, have substantially contributed to climate change. Despite the development of sustainable alternative energy sources aimed at reducing greenhouse gas emissions, we still rely heavily on fossil fuel-derived energy. Various CO<sub>2</sub> mitigation systems have been proposed to help reduce point-source emissions, including carbon capture and storage through chemical, geological, and biological means (Wang et al., 2008). The following studies focus on CO<sub>2</sub> capture and reuse using microalgae.

Microalgae are an abundant, polyphyletic group of microorganisms responsible for almost all of the primary production in aquatic systems and about half of global primary production via oxygenic photosynthesis (Kirchman 2012). Terrestrial plants have a comparable ecological role, but are less efficient at fixing CO<sub>2</sub>, exhibit slower growth, and thus have a lesser capacity for CO<sub>2</sub> bio-mitigation than microalgae (Wang et al., 2008). Microalgae-based mitigation systems have gained momentum, not only because of the organisms' high carbon fixation rates, but also because they accumulate valuable metabolites in high quantities that could make the entire process profitable (Wang et al. 2008). These metabolites include carbohydrates, lipids, proteins,

and pigments that are used as feedstocks for the development of different bioproducts.

Current research efforts aim to close the gap between proof of concept and profitability, as commodity bioproducts are not yet able to offset the costs associated with large-scale cultivation of microalgae for CO<sub>2</sub> capture (Wilson et al., 2016). These costs generally originate from initial construction of an open pond or closed photobioreactor (PBR hereafter) cultivation system, nutrients for the growth medium, as well as harvesting and dewatering the biomass (Wilson et al., 2014). Improving the cost-effectiveness of microalgae-based CO<sub>2</sub> capture and reuse involves optimizing every step of the process, from cultivation system design, to microalgal productivity, to downstream processing of the biomass. The following studies investigate several aspects of optimization of the freshwater chlorophyte, *Scenedesmus acutus* UTEX B72, currently being studied for CO<sub>2</sub> capture and reuse at a coal-fired power plant by colleagues at the University of Kentucky's Center for Applied Energy Research (CAER, Lexington, KY, USA).

## **1.2 Demonstration Facility**

Field studies conducted by CAER researchers take place at Duke Energy's East Bend Station located in Boone County, Kentucky, USA. The East Bend Station is a single unit, 650 MW plant that burns high sulfur coal (Wilson et al., 2016). It emits relatively low concentrations of NO<sub>x</sub> and SO<sub>x</sub> (~55 ppm NO<sub>x</sub> and ~25 ppm SO<sub>x</sub>) by utilizing a wet limestone scrubber for SO<sub>x</sub> control and selective catalytic reduction (SCR) with ammonia injection for NO<sub>x</sub> control

(Wilson et al., 2016). The flue gas is delivered to the cultivation system after the scrubber and SCR unit by a stainless-steel pipe (Wilson et al., 2016).

The algae are currently cultivated in a 1200 L vertical PBR using a low-cost growth medium and sparged with flue gas at a flow rate of 20 L min<sup>-1</sup> for 20 s every minute (Wilson et al., 2016). The PBR consists of two parallel rows of 36 clear tubes made of clear polyethylene terephthalate tubes connected by polyvinyl chloride pipes (Wilson et al., 2016). The rows are aligned so that shading is minimal. While the capital costs for closed PBRs are much higher than that for open pond systems, PBRs are preferred because they support greater areal productivities, as well as decrease the risk of CO<sub>2</sub> off-gassing, contamination, and water loss due to evaporation (Williams and Laurens 2010, Wilson et al., 2016). Additional details of the bioreactor design and the demonstration facility can be found in Wilson et al. (2016).

### **1.3 *Scenedesmus acutus***

Strain selection is an important consideration for CO<sub>2</sub> capture, because not all microalgal species are able to withstand industrial flue gas exposure and fluctuations in environmental conditions (e.g. light and temperature fluctuations). Chlorophytes are one of the most heavily studied groups of algae for industrial applications. Members of this group, including *Chlorella* sp. and *Scenedesmus* sp., have been extensively studied for waste-water treatment, CO<sub>2</sub> capture, and biofuel development (Hannon et al., 2011). Species in both genera have been isolated near coal-fired power plants, and cultivation experiments have shown successful growth at high temperatures and CO<sub>2</sub> concentrations as well as relevant levels of nitrogen and sulfur oxides (NO<sub>x</sub> and SO<sub>x</sub>), which are

characteristic of industrial flue gas emissions, making them ideal candidates for further study (Yen et al., 2015, Jiang et al., 2013, Morais and Costa 2007, Hanagata et al., 1992).

Out of 150 investigated strains of microalgae, *Scenedesmus acutus* UTEX B72 was selected for further study because of its fast and robust growth (Wilson, personal communication). Field studies by CAER researchers have demonstrated that *S. acutus* grows well at large scale (18,000 L) using flue gas as a CO<sub>2</sub> source, achieving a productivity of 39 g m<sup>-2</sup> d<sup>-1</sup> and a maximum carbon removal efficiency of 70% during summer months (Wilson et al., 2014).

Additionally, the harvested biomass has been investigated as potential feedstocks for bioplastic and biofuel applications. High protein content (35.3% of the total biomass) as well as considerable amounts of C16 and C18 fatty acids, which are favorable for the production of bioplastic and biodiesel, respectively, have been reported for this alga (Wilson et al., 2014, Santillan-Jimenez et al., 2016).

#### **1.4 Research Questions**

Despite these previous research, some fundamental questions remain to be explored in order to further optimize *S. acutus* for CO<sub>2</sub> capture and reuse at a coal-fired power plant. The present studies aim to answer the following research questions:

1. What is the effect of flue gas on growth and biomass composition of *S. acutus*?
2. What is the effect of nitrogen source on growth and biomass composition of *S. acutus*?
3. What organisms were present in a pilot-scale PBR over the 2016 harvest season?

## REFERENCES

- De Morais, M G, Costa J A V. 2007. Carbon dioxide fixation by *Chlorella kessleri*, *C. vulgaris*, *Scenedesmus obliquus* and *Spirulina* sp. cultivated in flasks and vertical tubular photobioreactors. *Biotechnology Letters*. 29(9): 1349-1352.
- Hanagata N, Takeuchi T, Fukujū Y. 1992. Tolerance of microalgae to high CO<sub>2</sub> and high temperature. *Phytochemistry*. 31(10): 3345-3348.
- Hannon M, Gimpel J, Miller T, Rasala B, Mayfield S. Biofuels from algae: challenges and potential. *Biofuels*. 1(5): 763-784.
- Jiang, Y, Zhang W, Wang J, Chen Y, Shen S, Liu T. 2013. Utilization of simulated flue gas for cultivation of *Scenedesmus dimorphus*. *Bioresource Technology*. 128: 359-364.
- Kirchman, David L. 2012. *Processes in Microbial Ecology*. Oxford University Press.
- Santillan-Jimenez E, Pace R, Marques S, Morgan T, McKelphin C, Mobley J, Crocker M. 2016. Extraction, characterization, purification and catalytic upgrading of algae lipids to fuel-like hydrocarbons. *Fuel*. 180: 668-678.
- Wang B, Li Y, Wu N, Lan CQ. 2008. CO<sub>2</sub> bio-mitigation using microalgae. *Appl Microbiol Biotechnol*. 79(5):707-718.
- Williams P J le B, Laurens L M L. 2010. Microalgae as biodiesel and biomass feedstocks: Review and analysis of the biochemistry, energetics and economics. *Energy Environ Sci*. 3: 554-590.
- Wilson M H, Groppo J, Placido A, Graham S, Morton III S A, Santillan-Jimenez E, Shea A, Crocker M, Crofcheck C, Andrews R. 2014. CO<sub>2</sub> recycling using microalgae for the production of fuels. *Applied Petrochemical Research*. 4(1): 41-53.
- Wilson M H, Mohler D T, Groppo J G, Grubbs T, Kesner S, Frazar E M, Shea A, Crofcheck C, Crocker M. 2016. Capture and recycle of industrial CO<sub>2</sub> emissions using microalgae. *Applied Petrochemical Research*. 6(3): 279-293.
- Yen H W, Ho S H, Chen C Y, Chang J S. 2015. CO<sub>2</sub>, NO<sub>x</sub> and SO<sub>x</sub> removal from flue gas via microalgae cultivation: a critical review. *Biotechnol J*. 10(6): 829-839.

## Chapter 2

### INFLUENCE OF FLUE GAS ON GROWTH AND BIOMASS COMPOSITION OF *SCENEDESMUS ACUTUS*

#### 2.1 Abstract

Microalgal-based carbon capture and reuse has been studied as a possible solution to reduce CO<sub>2</sub> emissions from point sources such as flue gas from power plants. *Scenedesmus acutus* is a freshwater chlorophyte that can successfully grow in the presence of flue gas and its biochemical composition is ideal for developing products such as bioplastic and biofuel. However, in order to continue optimizing the alga to improve the cost effectiveness of carbon capture and reuse, I studied how the flue gas influenced the growth and biochemical composition of *S. acutus* by exposing cultures to simulated flue gas and then compared it to growth in 9% CO<sub>2</sub>, and air (0.04% CO<sub>2</sub>). The biomass productivity was approximately 15 times greater when cultures were exposed to the simulated flue gas and 9% CO<sub>2</sub> despite a very low pH. The high CO<sub>2</sub> concentration in the simulated flue gas was the driving factor that promoted high biomass productivity, although the NO and SO<sub>2</sub> were not directly inhibiting growth. The high protein content and cetane numbers were particularly noteworthy for bio-plastic and biofuel production, respectively. I also investigated supplying the culture with an alternative inorganic carbon source such as bicarbonate or air (0.04% CO<sub>2</sub>) to maintain the health and biochemical composition of the alga in the event of an unplanned power outage when it is

deprived of high CO<sub>2</sub> from the flue gas. This experiment demonstrated that switching from high to low CO<sub>2</sub> resulted in a lower biomass yield, as well as reduced lipid and carbohydrate content. Although, adding solid sodium bicarbonate (5mM) promoted greater biomass productivity than if the cultures were solely supplemented with air. Cultures supplemented with NaHCO<sub>3</sub> also maintained high protein and saturated fatty acid content, as well as high cetane numbers which indicates bioplastic and biofuel could still be produced from the algal biomass even under this condition.

## **2.2 Introduction**

### **2.2.1 Influence of Flue Gas**

Coal accounts for the second largest share of global primary energy consumption at 28%, and emits more pollutants than all other fossil fuels (British Petroleum Company 2017). Emissions from coal-fired power plants, often referred to as flue gas, contain 10-20% carbon dioxide (CO<sub>2</sub>), as well as varying amounts of trace gases, including nitrogen and sulfur oxides (Sayre 2010). While carbon dioxide is a major concern as a greenhouse gas, nitric oxide (NO<sub>x</sub>) and sulfur dioxide (SO<sub>x</sub>) are the primary contributors to acid rain and smog. These oxides are also a significant public health concern, since they can increase the risk of respiratory tract infections in humans, as well as contribute to respiratory symptoms in healthy people and those with respiratory diseases (Chen et al., 2007). Globally, we still have a large dependency on energy derived from coal, but there is an ever-growing need to curb our carbon emissions not only from a public health standpoint, but to also combat the

devastating consequences of climate change. Microalgal-based carbon capture and reuse has been studied as a possible solution with the goal of capitalizing on the organisms' natural ability to incorporate inorganic carbon into its biomass, thus preventing the emissions from entering the atmosphere (Yen et al., 2015, Sayre 2010, Wang et al., 2008).

*Scenedesmus acutus* UTEX B72 (*S. acutus*) is a freshwater chlorophyte that has been studied for CO<sub>2</sub> capture and reuse. When grown in a pilot-scale closed photobioreactor (PBR) on an agriculture-grade urea-based medium, *S. acutus* was effective for CO<sub>2</sub> capture and reuse at Duke Energy's East Bend coal-fired power plant in Boone County, Kentucky (Wilson et al., 2014). A 2014 field study noted the carbon removal efficiency of the alga reached a maximum of 70% and the maximum biomass productivity of the alga was 39 g m<sup>-2</sup> d<sup>-1</sup> during the summer, at a scale of 18,000 L (Wilson et al., 2014). This is comparable to the rates of other well-used microalgal strains, and far above the Department of Energy's current minimum baseline (13 g m<sup>-2</sup> d<sup>-1</sup>) and the 2020 goal of 25 g m<sup>-2</sup> d<sup>-1</sup> (Wilson et al., 2014, US DOE 2010).

While *S. acutus* can successfully grow in the presence of flue gas, understanding how flue gas influences the growth and biochemical composition of this alga is essential for optimizing and improving CO<sub>2</sub> removal efficiency. A number of studies have examined the growth of microalgae, including *Scenedesmus* sp., under high CO<sub>2</sub> and simulated flue gas conditions (Huang et al., 2016, Mortensen and Gislerod 2016, Mudimu et al., 2015, Jiang et al., 2013, Papazi et al., 2008, Yang and Gao 2003, Hanagata et al., 1992), but few have studied *S. acutus* (Crofcheck et al., 2012). Among those that have, difficulties

arise when comparing results to published studies for related species, as intraspecific differences in growth rates and biomass composition can occur due to differences in cultivation conditions. Therefore, I investigated the influence of flue gas on the growth and biochemical composition of *S. acutus* under

### **2.2.2 Power Outage Mitigation**

Planned and unplanned power plant outages cease flue gas flow and deprive the alga of CO<sub>2</sub>. Understanding how these outages may compromise algal health is essential. Planned outages could be scheduled to coincide with culture harvest, so that the culture may be diluted to a minimum density before the outage thus minimizing losses. As the frequency and intensity of storms are expected to increase (Walsh et al., 2014), however, the threat of unplanned power outages should be considered. Unplanned outages require a different approach, because the biomass density may be too low to yield sufficient product. Conversely the lack of CO<sub>2</sub> could have detrimental effects on the biomass composition if the culture is left in the PBR. Any loss in biomass could considerably add to operational costs as well as the cost of the products developed downstream. On-site compressed CO<sub>2</sub> cylinders are not environmentally or economically feasible for such a large system. Therefore, when flue gas is unavailable, it is necessary to develop a strategy for supplying the culture with an alternative inorganic carbon source, such as supplementing the culture with bicarbonate.

Green algae use carbon concentrating mechanisms to assimilate bicarbonate under alkaline pH, and carbon assimilation studies have found that bicarbonate is the major carbon source for *Scenedesmus* sp. (Gardner et al.

2013). Gardner et al. (2013) evaluated the physiological effects of a different *Scenedesmus* strain by switching from 5% CO<sub>2</sub> to atmospheric CO<sub>2</sub> levels and supplementing with sodium bicarbonate as a way to induce the accumulation of the common precursor compound to biodiesel, triacylglycerol (TAG). Once switched to air, growth rates declined and cells continued to divide, but under certain concentrations of bicarbonate, division ceased and cells accumulated large amounts of TAGs (Gardner et al. 2013). However, our understanding of how switching from ~9% CO<sub>2</sub> in flue gas to atmospheric levels of CO<sub>2</sub>, or to other sources of carbon such as bicarbonate, alters productivity and biochemical composition is largely unknown for *S. acutus*. To assess these effects, *S. acutus* was grown on flue gas, then switched to one of three alternative inorganic carbon sources: atmospheric levels of CO<sub>2</sub> in compressed air (~400 ppm), carbon supplied from a saturated bicarbonate solution, or carbon supplied through addition of solid sodium bicarbonate. The results from this experiment will aid in the future development of standard operating procedures in the event that the culture is unable to be harvested during an unplanned power outage.

## **2.3 Methods**

### **2.3.1 Cultivation Setup**

*S. acutus* UTEX-B72 was obtained from the Culture Collection of Algae at the University of Texas at Austin. Stock cultures were grown in 500 ml glass Hybex bottles at 33°C under 10W Daylight 6000K LED lights (Fulight, Santa Ana, CA, USA) at an average intensity of 400 μmol photons m<sup>-2</sup> s<sup>-1</sup> on a 16:8 h light:dark cycle. The media used for cultivation contained 0.14 g L<sup>-1</sup> Triple

Super Phosphate, 0.068 g L<sup>-1</sup> Pot Ash, 0.026 g L<sup>-1</sup> Sprint 330 (iron chelate), and 0.13 g L<sup>-1</sup> urea (Chrofcheck et al., 2012). Cultures were positioned around the perimeter of a 15-position digital magnetic stirrer (RO 15, IKA, Staufen im Breisgau, Germany) and the alga was kept in continuous suspension by a 30 mm stir bar set to 110 rpm. Gas treatments included an air control (~0.04% CO<sub>2</sub>) and two additional treatments of 9% CO<sub>2</sub> (referred to hereafter as the CO<sub>2</sub> treatment) and simulated flue gas (9% CO<sub>2</sub>, 55 ppm NO, 25 ppm SO<sub>2</sub>). The treatment gases were premixed and balanced in N<sub>2</sub> (Keene Gas, Dover, DE, USA). All culture vessels were fitted with PTFE tubing and were continuously aerated with their respective gases at a flow rate between 2.3-2.5 mL min<sup>-1</sup>. Flow was controlled by individual 65-mm correlated flowmeters (Cole Parmer, Vernon Hills, IL, USA). Each treatment included four replicate bottles that were acclimated to their respective gases for three generations prior to starting the experiment. To begin the experiment, the appropriate volume of each culture was concentrated by centrifugation and then suspended in 400 mL of fresh media to obtain a biomass density of approximately 0.2-0.3 g L<sup>-1</sup>, with the exception of the control treatment, which accumulated less biomass during the acclimation phase and was concentrated to the initial density of 0.05±0.01 g L<sup>-1</sup>.

### **2.3.2 Growth Measurements**

Growth was monitored by oven dry weight measured by filtering 10 mL of culture on a pre-weighed 47 mm Grade C Sterlitech glass fiber filter, followed by drying at 100°C overnight, and then re-weighing the dry filter. Regression analysis was used to determine productivity rates (g biomass L<sup>-1</sup> day<sup>-1</sup>)

<sup>1</sup>) for each treatment. Specific growth rates were calculated for each treatment using the following equation:

$$\mu = \ln(\text{ODW}_f/\text{ODW}_i)/(t_f - t_i) \quad (1)$$

where  $\text{ODW}_{f/i}$  are the oven dry weight at final and initial time points, respectively, and  $t_{f/i}$  are the final and initial time in days, respectively.

The media was buffered with 0.5 M NaOH before the start of the experiment to bring the initial pH to approximately 7, but pH was otherwise unregulated during the experiment. pH was measured using a standard benchtop pH meter calibrated to NBS standard buffers. To determine urea and phosphate concentrations, samples were centrifuged at 5,000 rpm for 10 min and the supernatant was decanted into 20 mL scintillation vials and stored at -80°C until the analyses. Urea concentrations were determined colorimetrically based on a method by Zawada et al. 2009. Phosphate concentrations were determined using a Seal Nutrient Autoanalyzer (Mequon, WI, USA).

### **2.3.3 Biomass Characterization**

For total protein, lipid, carbohydrate, and fatty acid methyl ester (FAME) composition for each treatment, a 100 mL sample was pelleted by centrifugation (10 min at 5,000 rpm), freeze dried, and homogenized. Total nitrogen content was determined by CHN elemental analysis (ECS 4010 CHNSO analyzer, Costech Analytical Technologies, INC., Valencia, CA, USA), and protein content was subsequently calculated using the N-to-protein conversion factor of 4.78 (Templeton and Laurens 2015). Lipids were first extracted using chloroform and methanol (Folch et al. 1957) and quantified colorimetrically via the sulfo-phospho-vanillin method (Cheng et al. 2011). To determine FAME

composition, fatty acids were first separated from triacylglycerols and bonded to a methyl group through acid-catalyzed transesterification. FAME were then extracted with hexane, then identified and quantified as a percent of total FAME using gas chromatography on Agilent Technologies 7890B GC system (Santa Clara, CA, USA) (Van Wychen, Ramirez, and Laurens, 2013). Only fatty acids that made up greater than 2% of the total FAME composition were included in the analysis. Cetane numbers were calculated from the FAME content using equations in Islam et al. (2013). Total carbohydrate content was determined by a two-step sulfuric acid hydrolysis to break down the carbohydrates into monomers, which were then complexed with MBTH and quantified spectrophotometrically using a FLUOstar Omega plate reader (BMG Labtech, Offenburg, Germany) (Van Wychen and Laurens, 2015). All biochemical components were represented as a percentage of total biomass.

#### **2.3.4 Photochemical Measurements**

Chlorophyll a was extracted by filtering 5 mL of culture onto a 25 mm Grade C Sterlitech glass fiber filter, then placed in 90% acetone in the dark at -20°C overnight. Chlorophyll a concentration was measured using a 10-AU Turner Fluorometer (Turner Designs, Sunnyvale, California, USA). On days 0, 3, and 6, samples were dark acclimated for 20 min, and the single turnover maximum quantum yield of photosystem II ( $F_v/F_m$ ) was measured by a fast repetition rate fluorometer (FRRf) (Chelsea Technologies Group Ltd, West Molesey, UK) set to deliver 50  $\mu$ s flashlets of light over 200  $\mu$ s.

Gross photosynthesis to respiration ratios (P:R) were calculated by measuring photosynthetic oxygen evolution and consumption rates. Samples

were dark acclimated for 20 min in sealed 20 ml glass scintillation vials, fitted with a PreSens Fibox 4 oxygen electrode connected to a detector (Precision Sensing GmbH, Regensburg, Germany), in a water bath set to 33°C. Oxygen levels were continuously recorded for 20 min in the dark and 20 min of illumination at 200  $\mu\text{mol photons m}^{-2} \text{s}^{-1}$ , followed by another 20 min in the dark to record any post illumination respiratory activity. Dark respiration and net photosynthesis rates were then determined by linear regression during the initial dark stage and illumination stage, respectively. Gross photosynthesis was then calculated using the following equation:

$$P_{\text{gross}} = P_{\text{Net}} + R \quad (2)$$

Where  $P_{\text{gross}}$  is gross photosynthesis,  $P_{\text{Net}}$  is net photosynthesis and R is respiration.

### **2.3.5 Power Outage Mitigation Experimental Design**

Replicate *S. acutus* cultures exposed to flue gas in the previous experiment (n=4) were diluted with 200 mL of fresh urea media to lower the biomass to 0.2 g L<sup>-1</sup>, and the cultures were aerated with simulated flue gas (9% CO<sub>2</sub>, 55 ppm NO, 25 ppm SO<sub>2</sub>, balanced in N<sub>2</sub>) at 2.3-2.5 ml/min for four days. Dry weight was taken from days 0 to 4 while the cultures were still grown on flue gas. On day 4, the flue gas was shut off and all cultures were pooled to homogenize the four replicate cultures before splitting them into three treatments: 0.04% CO<sub>2</sub> (bubbled air), addition of sodium bicarbonate (NaHCO<sub>3</sub>) solution, or addition of solid NaHCO<sub>3</sub>. A saturated NaHCO<sub>3</sub> solution (0.95 M) was added to 400 mL of culture to achieve a final concentration of 5 mM. For the solid NaHCO<sub>3</sub> treatment, 168 mg of NaHCO<sub>3</sub> was added to 400 mL of

culture (final concentration to 5 mM). Each treatment was then split into 4 100 mL replicate Hybex vessels which were fitted with PTFE tubing and aerated with air at 2.3-2.5 ml/min and stirred as described above. All parameters described in sections 2.2.2-2.2.4 were measured on days 4 and 7 in this experiment.

### **2.3.6 Statistical analysis**

All statistical analyses were performed in R. Productivity, specific growth, photosynthesis and respiration rates were all determined using the linear model function (`lm()`). Significant differences between treatments were determined using the analysis of variance function (`aov()`), and least square means for multiple comparisons function (`lsmeans()`, in the `lsmeans` package) with a Tukey p-value adjustment. The assumptions for these tests were assessed visually and with the Shapiro-Wilk normality test and Levene's Test for Homogeneity of Variance.

## **2.4 Results**

### **2.4.1 Influence of Flue Gas on Growth of *S. acutus***

Growth of *S. acutus* was slow in the control (air only), and biomass accumulation occurred more rapidly in the CO<sub>2</sub> and flue gas treatments, with no significant difference between these two treatments ( $p > 0.05$ , Figure 1). However, the specific growth rates were significantly different between treatments (Table 1,  $p < 0.05$ ). The greatest specific growth rate was in the CO<sub>2</sub> treatment ( $0.389 \pm 0.021 \text{ d}^{-1}$ ), followed by the flue gas treatment ( $0.307 \pm 0.020 \text{ d}^{-1}$ ) and finally the control ( $0.217 \pm 0.087 \text{ d}^{-1}$ ). The biomass productivity rates for

the CO<sub>2</sub> (0.267±0.016 g L<sup>-1</sup> d<sup>-1</sup>) and flue gas treatments (0.269±0.039 g L<sup>-1</sup> d<sup>-1</sup>) were not significantly different, but were 15 times greater than the control (0.018±0.006 g L<sup>-1</sup> d<sup>-1</sup>) (Table 1, p<0.05).

The urea media was adjusted so that the initial pH for all treatments was between 6.5 and 7.0. The pH for the control increased to 9.7 ± 0.01 by day 6, whereas pH decreased to 4.2 ± 0.14 and 3.5 ± 0.19 in the CO<sub>2</sub> and flue gas treatments, respectively (Figure 2). The urea concentration declined by 67% in the control and by 95% in the CO<sub>2</sub> and flue gas treatments by day 3 (Table 2). Urea continued to decline more gradually from days 3 to 6, with final concentrations falling below the limits of detection in the CO<sub>2</sub> and flue gas treatments. The phosphate concentrations for each treatment followed a similar decline as urea but a larger proportion of phosphate remained in all treatments by day 6 (Table 3).

#### **2.4.2 Influence of Flue Gas on Biochemical Composition**

Biomass samples were taken on days 0, 3, and 6 to determine protein content, total lipid content, FAME profile, and the carbohydrate content for each treatment. CO<sub>2</sub> and flue gas treatments had significantly greater protein content than the control treatment on days 0 and 3 (p<0.05, Figure 3), but decreased to control levels by day 6. In all treatments, the lipid content (~33% of total biomass) was relatively high at the start of the experiment (Figure 4). On day 3, total lipids decreased in the CO<sub>2</sub> and flue gas treatments, and both were significantly less than the control (p<0.05). The final lipid content increased to an average of 25% of total biomass in the flue gas treatment, which was

comparable to that found in the control and about 10% greater than that in the CO<sub>2</sub> treatment, but this was not statistically significant.

In terms of overall FAME composition, the flue gas treatment had significantly greater saturated fatty acid content than the control on all days, but it was not significantly different from the CO<sub>2</sub> treatment ( $p < 0.05$ , Figure 5). The two gas treatments had significantly greater monounsaturated fatty acid content than the control on all days ( $p < 0.05$ , Figure 5). There were a few prominent fatty acids found among all treatments on all sampling days, including C16:0, C18:1n9c, and C18:1n9t (Appendix A, Figure 19). C18:2n6 was the only polyunsaturated fatty acid that made up at least 2% of the total composition, and it was only found in the control (Appendix A, Figure 19). The control also contained several other fatty acids that were not seen at all in the other treatments throughout the experiment, including C8:0, C10:0, C11:0, and C16:1 (Appendix A, Figure 19). The CO<sub>2</sub> and flue gas treatments had greater cetane numbers than the control (Table 4).

In contrast to the trends seen in lipid content, the flue gas treatment maintained relatively high carbohydrate content, at around 50% of the total biomass, throughout the experiment (Figure 6). On day 3 the flue gas treatment had the greatest carbohydrate content, followed by the CO<sub>2</sub> treatment, and then the control, which had 60% less carbohydrate content than the flue gas treatment, ( $p < 0.05$ ). By day 6, there was a slight decrease in carbohydrates in the flue gas treatment, but it was still significantly greater than the control ( $p < 0.05$ ).

### 2.4.3 Photochemical Measurements

Chlorophyll a content was significantly greater in the control than the gas treatments on all sampling days, but the chlorophyll a content in the flue gas treatment was significantly greater than that of the CO<sub>2</sub> treatment on day 3 ( $p < 0.05$ , Figure 7). In addition, the maximum quantum yield of PSII (Fv/Fm) remained relatively high in all treatments (Figure 8), and there were no significant differences between any condition, except for day 6, when the flue gas treatment had a significantly greater Fv/Fm than the CO<sub>2</sub> treatment. The P:R of the flue gas treatment was significantly greater than the control and CO<sub>2</sub> treatment on day 3 (Figure 9,  $p < 0.05$ ), but was not significantly different from the control by day 6. The CO<sub>2</sub> treatment had slightly greater P:R on day 0 but remained significantly lower than both the control and flue gas treatment on days 3 and 6 ( $p < 0.05$ ).

### 2.4.4 Power Outage Mitigation

The biomass productivity of cultures exposed to flue gas ( $0.23 \text{ g L}^{-1} \text{ day}^{-1}$ ) for the first four days was not significantly different from that seen in the previous experiment ( $p < 0.05$ ). After the flue gas was shut off, the greatest biomass productivity and specific growth rates were noted in the cultures amended with NaHCO<sub>3</sub>, although there were small, albeit significant, differences in these rates between the two NaHCO<sub>3</sub> treatments (Table 5, Figure 10). Whereas, when cultures were solely bubbled with air the biomass density declined (Figure 10). Importantly, the productivity and specific growth rates of all treatments were still significantly less than that of cultures maintained on flue gas ( $p < 0.05$ ). The pH increased in all treatments after the flue gas was shut off,

and as expected, it was the greatest in the two NaHCO<sub>3</sub> treatments (Figure 11). Phosphate and urea concentrations were depleted by approximately 80% and 90%, respectively, when the flue gas was turned off on day 4. By day 7, only 10% of phosphate remained in all treatments, and urea was completely exhausted in the flue gas and air treatments, but 6% and 9% of urea remained in the solid NaHCO<sub>3</sub> and NaHCO<sub>3</sub> solution treatments, respectively.

Despite significant differences in growth, the biomass composition remained similar for air-grown cultures compared to those receiving bicarbonate supplementation. However, significant differences were observed in biomass composition compared to those maintained on flue gas. There was a slight decrease in protein content in all treatments after the flue gas was shut off, but all treatments still contained 25% of total biomass as protein on day 7, which was significantly greater than that in cultures maintained on flue gas (Figure 12,  $p < 0.01$ ). In contrast, there was a slight increase in lipid content in all treatments after flue gas was shut off, although the total lipids were 5% less ( $p < 0.05$ ) in all treatments compared to cultures when flue gas supply was not interrupted (Figure 13). Saturated fatty acid content in all treatments was significantly greater than flue gas maintained cultures on day 7 ( $p < 0.05$ , Figure 14). Conversely, monounsaturated fatty acid content in all treatments was significantly less than in flue gas maintained cultures on day 7 ( $p < 0.05$ ). A few fatty acids were common across all samples before and after the flue gas disruption, including C16:0, C18:0, C18:1n9c/t, and C20:0 (Appendix A, Figure 20). C22:6n3 was the only polyunsaturated fatty acid that contributed to 2% or more of the total FAME content and it was only seen on day 4 prior to flue gas

disruption (Appendix A, Figure 20). Average cetane numbers for air, flue gas, solid NaHCO<sub>3</sub>, and NaHCO<sub>3</sub> solution on day 7 were 67, 65, 66, and 65, respectively. There was a decrease in carbohydrates in all treatments after the flue gas was shut off (Figure 15). On day 7, carbohydrate content was significantly lower in the air and bicarbonate cultures than in flue gas maintained cultures ( $p < 0.05$ ).

Chlorophyll a content increased in all treatments and was significantly greater than that of the flue gas maintained cultures on day 7 (Figure 16). Interestingly, Fv/Fm increased on day 7 in both NaHCO<sub>3</sub> treatments, despite the low nutrient concentrations observed (Figure 17). Fv/Fm decreased in air-grown cultures, but all treatments were significantly greater than that of cultures maintained on the flue gas ( $p < 0.05$ ). There was an increase in respiration (normalized to total carbon content), which was also reflected in the decline in P:R for all treatments after the flue gas was shut off, and was significantly lower than that for flue gas maintained cultures on day 7 ( $p < 0.05$ , Figure 18). The lowest P:R was noted in the NaHCO<sub>3</sub> solution treatment, followed by the solid NaHCO<sub>3</sub> treatment.

## **2.5 Discussion**

### **2.5.1 Influence of Flue Gas on Growth and Biochemical Composition of *S. acutus***

The goal of this study was to assess how different gases influence the growth and biochemical composition of a green alga commonly utilized in commercial settings. The choice of the simulated flue gas used here was to approximate culture conditions to those used in field studies at a pilot outdoor

PBR connected to a coal-fired power plant in Kentucky (Wilson et al., 2014). While we were able to replicate the growth temperature and total photoperiod, a limitation of our experimental design was that the light intensity was lower than that recorded in the outdoor PBR system but still higher than what is typically used in many other studies (Jiang et al., 2013, Moretensen and Gislerod 2016). Likewise, while flue gas is intermittently sparged into the pilot PBR, we used a simplified constant gas supply in our flue gas and CO<sub>2</sub> treatment cultures.

Despite a much lower pH in this experiment as compared to the outdoor PBR (Wilson et al, 2016), the productivity of *S. acutus* was significantly greater when grown on flue gas when compared to air alone and also greater than that reported for *S. acutus* grown on flue gas in the pilot PBR. While the flue gas did not inhibit productivity, growth on this gas was not significantly different from that in 9% CO<sub>2</sub>, thereby suggesting that the high CO<sub>2</sub> concentration in the flue gas was more important in promoting growth than the NO and SO<sub>2</sub> trace gases. Fv/Fm values for the flue gas and CO<sub>2</sub> treatments were also similar to those of the air-grown control, which further indicated that the high CO<sub>2</sub> concentrations in these treatments were not inhibiting photochemistry.

These results are in agreement with previous studies that noted increased biomass productivity of other economically important chlorophytes, such as *Chlorella* sp., *Chlamydomonas* sp., and other *Scenedesmus* sp., when grown in high CO<sub>2</sub> concentrations (Mudimu et al., 2015, Papazi et al., 2008, Yang and Gao 2003, Hanagata et al., 1992). They are also consistent with studies that evaluated the use of microalgae to biologically capture CO<sub>2</sub> from industrial flue gas sources (Mortensen and Gislerod 2016, Jiang et al., 2013, Huang et al.,

2016). For example, Hanagata et al. (1992) showed that *Scenedesmus* sp. successfully grows in up to 80% CO<sub>2</sub>; Jiang et al. (2013) reported that *Scenedesmus* sp. grew well at NO concentrations of 150-500 ppm and SO<sub>2</sub> concentrations below 100 ppm, which are much higher than in the flue gas used in this experiment.

At current atmospheric CO<sub>2</sub> levels (0.04%), ribulose-1,5-bisphosphate carboxylase/oxygenase (RuBisCO), operates well below its maximum capacity because this low CO<sub>2</sub> concentration does not saturate carboxylation (Borowitzka et al., 2016). Additionally, because of RuBisCO's dual role as a carboxylase and oxygenase, CO<sub>2</sub> and oxygen compete for the active site, which further decreases the efficiency of the enzyme (Borowitzka et al., 2016). Thus, high density cultures, similar to those used in most large-scale PBR systems, when grown solely on air are considered to be carbon limited (or CO<sub>2</sub>-limited). To combat this, CO<sub>2</sub>-limited cells employ energy-dependent carbon concentrating mechanisms (CCMs) that increase the CO<sub>2</sub> concentration around RuBisCO to increase its carboxylase activity (Borowitzka et al., 2016). However, due to the high energetic demand of employing CCMs, air-grown cells may be diverting a significant amount energy from carbon fixation and growth, to CCM activity, and why growth is much substantially slower in these cultures. Whereas in cultures treated with CO<sub>2</sub> and flue gas, the biomass productivity is much higher because the high CO<sub>2</sub> concentration alleviates the need for CCM activity and its associated energetic demand (Solovchenko and Khozin-Goldberg 2013).

In this experiment, pH was unregulated and the introduction of excess CO<sub>2</sub> caused the pH to decline considerably in the CO<sub>2</sub> and flue gas treatments.

Additionally, the final pH in the flue gas treatment (3.5) was almost one pH unit below that of the final pH in the CO<sub>2</sub> treatment. This was probably due to the accumulation of NO and SO<sub>2</sub> in the media (Yen et al., 2015, Jiang et al. 2013, Lee et al., 2002, Maeda et al., 1995). It was surprising that the cultures grew faster in such acidic conditions, considering the optimum pH for growth for most microalgae is near neutral (Juneja et al., 2013). Many algal species, however, have adapted to fluctuations in pH often seen in freshwater environments by regulating their internal pH (Juneja et al., 2013, Gehl and Colman 1984, Goldman et al., 1982). Some freshwater green algae, including *Scenedesmus*, can maintain a near neutral internal pH even under low external pH conditions (Gehl and Colman 1984, Lane and Burris 1981). This would allow for normal cell functions to proceed, although it would be necessary for cells to allocate a significant amount of energy to proton pumping via P-type H<sup>+</sup> ATPases found on the plasma membrane (Juneja et al., 2013, Taylor et al., 2012). While there was an increase in *S. acutus* biomass productivity in 9% CO<sub>2</sub> and flue gas, maximum productivity might not have been reached in these treatments, because the cells diverted energy from CO<sub>2</sub> fixation and growth to such proton pumping (Gerloff-Elias et al., 2005). To offset the low pH, intermittent flue gas sparging, instead of continuous aeration, would allow for greater stability in culture pH, which could further increase biomass productivity as well as CO<sub>2</sub> fixation efficiency (Jiang et al. 2013). As mentioned above, this strategy is employed in the pilot PBR at the East Bend Station where gas is sparged for 20 seconds and then turned off for 40 seconds, and the pH of the pilot PBR system is held to a range of 6-7 (Wilson, personal communication).

Higher biomass productivity in the flue gas and CO<sub>2</sub> grown cultures was also reflected in the greater depletion of urea over phosphate compared to the air grown cultures. Likewise, the larger urea depletion than that of the phosphate in all treatments indicates that nitrogen became the first limiting nutrient as the cultures entered stationary phase. Furthermore, other work has shown that sub-inhibitory levels of NO promotes microalgal growth, as the NO is used as an additional nitrogen source (Yen et al. 2015, Matsumoto et al., 1997, Nagase et al., 1997). Specifically, as the NO is dissolved into the media, it is oxidized to form nitrite (NO<sub>2</sub><sup>-</sup>) via inlet gas or photosynthetically derived oxygen (Nagase et al., 1997), and the NO<sub>2</sub><sup>-</sup> is then taken up and assimilated by the algae (Nagase et al., 1997). Dissolution and removal of NO by the algae was not directly measured in this experiment, but a small amount of nitrite was detected (approximately 15 μmol L<sup>-1</sup> NO<sub>2</sub><sup>-</sup>), which could provide some evidence of using NO in this fashion. Nevertheless, if such additional nitrogen was available to the flue gas cultures, it did not result in increased productivity when compared to cultures grown on CO<sub>2</sub> alone.

Evaluating the effect of flue gas on biomass composition is important in order to gain a better understanding of how the major biochemical constituents change in *S. acutus* in response to high CO<sub>2</sub> and the trace gases. The biomass composition of *S. acutus* was expected to change in all treatments as the culture aged and nutrient concentrations declined. Protein content (% of total biomass) was of particular importance in this study, since a future application is to harvest *S. acutus* for production of biodegradable plastic from this fraction. Bioplastic from protein capitalizes on the fact that proteins are naturally occurring

polymers and therefore do not require polymer synthesis (Wang et al., 2016). The high protein content and biomass yields make algae good candidates for bioplastic production, compared to other bioplastic feedstocks like soy protein (Wang et al., 2016). Although unlike soy protein it's not feasible to isolate the algal protein before the modification process and why the lipid and carbohydrate fractions still need to be considered as they can influence the quality of the bioplastic (Wang et al., 2016).

When exposed to CO<sub>2</sub> and flue gas, protein content was enhanced by 25% during log phase growth (day 3). Sarat et al., 2016 also found that protein content in *S. obtusus* increased by 15% when grown under 10% CO<sub>2</sub>. In this study, *S. acutus* protein content was about 30% on day 3, which is comparable to that reported for *S. acutus* grown using flue gas in an outdoor pilot-PBR (Santillan-Jimenez et al., 2016), as well as that for *S. obtusus* in Sarat et al. (2016). Protein synthesis is largely dependent on nitrogen availability, as nitrogen is a main component in amino acids, and so as nitrogen is depleted from the media, protein content will likely decrease (Juneja et al., 2013), as seen on day 6 in Figure 3. The air-grown cultures had less protein than the two gas treatments on all sampling days which is reflected in the low biomass productivity under this condition. However, the air-grown cultures had significantly greater chlorophyll a content (an N-rich pigment) than the two gas treatments which suggests that those cells were not allocating as much protein to light harvesting complexes and energy capture as the air grown cells, despite their high biomass productivities. This could be another indication of the high

CO<sub>2</sub> concentration alleviating the energetic demand of employing strategies like CCMs.

Other studies have noted increased lipids with increased CO<sub>2</sub> concentration in *Scenedesmus* and *Chlorella* sp., as lipid biosynthesis is a sink for excess products of carbon fixation, and it is thought that channeling these products to energy rich compounds may be an adaptation to high CO<sub>2</sub> tolerance (Sarat et al., 2016, Xia et al., 2013, Solovchenko and Goldberg 2013). This was not the case in this experiment, as there were less lipids in cultures grown in flue gas and CO<sub>2</sub> than air-grown cultures in log and stationary phases. Rather, the cells in the flue gas and CO<sub>2</sub> treatments stored their fixed carbon as carbohydrates, which is the primary sink for carbon. The ratio of gross photosynthesis to respiration (P:R) in the flue gas cultures was significantly greater than that of the other cultures during log phase growth (Figure 9; day 3), which further suggests that the flue gas cultures were not losing large amounts of carbohydrates to respiration. At nearly 50% of the total biomass, the carbohydrate content in *S. acutus* could be extracted and utilized as a feedstock for fermentation into bio-ethanol, which would increase the purity of the protein fraction bio-plastic production (Laurens et al., 2015).

There was a clear trend seen in fatty acid composition where the CO<sub>2</sub> and flue gas grown cultures had more saturated and monounsaturated fatty acids than the control. This shift to increased saturated fatty acid content, in particular long-chain saturated fatty acids, has been seen in some microalgae exposed to high CO<sub>2</sub> concentrations (Singh et al., 2016, Juneja et al., 2013). The high saturated and monounsaturated fatty acid content was also reflected in the higher

cetane numbers for these treatments. Cetane number is a diesel fuel standard used to indicate good ignition quality, suitable cold filter plugging point, low pollutant content, correct density, and viscosity (Islam et al., 2013). The cetane numbers reported for *S. acutus* were greater than the minimum cetane number of 47 under all conditions, thereby indicating that this organism is a good candidate for the production of biodiesel (ASTM D6751, 2002). In addition, palmitic (C16:0) and oleic (C18:1) acids made up a large proportion of the FAME composition, and is consistent to that reported for *S. acutus* grown on flue gas in the pilot PBR (Wilson et al., 2014).

There were polyunsaturated fatty acids in the CO<sub>2</sub> and flue gas grown cultures, but at very low amounts. However, *S. acutus* grown in the field and other species of *Scenedesmus* were reported to have as much as 50% of the total fatty acids as polyunsaturated fatty acids (Ji et al., 2017). This difference in fatty acid composition could be due to the low pH in this experiment versus the near neutral pH seen in the field and in these other experiments (Ji et al., 2017). Increased saturated fatty acid content in microalgae is another response to increased external acidity, since saturation of membrane fatty acids reduces its fluidity and inhibits proton infiltration (Juneja et al., 2013). This difference highlights the idea that fatty acid content and composition in microalgae is largely species-specific and can significantly change under different environmental conditions (Ji et al., 2017, Juneja et al., 2013).

*S. acutus* not only showed a high tolerance to flue gas, but the robustness of this species was also demonstrated by the enhanced productivity despite very low pH. The high CO<sub>2</sub> concentration was the driving factor that promoted high

biomass productivity, although it was determined that the NO and SO<sub>2</sub> were not directly inhibiting growth. The alga also has a biochemical composition that has the potential to be fractionated to make a variety of bio-products. The high protein content and cetane numbers are particularly noteworthy for bio-plastic and biofuel production, respectively. *S. acutus* is an ideal candidate for carbon capture and reuse at coal-fired power plants.

### **2.5.2 Power Outage Mitigation**

In the event of an unplanned power outage, algae would be deprived of high CO<sub>2</sub> from the flue gas. If the alga is unable to be harvested at that time, the culture must be supplied with an alternative source of inorganic carbon to maintain the health of the culture. This experiment aimed to identify differences in growth and biochemical composition of *S. acutus* that would occur in the event of a power outage, where the culture could be transitioned from growing on flue gas to either (1) a stream of atmospheric air, (2) a sodium bicarbonate solution, or (3) solid sodium bicarbonate.

Differences in CO<sub>2</sub> concentration are a main factor that drive differences in *S. acutus* growth and biochemical composition. Here, it was apparent that switching from 9% CO<sub>2</sub> to the alternative inorganic carbon sources tested in this experiment resulted in a CO<sub>2</sub>-limited condition. This also corresponded to a lower biomass yield as well as reduced carbohydrate and lipid content compared to cultures maintained on flue gas. Reducing the concentration to 400 ppm CO<sub>2</sub> led to an immediate decrease in biomass. To maintain a higher biomass yield during a power outage, NaHCO<sub>3</sub> addition is the better alternative. While the difference in biomass productivity between cultures supplemented with solid

NaHCO<sub>3</sub> and the NaHCO<sub>3</sub> solution was small albeit significant, logistically it would be easier to add solid NaHCO<sub>3</sub> in the event of a power outage rather than making a NaHCO<sub>3</sub> solution onsite. Therefore, supplementation of solid NaHCO<sub>3</sub> to the culture appears to be the best alternative inorganic carbon source.

While not measured directly here, it is assumed that the microalgae in these treatments were not only experiencing an increase in alkalinity, but also a shift in carbon species from dissolved CO<sub>2</sub> to HCO<sub>3</sub><sup>-</sup>, which is associated with a myriad of physiological changes. It is known that many microalgae can use HCO<sub>3</sub><sup>-</sup> as a source of inorganic carbon through the use of the enzyme carbonic anhydrase (CA) which converts HCO<sub>3</sub><sup>-</sup> to CO<sub>2</sub> (Borowitzka et al., 2016, Bhatti and Colman 2008). It has been shown in *Chlamydomonas reinhardtii*, however, that under high CO<sub>2</sub> there is a complete degradation of CA associated with the inhibition of active transport of bicarbonate (Borowitzka et al., 2016, Bhatti and Colman 2008). Upon reintroducing the alga to a low CO<sub>2</sub> concentration there must be a swift upregulation and expression of CA for the cells to use HCO<sub>3</sub><sup>-</sup>. This readjustment may contribute to the slower growth seen in the *S. acutus* cultures amended with NaHCO<sub>3</sub> compared to the flue gas maintained cultures.

Careful consideration was taken to determine the appropriate NaHCO<sub>3</sub> concentration in this study. Gardner et al. (2013), demonstrated that supplementing cultures of *Scenedesmus* sp. WC-1 with NaHCO<sub>3</sub> concentrations as low as 10 mM and 15 mM led to a delayed and complete cessation of the cell cycle, respectively, as well as induced greater TAG accumulation. Although, the addition of 5 mM NaHCO<sub>3</sub> allowed cells to continue to divide, and TAGs did not accumulate to the extent seen in the higher NaHCO<sub>3</sub> concentrations

(Gardner et al., 2013). Supplementing the culture with a low concentration of  $\text{NaHCO}_3$  is a viable option in the event of a power outage to not only maintain growth, but also to maintain the desired biochemical composition, especially in terms of protein for the development of bio-plastic.

Protein content remained high in all treatments, even though urea concentrations were already low when the flue gas was shut off, which is promising for plastic production from protein despite the power outage. Lipid content increased in all cultures by day 7, which was expected with the decreasing urea concentration and the addition of bicarbonate (Gardner et al., 2013). Although the lipid content in all treatments was 5% less than that seen in the flue gas cultures on day 7. In terms of the FAME composition and content, the bicarbonate treatments maintained a very similar profile to that of the cultures on day 4 in that the majority were saturated fatty acids. The high saturated fatty acid content was also reflected in the high cetane numbers in these treatments, which support the idea that *S. acutus* is still a good candidate for biofuel production even under this condition. The carbohydrate content in all treatments was approximately half of that of the flue gas cultures on day 7. This decrease in carbohydrate content as well as the decrease in  $\text{P}_{\text{gross}}:\text{R}$  could indicate that the cells were respiring some of their carbohydrate stores as a source of energy, possibly for CCM up-regulation under the low  $\text{CO}_2$  condition.

Biomass losses due to unplanned power outages could significantly add to operating costs. Therefore, it is necessary to develop standard operating procedures to maintain the health, productivity, and biochemical composition of the microalgae during these outages, especially as the frequency and severity of

storms are expected to increase that could lead to more frequent outages. This experiment demonstrated that switching from high to low CO<sub>2</sub> concentrations resulted in a lower biomass yield, and reduced lipid and carbohydrate content. However, adding solid NaHCO<sub>3</sub> to achieve a final concentration of 5 mM in the culture promoted greater biomass productivity than if the culture was solely supplemented with air. Cultures supplemented with NaHCO<sub>3</sub> also maintained high protein and saturated fatty acid content, as well as high cetane numbers which indicates bioplastic and biofuel could still be produced from the algal biomass even under this condition. The addition of solid NaHCO<sub>3</sub> is a viable option to maintain the health and biochemical composition of the algae in the event of a power outage

Table 1. Biomass productivity and specific growth rates of *S. acutus* during log phase growth when grown under air (0.04% CO<sub>2</sub>), 9% CO<sub>2</sub>, and simulated flue gas (9% CO<sub>2</sub>, 55 ppm NO, 25 ppm SO<sub>2</sub>). Values are means ± SD. Letters denote significant differences between treatments (p<0.05).

	Treatment		
	Air	9% CO <sub>2</sub>	Flue Gas
Productivity (g L <sup>-1</sup> d <sup>-1</sup> )	0.018±0.006 <sup>A</sup>	0.267±0.016 <sup>B</sup>	0.269±0.039 <sup>B</sup>
Specific growth rate (d <sup>-1</sup> )	0.217±0.087 <sup>A</sup>	0.389±0.021 <sup>B</sup>	0.307±0.020 <sup>C</sup>

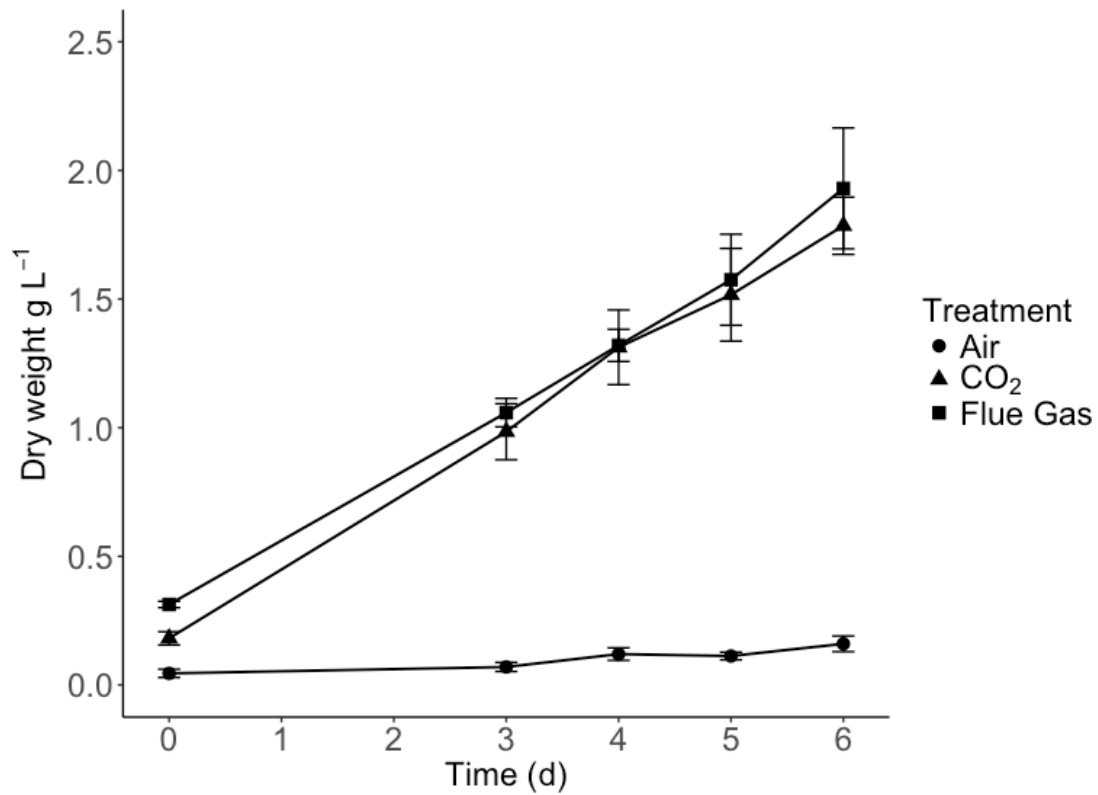


Figure 1. Growth of *S. acutus* cultures when grown under air (0.04% CO<sub>2</sub>), 9%CO<sub>2</sub>, and simulated flue gas (9% CO<sub>2</sub>, 55 ppm NO, 25 ppm SO<sub>2</sub>). Values are means ± SD.

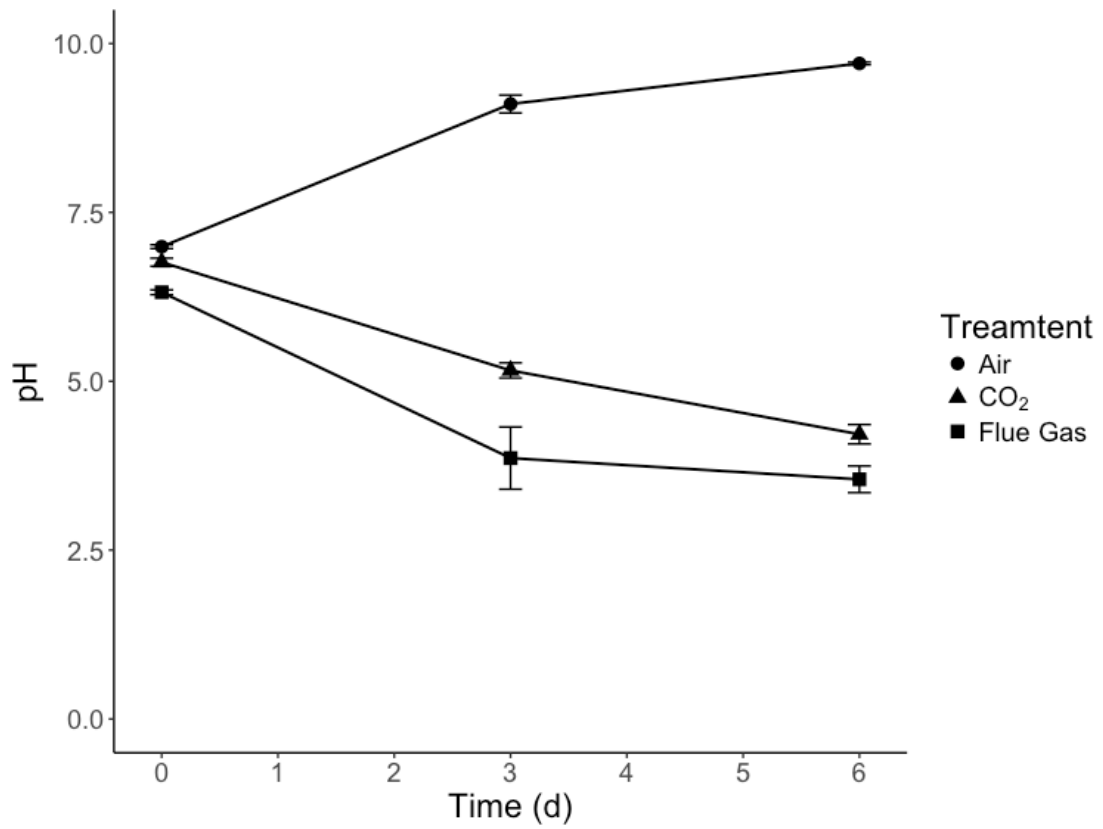


Figure 2. pH of *S. acutus* cultures when grown under air (0.04% CO<sub>2</sub>), 9%CO<sub>2</sub>, and simulated flue gas (9% CO<sub>2</sub>, 50 ppm NO, 25 ppm SO<sub>2</sub>). Values are means  $\pm$  SD.

Table 2. Concentrations of urea in *S. acutus* cultures when grown under air (0.04% CO<sub>2</sub>), 9%CO<sub>2</sub>, and simulated flue gas (9% CO<sub>2</sub>, 50 ppm NO, 25 ppm SO<sub>2</sub>). Values are means ± SD.

	Day		
	0	3	6
Air	1950.0 ± 35.3	660.5 ± 8.1	508.8 ± 61.9
9% CO <sub>2</sub>	1963.2 ± 88.9	122.2 ± 30.4	0
Flue Gas	1961.5 ± 20.8	133.3 ± 49.9	0

Table 3. Concentrations of phosphate in *S. acutus* cultures grown under air (0.04% CO<sub>2</sub>), 9%CO<sub>2</sub>, and simulated flue gas (9% CO<sub>2</sub>, 50 ppm NO, 25 ppm SO<sub>2</sub>). Values are means ± SD.

	Day		
	0	3	6
Air	736.7 ± 49.0	650.1 ± 42.4	326.0 ± 42.7
9% CO <sub>2</sub>	731.9 ± 99.0	462.2 ± 28.2	73.1 ± 27.2
Flue Gas	715.1 ± 87.1	487.4 ± 42.1	119.7 ± 41.8

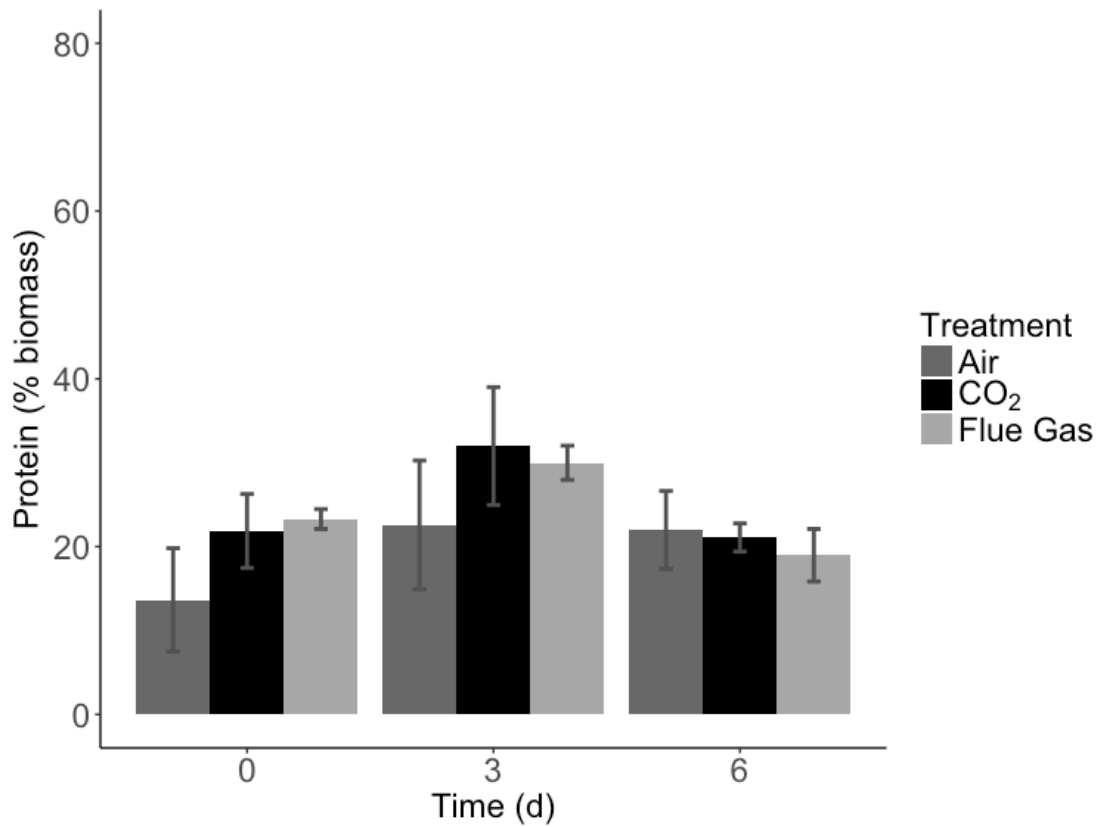


Figure 3. Protein content as a percentage of the total biomass in *S. acutus* grown under air (0.04% CO<sub>2</sub>), 9% CO<sub>2</sub>, and simulated flue gas (9% CO<sub>2</sub>, 55 ppm NO, 25 ppm SO<sub>2</sub>). Values are means ± SD.

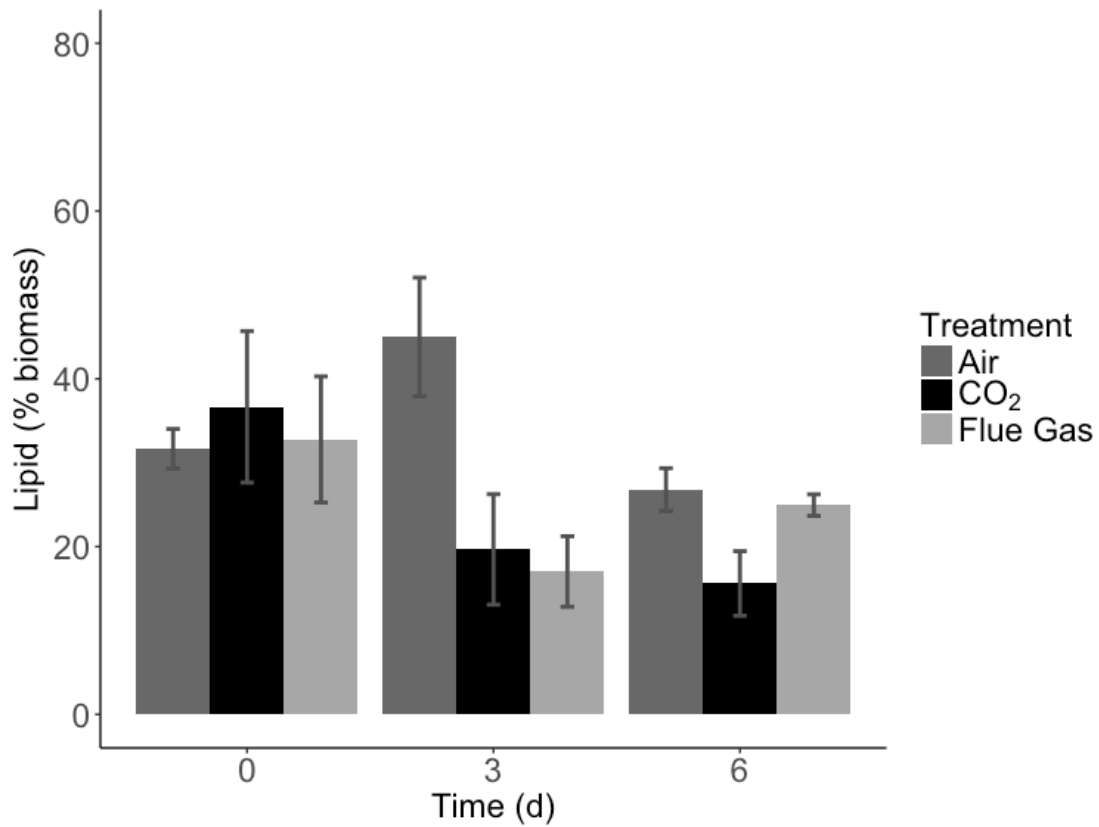


Figure 4. Total lipid content as a percentage of the total biomass in *S. acutus* grown under air (0.04% CO<sub>2</sub>), 9% CO<sub>2</sub>, and simulated flue gas (9% CO<sub>2</sub>, 55 ppm NO, 25 ppm SO<sub>2</sub>). Values are means  $\pm$  SD.

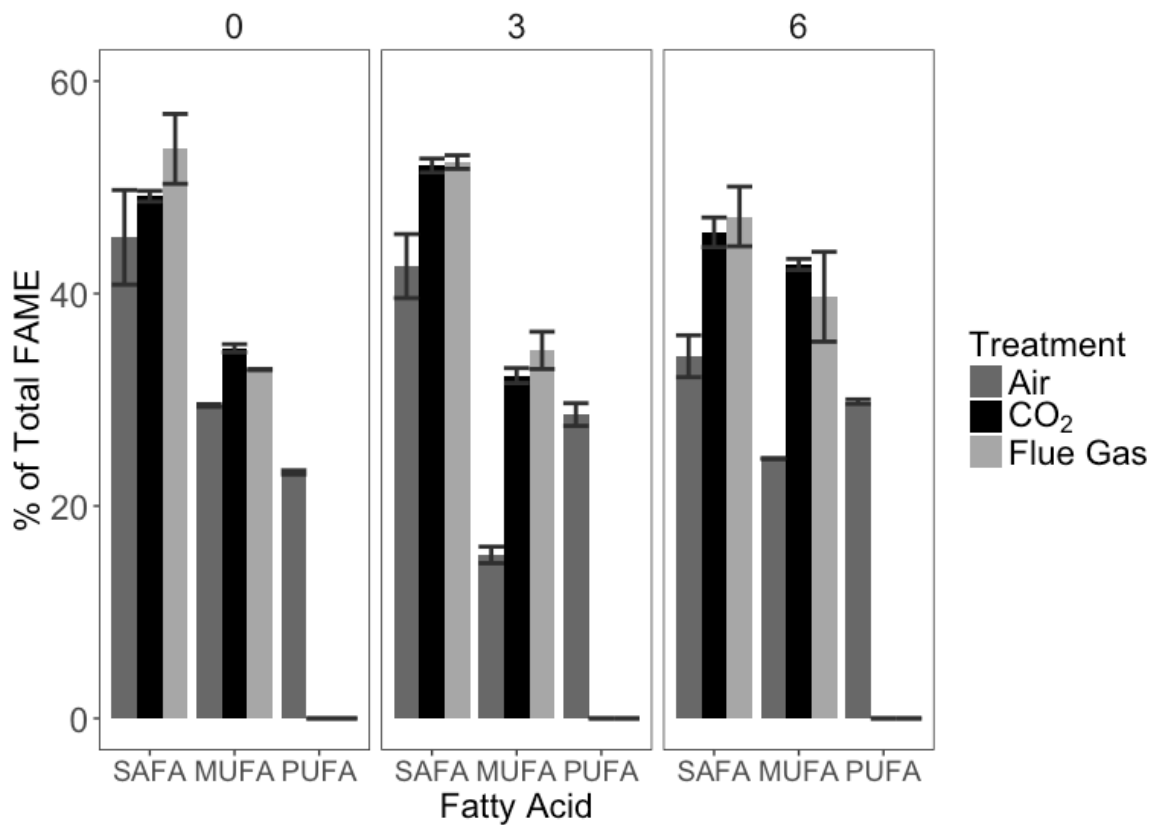


Figure 5. Saturated (SAFA), monounsaturated (MUFA), and polyunsaturated (PUFA) fatty acid content for *S. acutus* grown under air (0.04% CO<sub>2</sub>), 9% CO<sub>2</sub>, and simulated flue gas (9% CO<sub>2</sub>, 55 ppm NO, 25 ppm SO<sub>2</sub>). Values are percent means  $\pm$  SD of the total fatty acid methyl ester (FAME) content. Only fatty acids that contributed to 2% or more of the total FAME composition were included in the calculation of each fatty acid.

Table 4. Average cetane number for *S. acutus* FAME content grown under air, 9% CO<sub>2</sub>, and simulated flue gas (9% CO<sub>2</sub>, 55 ppm NO, 25 ppm SO<sub>2</sub>).

	0	3	6	Overall
Air	58	59	59	58
9% CO <sub>2</sub>	65	68	65	66
Flue Gas	65	68	66	66

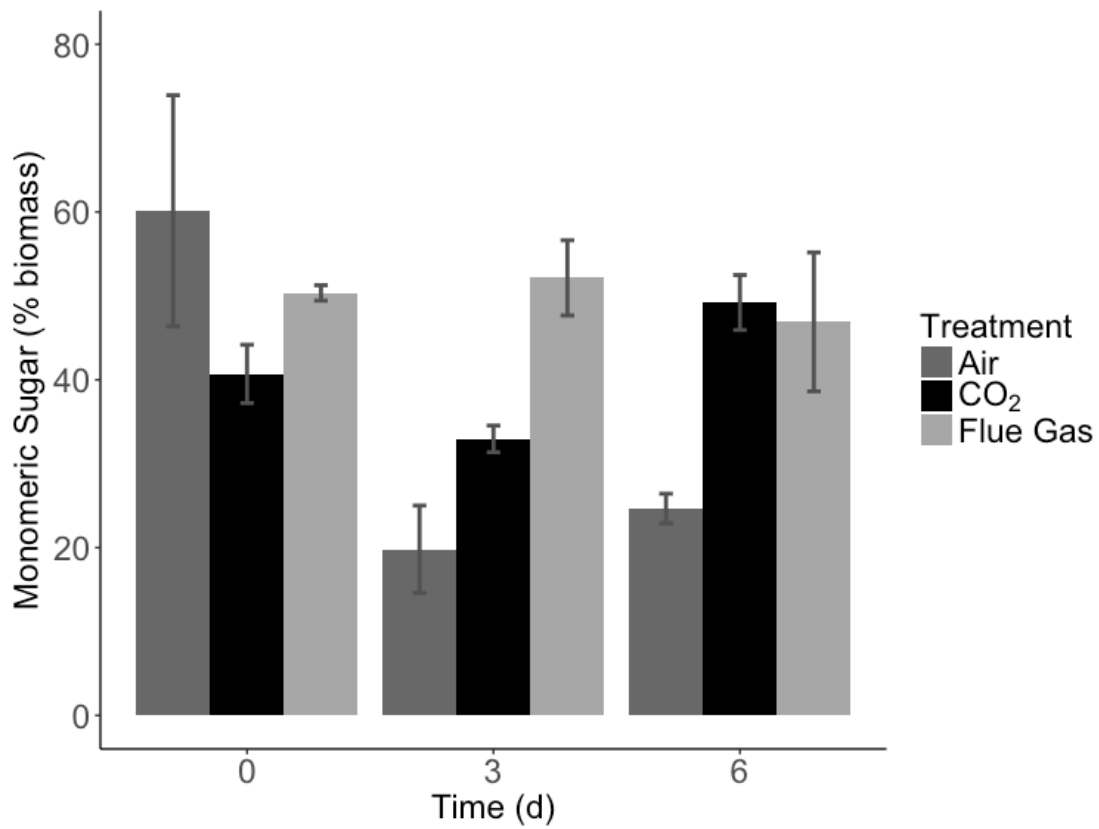


Figure 6. Total carbohydrate content as a percentage of the total biomass in *S. acutus* grown under air (0.04% CO<sub>2</sub>), 9% CO<sub>2</sub>, and simulated flue gas (9% CO<sub>2</sub>, 55 ppm NO, 25 ppm SO<sub>2</sub>). Values are means  $\pm$  SD.

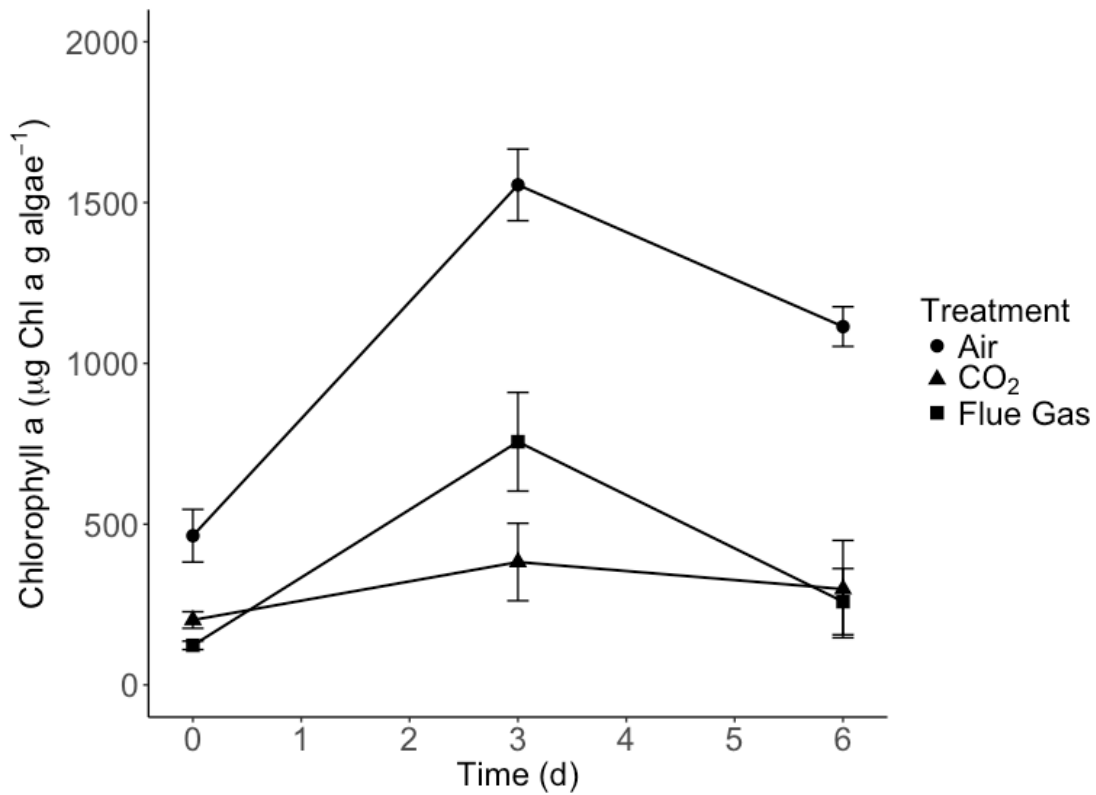


Figure 7. Chlorophyll a content per gram of algal biomass of *S. acutus* when grown under air (0.04% CO<sub>2</sub>), 9% CO<sub>2</sub>, and simulated flue gas (9% CO<sub>2</sub>, 55 ppm NO, 25 ppm SO<sub>2</sub>). Values are means  $\pm$  SD.

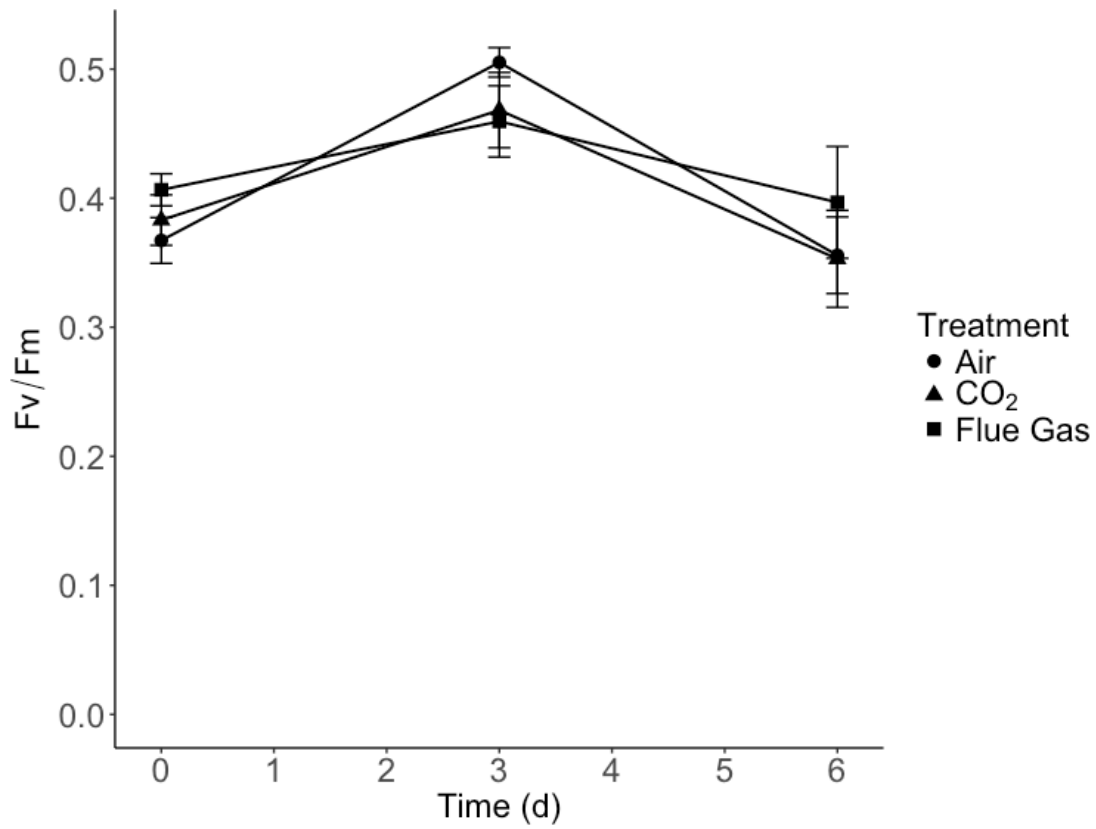


Figure 8. Maximum quantum yield of PSII (single turnover) of *S. acutus* when grown under air (0.04% CO<sub>2</sub>), 9% CO<sub>2</sub>, and simulated flue gas (9% CO<sub>2</sub>, 55 ppm NO, 25 ppm SO<sub>2</sub>). Values are means  $\pm$  SD.

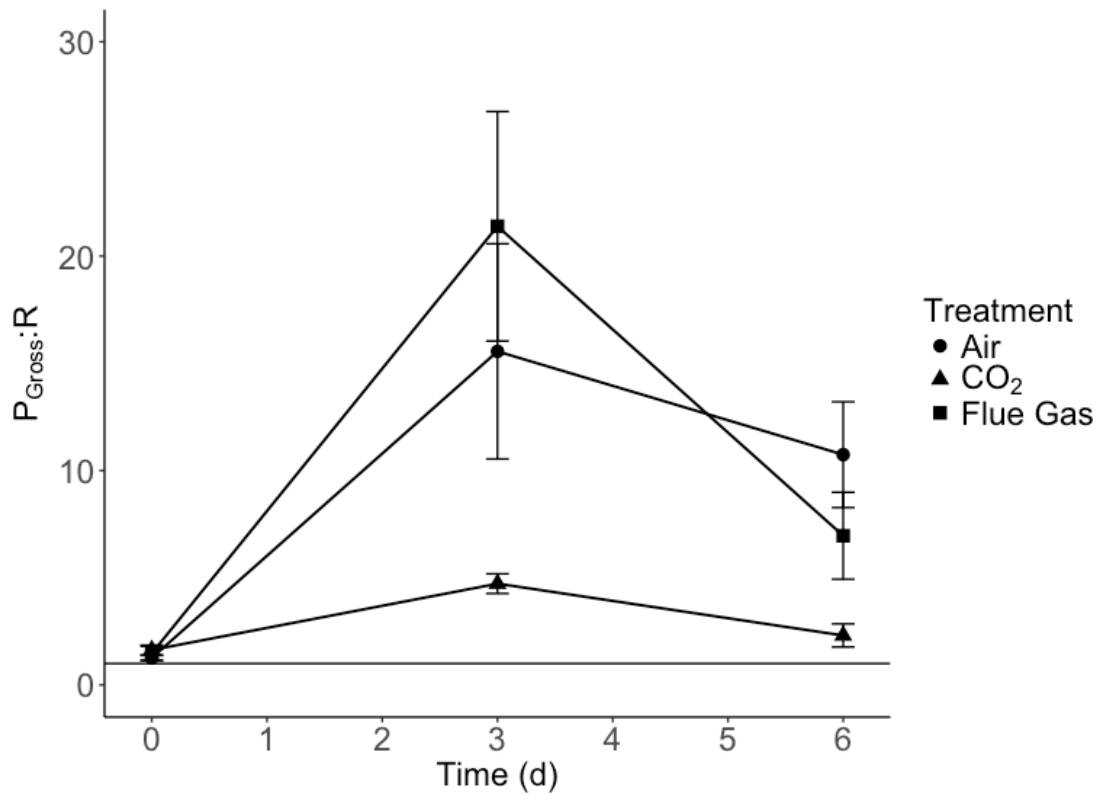


Figure 9. Gross photosynthesis to respiration ratios for *S. acutus* when grown under air (0.04% CO<sub>2</sub>), 9% CO<sub>2</sub>, and simulated flue gas (9% CO<sub>2</sub>, 55 ppm NO, 25 ppm SO<sub>2</sub>). Black solid line represents the 1:1 line. Values are means ± SD.

Table 5. Productivity and specific growth rates of *S. acutus* cultures maintained on flue gas compared to those amended with bicarbonate or air from days 4 to 7. Letters denote significant differences between treatments ( $p < 0.05$ ).

	Flue Gas	Air	Solid NaHCO <sub>3</sub>	NaHCO <sub>3</sub> Solution
Productivity (g L <sup>-1</sup> day <sup>-1</sup> )	0.260 ± 0.084 <sup>A</sup>	-0.028 ± 0.012 <sup>B</sup>	0.079 ± 0.02 <sup>C</sup>	0.048 ± 0.016 <sup>D</sup>
Specific growth rate (μ)	0.270 ± 0.027 <sup>A</sup>	-0.033 ± 0.042 <sup>B</sup>	0.061 ± 0.017 <sup>C</sup>	0.039 ± 0.013 <sup>D</sup>

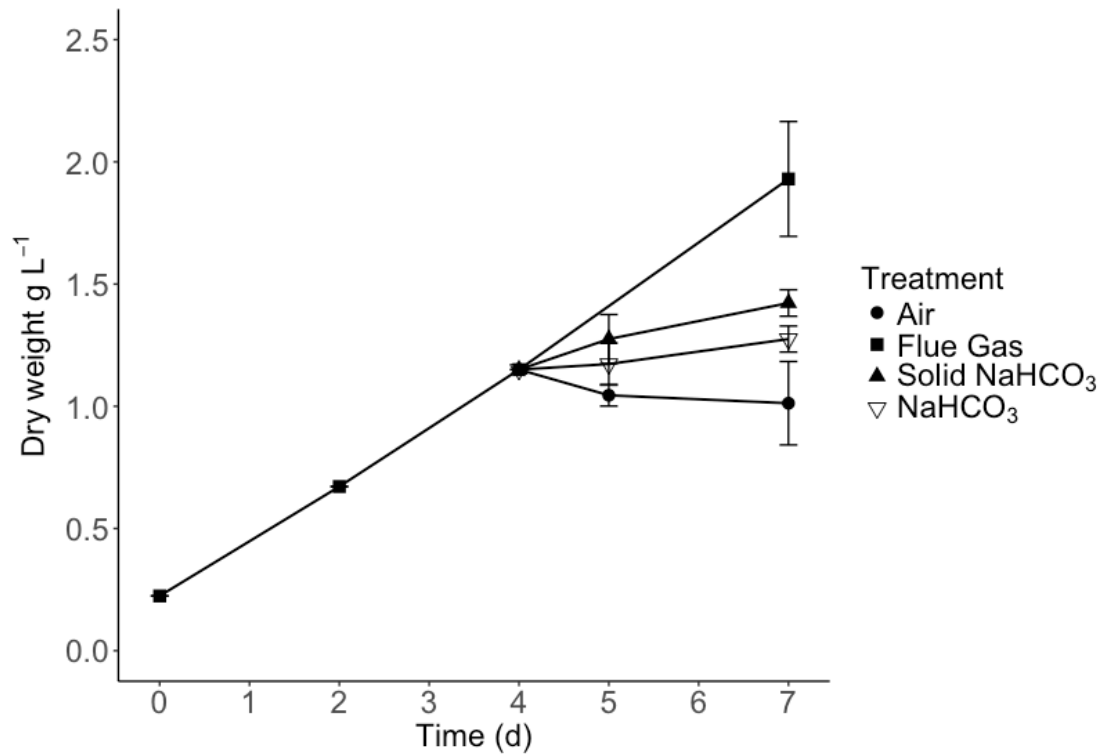


Figure 10. Growth of *S. acutus* cultures before and after flue gas was shut off and cultures were supplemented with bicarbonate or air. Values are means  $\pm$  SD. Arrow indicates when flue gas was shut off.

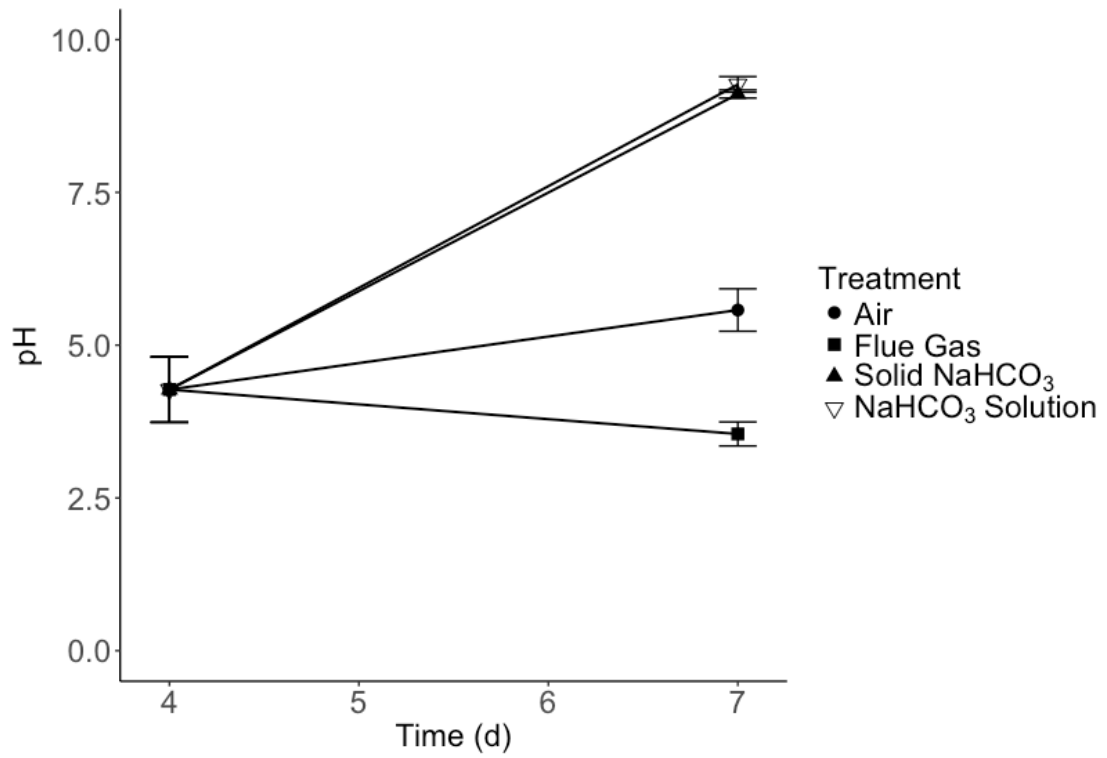


Figure 11. pH in *S. acutus* cultures before and after flue gas was shut off and cultures were supplemented with bicarbonate or air. Values are means  $\pm$  SD.

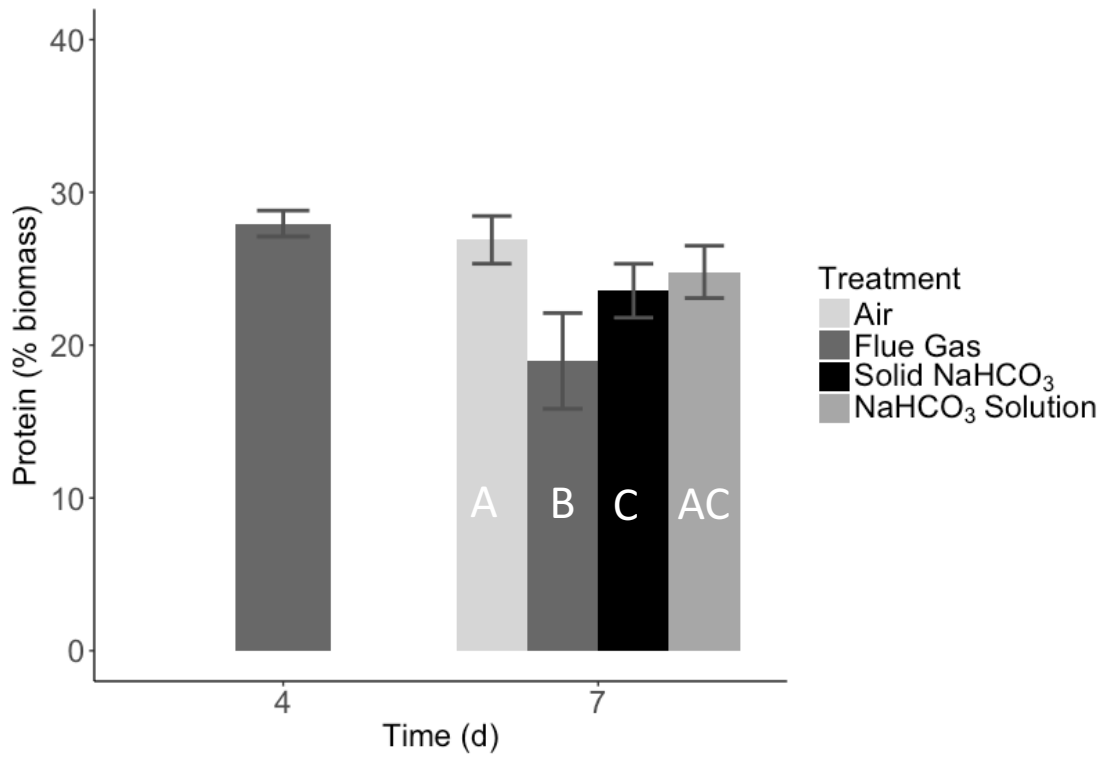


Figure 12. Protein content (% of biomass) in *S. acutus* before (day 4) and after (day 7) flue gas was shut off and cultures were supplemented with bicarbonate or air. Values are means  $\pm$  SD.

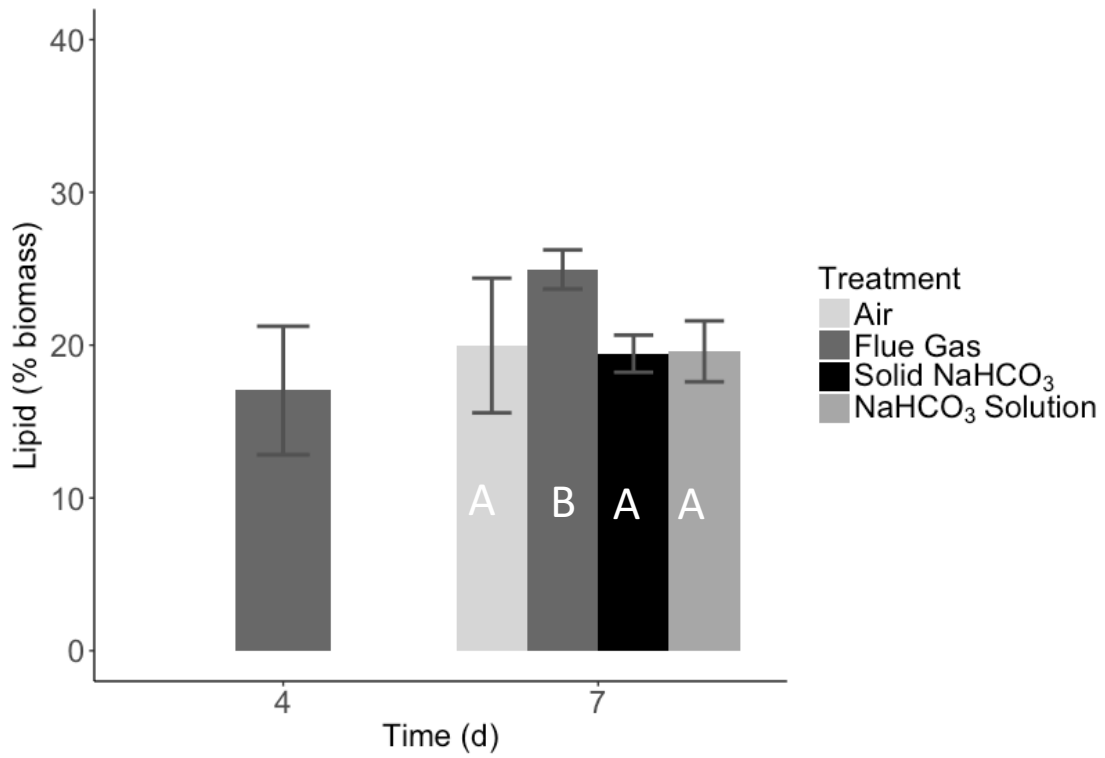


Figure 13. Lipid content (% of biomass) in *S. acutus* before and after flue gas was shut off and cultures were supplemented with bicarbonate or air. Values are means  $\pm$  SD.

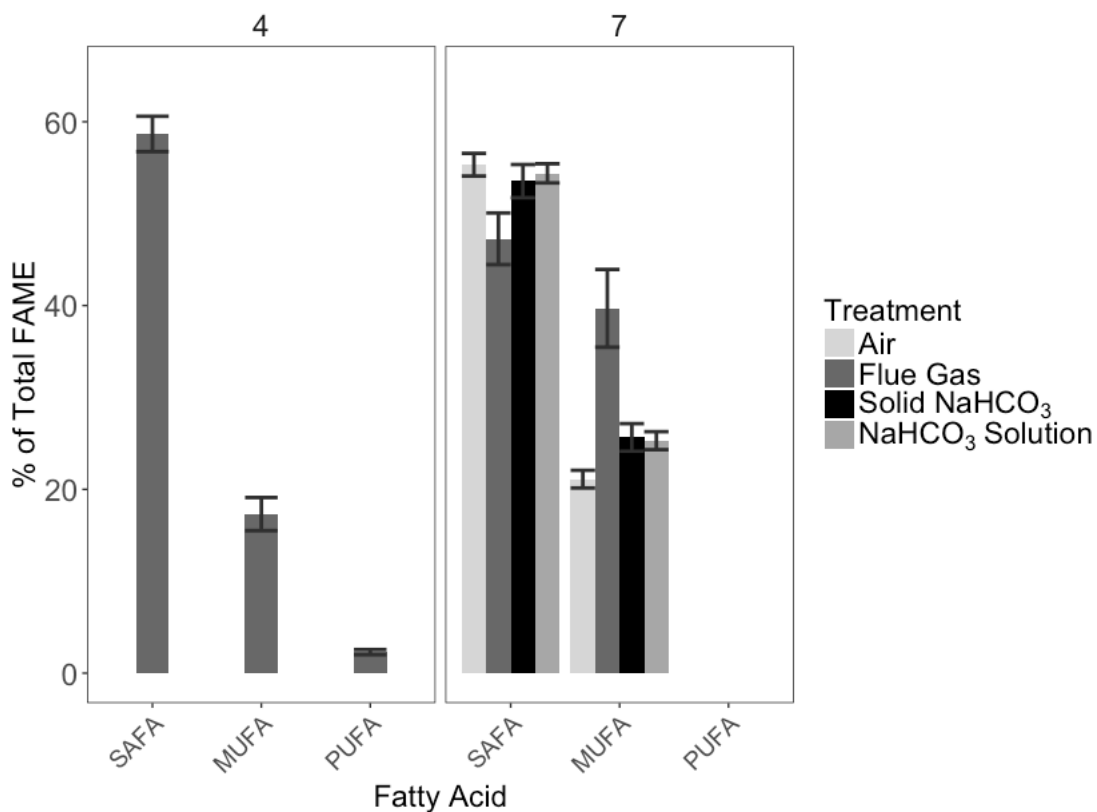


Figure 14. Saturated (SAFA), monounsaturated (MUFA), and polyunsaturated (PUFA) fatty acid content for *S. acutus* before and after flue gas was shut off and cultures were supplemented with bicarbonate or air. Values are percent means  $\pm$  SD of the total fatty acid methyl ester (FAME) content. Only fatty acids that contributed to 2% or more of the total FAME composition were included in the calculation of each fatty acid

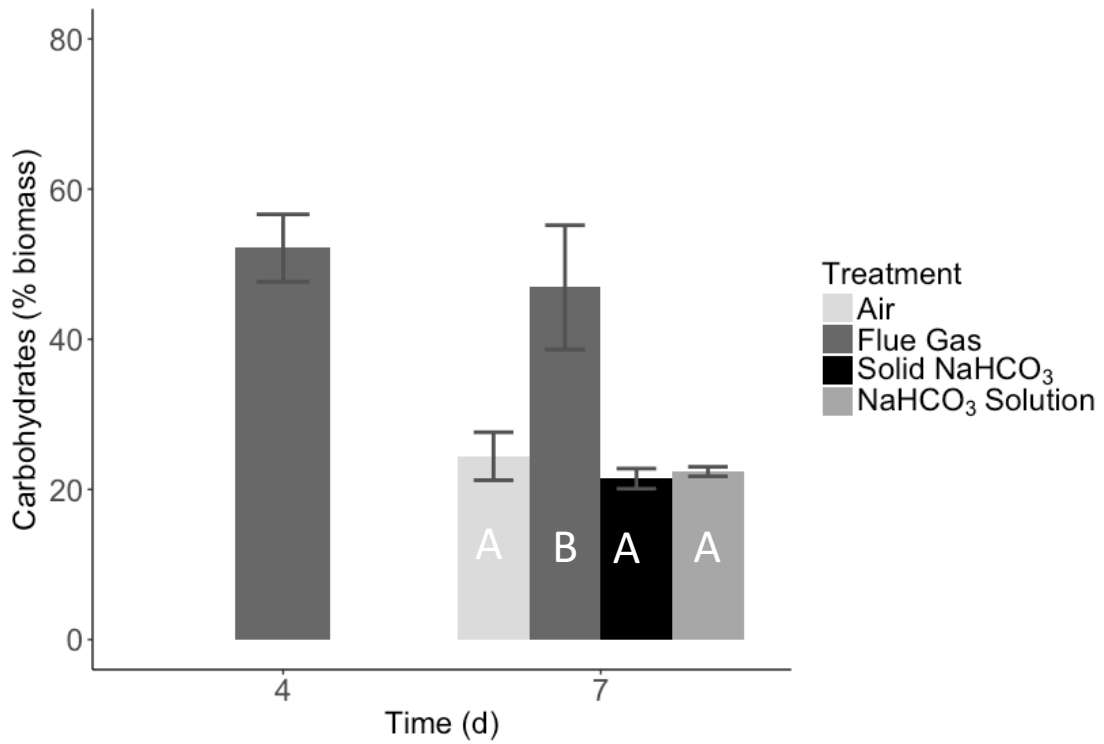


Figure 15. Carbohydrate content (% of biomass) in *S. acutus* before and after flue gas was shut off and cultures were supplemented with bicarbonate or air. Values are mean  $\pm$  SD.

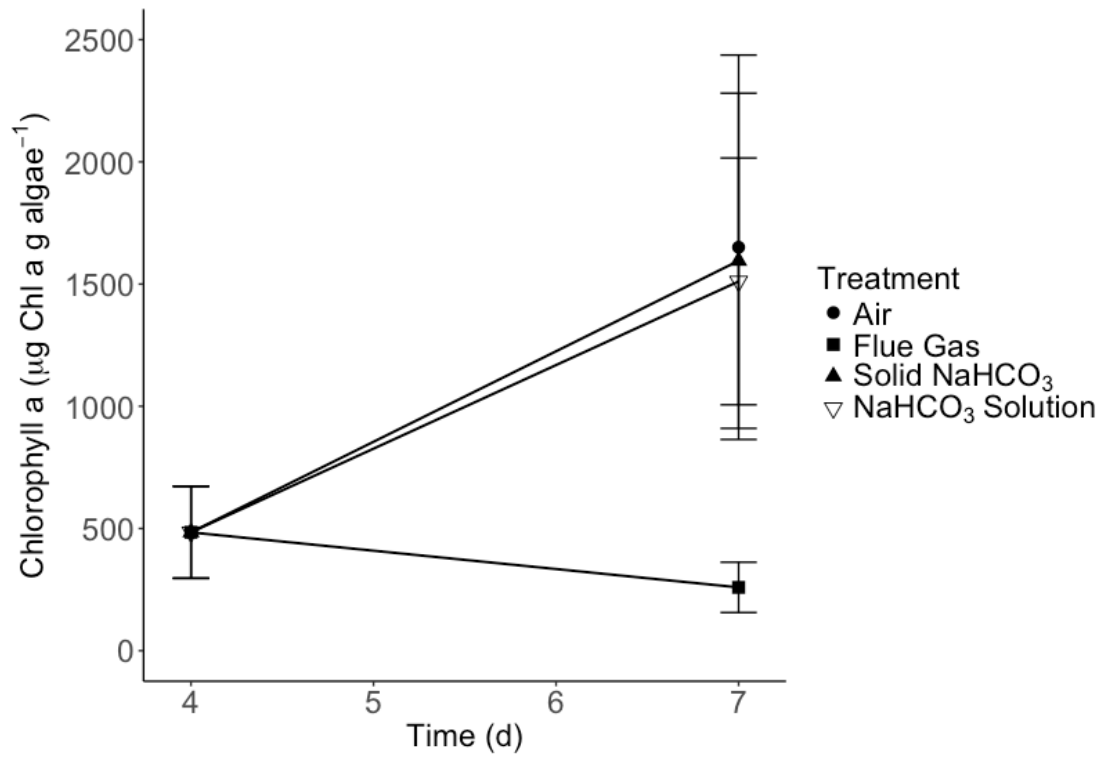


Figure 16. Chlorophyll a content of *S. acutus* normalized to grams of algal biomass before and after flue gas was shut off and cultures were supplemented with bicarbonate or air. Values are mean  $\pm$  SD.

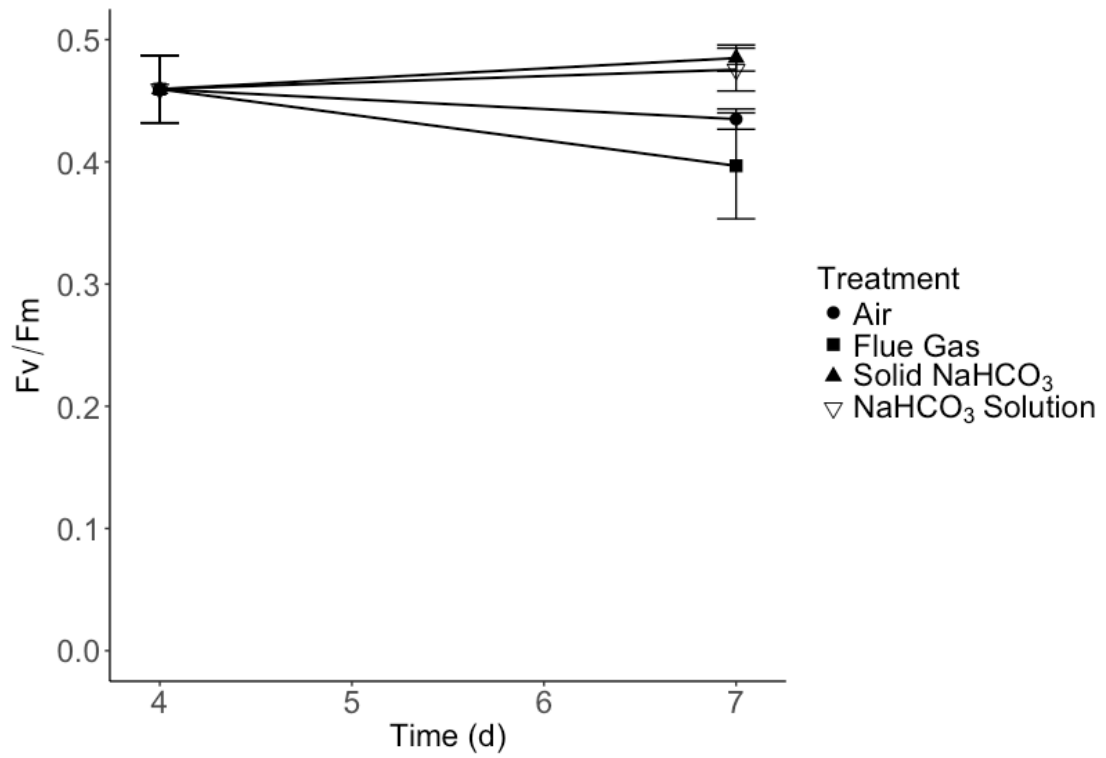


Figure 17. Maximum quantum yield of PSII (Fv/Fm) of *S. acutus* before and after flue gas was shut off and cultures were supplemented with bicarbonate or air. Values are mean  $\pm$  SD.

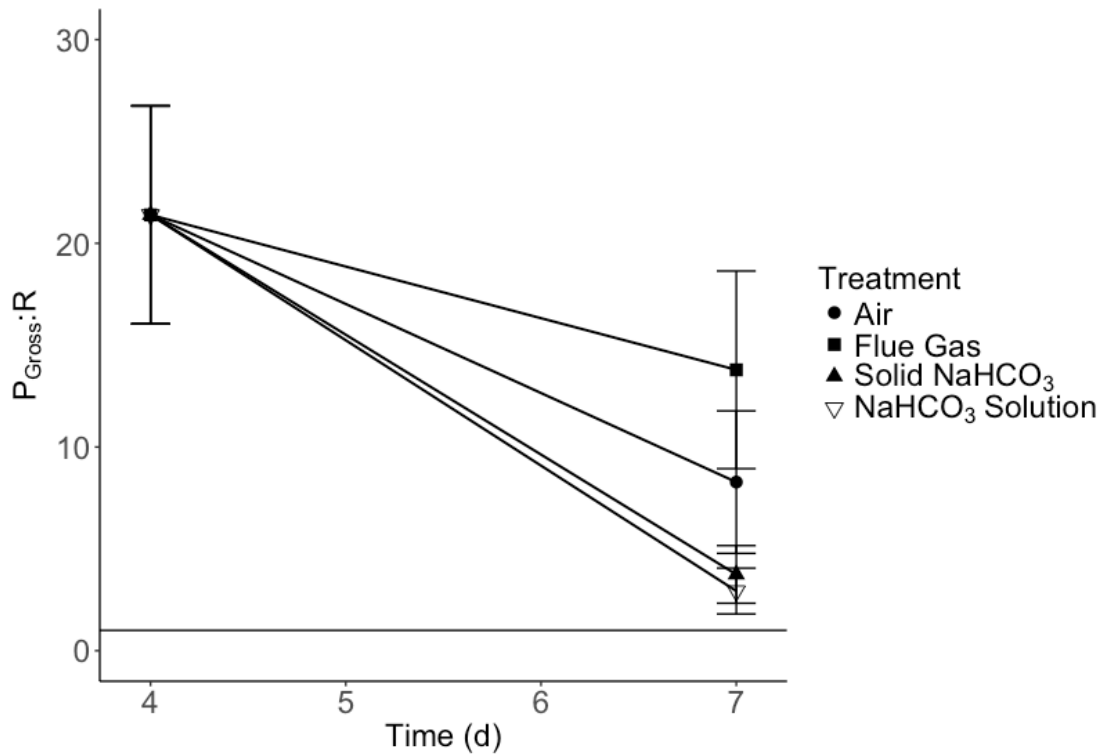


Figure 18. Gross photosynthesis to respiration ratios (P:R) for *S. acutus* before and after flue gas was shut off and cultures were supplemented with bicarbonate or air. Black solid line represents the 1:1 line. Values are means  $\pm$  SD.

## REFERENCES

- ASTM. 2002. D 6751-Standard Specification for Biodiesel Fuel (B100) Blend Stock for Distillate Fuels. American Society for Testing and Materials International, West Conshohocken, Penn.
- Bhatti S, Colman B. 2008. Inorganic carbon acquisition in some synurophyte algae. *Physiol Plant*. 133(1): 33-40.
- Borowitzka, M, Beardall J, Raven J A. 2016. *The Physiology of Microalgae*. Springer International Publishing.
- British Petroleum Company. 2017. BP Statistical Review of World Energy. BP Press
- Chen, TM, Gokhale J., Shofer S., Kushner WG. 2007. Outdoor air pollution: nitrogen dioxide, sulfur dioxide, and carbon monoxide health effects. *Am J Med Sci*. 333(4): 249-56.
- Cheng, Yu-Shen, Yi Zheng, and Jean VanderGheynst. 2011. Rapid Quantitative Analysis of Lipids Using a Colorimetric Method in a Microplate Format. *Lipids* 46: 95-103
- Crofcheck C, E X, Shea A, Montross M, Crocker M, Andrews R. 2012. Influence of media composition on the growth rate of *Chlorella vulgaris* and *Scenedesmus acutus* utilized for CO<sub>2</sub> mitigation. *J Biochem Tech*. 4(2): 589-594.
- Folch J, Lees M, Sloane Stanley G H. 1957. A simple method for the isolation and purification of total lipids from animal tissues. *J Biol Chem*. 226(1): 497-509.
- Gardner R D, Lohman E J, Cooksey K E, Gerlach R, Peyton B M. Cellular cycling, carbon utilization, and photosynthetic oxygen production during bicarbonate-induced triacylglycerol accumulation in a *Scenedesmus* sp. *Energies*. 6: 6060-6076.
- Gehl K A, Colman B. 1985. Effect of external pH on the internal pH of *Chlorella saccharophila*. *Plant Physiol*. 77: 917-921.
- Gerloff-Elias A, Spijkerman E, Proschold T. 2005. Effect of external pH on the growth, photosynthesis and photosynthetic electron transport of

- Chlamydomonas acidophila* Negoro, isolated from an extremely acidic lake (pH 2.6). *Plant, Cell and Environment*. 28: 1218-1229.
- Goldman J C, Azov Y, Riley C B, Dennett M R. 1982. The effect of pH in intensive microalgal cultures. I. Biomass regulation.
- Hanagata N, Takeuchi T, Fukuju Y. 1992. Tolerance of microalgae to high CO<sub>2</sub> and high temperature. *Phytochemistry*. 31(10): 3345-3348.
- Huang G, Wang J, Kuang Y, He H. Effects of SO<sub>2</sub> and NO<sub>2</sub> in flue gas on CO<sub>2</sub> sequestration and intracellular microstructures analysis of *Chlorella* sp. *Research and Reviews: Journal of Microbiology and Biotechnology*. 5(3): 60-67.
- Ji M, Yun H, Hwang J, Salama E, Jeon B, Choi J. 2017. Effect of flue gas CO<sub>2</sub> on the growth, carbohydrate and fatty acid composition of a green microalga *Scenedesmus obliquus* for biofuel production. *Environmental Technology*. 38(16): 2085-2092.
- Jiang, Y, Zhang W, Wang J, Chen Y, Shen S, Liu T. 2013. Utilization of simulated flue gas for cultivation of *Scenedesmus dimorphus*. *Bioresource Technology*. 128: 359-364.
- Juneja A, Ceballos R M, Murthy G S. 2013. Effects of environmental factors and nutrient availability on the biochemical composition of algae for biofuels production: a review. *Energies*. 6: 4607-4638.
- Lane A E, Burris J E. Effects of environmental pH on the internal pH of *Chlorella pyrenoidosa*, *Scenedesmus quadricauda*, and *Euglena mutabilis*. *Plant Physiol*. 68: 439-442.
- Laurens L M L, Nagle N, Davis R, Sweeney N, Van Wychen S, Lowell A, Pienkos P T. 2015. Acid-catalyzed algal biomass pretreatment for integrated lipid and carbohydrate-based biofuels production. *Green Chemistry*. 17: 1145.
- Lee J S, Kim D K, Lee J P, Park S C, Koh J H, Cho H S, Kim S W. 2002. Effects of SO<sub>2</sub> and NO on growth of *Chlorella* sp. KR-1. *Bioresource Technology*. 82: 1-4.
- Maeda K, Owada M, Kimura N, Omata K, Karube I. 1995. CO<sub>2</sub> fixation from the flue gas on coal-fired thermal power plant by microalgae. *Energy Conversion and Management*. 36(6-9): 717-720.

- Matsumoto H, Hamasaki A, Sioji N, Ikuta Y. 1997. Influence of CO<sub>2</sub>, SO<sub>2</sub>, and NO in flue gas on microalgae productivity. *J Chem. Eng. Jpn.* 30:620-624.
- Mortensen L M, Gislerød H R. The growth of *Chlorella sorokiniana* as influenced by CO<sub>2</sub>, light, and flue gas. *J Appl Phycol.* 28: 813-820.
- Mudimu O, Rybalka N, Bauersachs T, Friedl T, Schulz R. Influence of different CO<sub>2</sub> concentrations on microalgae growth,  $\alpha$ -tocopherol content and fatty acid composition. *Geomicrobiology Journal.* 32: 291-303.
- Nagase H, Yoshihara K I, Eguchi K, Yokota Y, Matsui R, Hirata K, Miyamoto K. 1997. Characteristics of biological NO<sub>x</sub> removal from flue gas in a *Dunaliella tertiolecta* culture system. *Journal of Fermentation and Bioengineering.* 83(5): 461-465.
- Papazi, A, Makridis P, Divanach P, Kotzabasis K. 2008. Bioenergetic changes in the microalgal photosynthetic apparatus by extremely high CO<sub>2</sub> concentrations induce an intense biomass production. *Physiologia Plantarum.* 132: 338-349.
- Santillan-Jimenez E, Pace R, Marques S, Morgan T, McKelphin C, Mobley J, Crocker M. Extraction, characterization, purification and catalytic upgrading of algae lipids to fuel-like hydrocarbons. *Fuel.* 180: 668-678.
- Sarat, CT, Deepak RS, Maneesh KM, Mukherji S, Chauhan VS, Sarada R, Mudliar SN. 2016. Evaluation of indigenous fresh water microalga *Scenedesmus obtusus* for feed and fuel applications: Effect of carbon dioxide, light and nutrient sources on growth and biochemical characteristics. *Bioresource Technology.* 207:430-439.
- Sayre, R. 2010. Microalgae: The potential for carbon capture. *BioScience* 60(9): 722-727.
- Singh RS, Pandey A, Gnansounou E. 2016. *Biofuels: Production and Future Perspectives.* CRC Press.
- Solovchenko A, Khozin-Goldberg I. High-CO<sub>2</sub> tolerance in microalgae: possible mechanisms and implication for biotechnology and bioremediation. *Biotechnology Letters.* 35: 1745-1752.
- Taylor AR, Brownlee C, Wheeler GL. 2012. Proton channels in algae: reasons to be excited. *Trends in Plant Science.* 17(11): 675-684.

- Templeton DW, Laurens LML. 2015. Nitrogen-to-protein conversion factors revisited for applications of microalgal biomass conversion to food, feed and fuel. *Algal Research*. 11: 359-367.
- US DOE. 2010. National Algal Biofuels Technology Roadmap. US Department of Energy, Office of Energy Efficiency and Renewable Energy, Biomass Program.
- Van Wychen S, Laurens LML. 2015. Determination of Total Carbohydrates in Algal Biomass. NREL/TP-5100-60957. Golden, CO: National Renewable Energy Laboratory.
- Van Wychen S, Ramirez K, Laurens LML. 2015. Determination of Total Lipids as Fatty Acid Methyl Esters (FAME) by in situ Transesterification. NREL/TP-5100- 60958. Golden, CO: National Renewable Energy Laboratory.
- Walsh, J, Wuebbles D, Hayhoe K, Kossin J, Kunkel K, Stephens G, Thorne P, Vose R, Wehner M, Willis J, Anderson D, Doney S, Feely R, Hennon P, Kharin V, Knutson T, Landerer F, Lenton T, Kennedy J, Somerville J. 2014. Chapter. 2: Our Changing Climate. *Climate Change Impacts in the United States: The Third National Climate Assessment*, J. M. Melillo, Terese (T.C.) Richmond, and G. W. Yohe, Eds., U.S. Global Change Research Program, 19-67.
- Wang B, Li Y, Wu N, Lan CQ. 2008. CO<sub>2</sub> bio-mitigation using microalgae. *Appl Microbiol Biotechnol*. 79(5):707-718.
- Wilson MH, Groppo J, Placido A, Graham S, Morton III S A, Santillan-Jimenez E, Shea A, Crocker M, Crofcheck C, Andrews R. 2014. CO<sub>2</sub> recycling using microalgae for the production of fuels. *Applied Petrochemical Research*. 4(1): 41-53.
- Xia J, Gong S, Jin X, Wan M, Nie Z. 2013. Effects of simulated flue gases on growth and lipid production of *Chlorella sorokiniana* CS-01. *J Cent South Univ*. 20: 730-736.
- Yang Y, Gao K. 2003. Effects of CO<sub>2</sub> concentrations on the freshwater microalgae, *Chlamydomonas reinhardtii*, *Chlorella pyrenoidosa* and *Scenedesmus obliquus* (Chlorophyta). *J Appl Phycol*. 00:1-11.

Yen HW, Ho SH, Chen CY, Chang JS. 2015. CO<sub>2</sub>, NO<sub>x</sub> and SO<sub>x</sub> removal from flue gas via microalgae cultivation: a critical review. *Biotechnol J.* 10(6): 829-839.

Zawada RJ, Kwan P, Olszewski KL, Llinas M, Huang SG. 2009. Quantitative determination of urea concentrations in cell culture medium. *Biochem. Cell Biol.* 87: 541-544

## Chapter 3

### INFLUENCE OF NITROGEN SOURCE ON GROWTH AND BIOMASS COMPOSITION OF *SCENEDESMUS ACUTUS*

#### 3.1 Abstract

The high production costs of growing algae for carbon capture and reuse from industrial flue gas sources has prohibited the process from being cost-effective when developing commodity products from the biomass. Continuously supplying the cultures with nitrogen contributes to these production costs. This study investigated the growth and biochemical composition of *Scenedesmus acutus* when using sodium nitrate versus urea, a much cheaper source of nitrogen, under several gas compositions (e.g. air, 9% CO<sub>2</sub>, and simulated flue gas). The cultivation conditions used in this experiment approximated those used in outdoor pilot studies of *S. acutus* in order to determine which N source is the most appropriate for optimizing *S. acutus* growth for CO<sub>2</sub> mitigation at a coal-fired power plant. Urea supported greater biomass productivity and protein content as well as high cetane numbers which is ideal for carbon capture and the production of bio-plastic and biofuel, respectively. From these results and the fact that it is more economical, urea is the most appropriate N source for large-scale cultivation of *S. acutus* for carbon capture and reuse at a coal-fired power plant.

### 3.2 Introduction

Large scale algae cultivation for capturing carbon in industrial flue gas sources and the subsequent development of commodity products from the biomass is not yet a cost-effective process (Wilson et al., 2014). There are operating costs associated with growing the biomass, particularly with supplying nutrients. Aside from carbon, which is supplied in the flue gas stream, prominent nutrients including nitrogen and phosphorous, must be continuously amended to the culture medium. Nitrogen (N) is of particular interest in applied algal research as many studies have found that manipulation of the N source and concentration can increase lipid accumulation in commercially relevant algal strains such as *Chlorella* sp., *Nannochloropsis* sp., and *Scenedesmus* sp. which is ideal for biofuel production (Fakhry and El Maghraby 2015, Lin and Lin 2010, Sunja et al., 2011).

Many eukaryotic microalgae are known to use a variety of N sources, both organic and inorganic, although any differences in biomass productivity and biochemical composition of algae using different N sources are often strain-specific and influenced by other abiotic factors including light and temperature (Borowitzka et al., 2016). *Scenedesmus acutus* (*S. acutus*), a freshwater chlorophyte, is currently being evaluated for carbon capture and reuse at a coal-fired power plant in Kentucky (Wilson et al., 2014, Wilson et al., 2016). To improve the cost effectiveness of the carbon capture process, urea was investigated as a cheaper alternative to nitrate (Chrofcheck et al., 2012). Crofcheck et. al (2012) compared growth rates of *S. acutus* cultured under 5% CO<sub>2</sub> using M-8 media amended with either potassium nitrate or urea and found that *S. acutus* growth rates were not significantly different. From this result and

subsequent experiments, they were able to refine a urea-based media recipe to use the least amount of urea, thus minimizing cost while still promoting maximal algal productivity. However, a preliminary study in our laboratory indicated that *S. acutus* grew better using sodium nitrate when grown in 9% CO<sub>2</sub>, which prompted a more comprehensive study that approximated cultivation conditions used in outdoor pilot studies at Duke Energy's East Bend Station in Boone County, Kentucky.

N is required for amino acid and ultimately protein synthesis, and microalgae have relatively high N requirements, as some species are composed of up to 50% protein by weight (Falkowski and Raven 2007). In order to be assimilated into cellular constituents, all forms of N must first be reduced to ammonium or ammonia (NH<sub>4</sub><sup>+</sup>, NH<sub>3</sub>). This is done through two different pathways for nitrate and urea. Nitrate assimilation requires several types of energy dependent transporters and two enzymes, nitrate reductase and nitrite reductase, which both require photosynthetically derived NADH as well as Fe and Mo cofactors (Falkowski and Raven 2007). Urea also requires active transport into the cell and in many microalgae and it is metabolized by the urease enzyme; however, Leftely and Syrett (1973) noted that the chlorophytes (including *Scenedesmus* sp.) lack a urease gene, and instead utilize the urea amidolyase enzyme complex (UALase). For other chlorophytes, such as *Chlamydomonas reinhardtii* that the UALase complex requires two distinct enzymes, urea carboxylase and allophanate hydrolase, which require ATP and Mg<sup>2+</sup> and K<sup>+</sup> cofactors to generate ammonia and bicarbonate (Solomon et al., 2010, Leftely and Syrett 1973). The high energy requirements of these enzymes

may have significant implications for the growth of the microalgae, since energy resources may be redirected to N assimilation at the expense of CO<sub>2</sub> fixation and biomass production.

The present study compares the growth and biochemical composition of *S. acutus* under different nitrogen sources (e.g. urea, sodium nitrate) under several gas compositions, including air, 9% CO<sub>2</sub>, and simulated flue gas (9% CO<sub>2</sub>, 55 ppm NO, 25 ppm SO<sub>2</sub>). Additionally, the cultures were grown under a higher irradiance and temperature than most laboratory studies that have investigated N source on growth of *Scenedesmus* sp. thus far (Vasileva et al., 2015, Arumugan et al., 2013, Crofcheck et al., 2012). These results will allow us to determine which N source is the most appropriate for optimizing *S. acutus* growth for CO<sub>2</sub> mitigation.

### **3.3 Methods**

#### **3.3.1 Cultivation setup**

The media components and concentrations used in this experiment were based on an original urea-based recipe (Table 6, Crofcheck et al., 2012). All components were agriculture grade except for the sodium nitrate, which was ACS reagent grade. Nitrogen sources were equalized based on moles of nitrogen. The media was adjusted with 0.5M NaOH to bring the pH to approximately 7.0 at the start of the experiment.

*S. acutus* UTEX-B72 was obtained from the Culture Collection of Algae at the University of Texas at Austin. Stock cultures were acclimated to their respective media for three generations. The cultures were grown in 500 mL

glass Hybex bottles at 33°C under 10W Daylight 6000K LED lights (Fulight, Santa Ana, CA, USA) at an average intensity of 400  $\mu\text{mol photons m}^{-2} \text{ s}^{-1}$  on a 16:8 light:dark cycle. Cultures were positioned around the perimeter of a 15-position digital magnetic stirrer (RO 15, IKA, Staufen im Breisgau, Germany), and the alga was kept in continuous suspension by a 30 mm stir bar set to 110 rpm. All culture vessels were fitted with PTFE tubing for aeration with one of three gases, air ( $\sim 0.04\%$   $\text{CO}_2$ ), 9%  $\text{CO}_2$  balanced in  $\text{N}_2$ , or simulated flue gas which consisted of 9%  $\text{CO}_2$ , 55 ppm  $\text{NO}$ , 25 ppm  $\text{SO}_2$ , balanced in  $\text{N}_2$  (Keene Gas, Dover, DE, USA). Flow was controlled for each replicate by individual 65-mm correlated flowmeters and maintained at a flow rate of 2.3-2.5  $\text{mL min}^{-1}$  (Cole Parmer, Vernon Hills, IL, USA). Both treatments had four replicates grown under each gas composition. To begin the experiment, the appropriate volume of each stock culture was centrifuged at 3000 rpm for 2 minutes, then resuspended in 400 mL of fresh media to obtain a biomass density of about 0.2-0.3  $\text{g L}^{-1}$ . Both N treatments had four replicates per gas source. Note that both treatments grown under air did not accumulate enough biomass during the acclimation period to have a starting biomass of 0.2  $\text{g L}^{-1}$ . The initial biomass densities when grown in air were  $0.08 \pm 0.02 \text{ g L}^{-1}$  and  $0.05 \pm 0.01 \text{ g L}^{-1}$  in the sodium nitrate and urea treatments, respectively.

### **3.3.2 Growth measurements**

All cultures were grown in batch for a period of six days. Growth was monitored using oven dry weight (ODW) by filtering 10 mL of cultures on a pre-weighted 47 mm Grade C Sterlitech glass fiber filter, drying at 100°C, then re-weighing the dry filter. Productivity for each treatment was measured using

regression analysis of the ODW taken on days 0, 3, 4, 5, and 6. Specific growth rates were calculated for each treatment using Equation 1 (see section 2.2.2). pH was measured using a standard benchtop meter on days 0, 3, and 6 of the experiment.

Nitrate and phosphate concentrations were determined using a Seal Nutrient Auto-analyzer. Briefly, samples were taken on days 0, 3, and 6, centrifuged at 5000 rpm for 10 min and the supernatant was decanted into 20 mL plastic scintillation vials. Urea concentrations were determined colorimetrically based on a method by Zawada et al. 2009.

### **3.3.3 Biomass Characterization**

To determine the breakdown of total carbohydrates, total lipids, fatty acid methyl ester (FAME) composition, and protein content for each treatment, about 100 mL of sample was pelleted by centrifugation (10 min, 5,000 rpm), freeze-dried and homogenized. Total nitrogen content was determined by CHN elemental analysis (ECS 4010 CHNSO Analyzer, Costech Analytical Technologies, INC., Valencia, CA), and protein content was subsequently calculated using the N-to-protein conversion factor 4.78 (Templeton and Laurens 2015). Lipids were first extracted using chloroform and methanol (Folch et al., 1957) and quantified colorimetrically using a sulfo-phospho-vanillin method (Cheng et al., 2011). To determine the FAME composition, the fatty acids are first separated from triacylglycerols and bonded to a methyl group through acid-catalyzed transesterification. FAME were then extracted with hexane, then identified and quantified as a percentage of the total FAME using gas chromatography on Agilent Technologies 7890B GC system (Santa Clara,

CA) (Van Wychen, Ramirez, and Laurens 2013). Cetane numbers were calculated from the FAME content using equations in Islam et al. (2013). Total carbohydrate content was determined by a two-step sulfuric acid hydrolysis to break down the carbohydrates into monomers, which were then complexed with MBTH and quantified spectrophotometrically using a FLUOstar Omega plate reader (BMG Labtech, Offenburg, Germany) (Van Wychen and Laurens, 2015). All biochemical components were represented as a percentage of total biomass.

### **3.3.4 Photochemical Measurements**

Chlorophyll a concentration was determined on days 0, 3, and 6 by filtering 5 mL of culture onto a Sterlitech Grade C 25mm filter and extracting the pigment in 90% acetone at -20°C in the dark overnight. Chlorophyll a concentration was measured using a 10-AU Turner Fluorometer (Turner Designs, Sunnyvale, California) and normalized to grams of algae biomass. On days 0, 3, and 6 samples were dark acclimated for 20 min, and the single turnover maximum quantum yield of photosystem II ( $F_v/F_m$ ) was measured by a fast repetition rate fluorometer (FRRf) (Chelsea Technologies Group Ltd, West Molesey, UK) set to deliver 50  $\mu$ s flashlets of light over 200  $\mu$ s.

Gross photosynthetic to respiration ratios (P:R) were calculated by measuring photosynthetic oxygen evolution and oxygen consumption rates on days 0, 3, and 6. Samples were dark acclimated for 20 min in sealed 20 mL glass scintillation vials, then they were fitted with a PreSens Fibox 4 oxygen electrodes connected to a detector (Precision Sensing GmbH, Regensburg, Germany), in a water bath at 33°C. Oxygen levels were continuously recorded over 3 stages: 20 min in the dark, followed by 20 min illuminated at 200  $\mu$ mol

photons  $\text{m}^{-2} \text{s}^{-1}$ , and then another 20 min in the dark. Dark respiration and net photosynthesis rates were then determined by linear regression analysis during the initial dark stage and illumination stage, respectively. Gross photosynthesis was then calculated using equation 2 (see section 2.2.4).

### **3.3.5 Statistical analysis**

All statistical analyses were performed in R. Productivity, specific growth, photosynthesis and respiration rates were all determined using the linear model function (`lm()`). Significant differences between treatments were determined using the Student's t-test function, (`t.test()`). The assumptions for this test was assessed visually and with the Shapiro-Wilk normality test, as well as Levene's Test for Homogeneity of Variance.

## **3.4 Results**

### **3.4.1 Influence of N Source on Growth of *S. acutus***

The growth of *S. acutus* was monitored using dry weights to determine if urea or sodium nitrate supported the best growth under three different gas compositions: air, 9%  $\text{CO}_2$ , and flue gas (Figure 21A-C). Growth was slow for both N sources when grown on air, but it is apparent that urea was favorable as the productivity and specific growth rates were about three-fold greater than sodium nitrate amended cultures (Table 7,  $p < 0.05$ ). When grown under 9%  $\text{CO}_2$ , growth was faster than that in air for both N sources initially, but growth began to plateau in the sodium nitrate cultures after the density reached about 1.0 g/L (day 3), which resulted in significantly lower productivity and specific growth rates than growth in urea ( $p < 0.05$ , Table 7). Growth was similar between N

source when grown on flue gas, and contrary to growth in the other gases, cultures using sodium nitrate exhibited slightly greater productivity and specific growth rates but this was only significant for specific growth ( $p < 0.05$ ; Table 7). The pH increased in all cultures grown in air, regardless of N source (Figure 21D). However, in 9% CO<sub>2</sub> and flue gas, the pH decreased in the urea amended cultures but remained near neutral in the nitrate treatment (Figure 21E-F).

There were large differences in nutrient uptake patterns between the N sources. In air, cultures using sodium nitrate only exhausted approximately 10% of N in the media over the entire experiment, whereas 65% of N was consumed within the first three days in cultures using urea (Figure 22A). Differential N consumption was also seen when cultures were grown under CO<sub>2</sub> and to a lesser extent in flue gas, where cultures using sodium nitrate only consumed about 50% and 80% of N by day 3, respectively, but cultures using urea consumed upwards up 95% of their N supply in both gases (Figure 22B-C). However, sodium nitrate cultures depleted 5%, 20%, and 55% more phosphate than urea cultures by day 3 in air, CO<sub>2</sub>, and flue gas, respectively ( $p < 0.05$ , Figure 22D-F).

### **3.4.2 Influence of N Source on Biochemical Composition of *S. acutus***

To compare the effect of N source on the biochemical composition of *S. acutus*, biomass samples were taken on days 0, 3, and 6 for protein, total lipids, FAME profile, and carbohydrate content. There was greater protein content in cultures using urea in all gases on all days (Figure 23). Notably, cultures grown using urea in CO<sub>2</sub> and flue gas reached peak protein content on day 3, at 31% and 29%, respectively, both significantly greater than that obtained with sodium nitrate ( $p < 0.05$ ).

The lipid content was greatest overall in air grown cultures, reaching approximately 45% of the total biomass on day 3 for both N sources (Figure 24). This high lipid content did not last in cultures using urea as it decreased by about half by day 6, while lipid content slightly increased to about 50% of the total biomass in sodium nitrate cultures. In CO<sub>2</sub> and flue gas, the lipid content in both N sources remained relatively low, with final yields at 15% and 25% of the total biomass obtained with urea, respectively, and about 20% obtained with sodium nitrate for both gases. The final lipid content was significantly different between the nitrate and urea amended cultures when grown in flue gas ( $p < 0.05$ ).

Although the total lipid content was generally similar between N sources when grown in air, 50-60% of the total FAME content was saturated fatty acids when grown using sodium nitrate, which was significantly greater than that for urea grown cultures ( $p < 0.05$ , Figure 25). Of these fatty acids, C8:0, C10:0, and C16:0 were prominent for both N sources, while C14:0, C15:0, C17:0, and C20:0 were generally only seen in cultures grown using sodium nitrate (Appendix B, Figure 31). The cultures grown using sodium nitrate under air also had significantly greater monounsaturated fatty acid content, reaching about 30% of the total FAME by day 6 ( $p < 0.05$ ). Cultures using either N source had between 20-30% polyunsaturated fatty acids when grown in air, with the exception of the sodium nitrate cultures which dropped to approximately 8% of the total FAME content by day 6 (Figure 25). Prominent polyunsaturated fatty acids included C18:2, C20:5n3, and C18:3n6 in the sodium nitrate cultures, and C18:2n6 in the urea cultures (Appendix B, Figures 31-33).

Under 9% CO<sub>2</sub> and flue gas, saturated fatty acid content was significantly greater in the urea amended cultures, at about 50% the total FAME content (Figure 26-27, p<0.05). In those cultures, as well as the sodium nitrate amended cultures, C16:0 and C20:0 were prominent saturated fatty acids (Figure 32). Monounsaturated fatty acid content increased on average to 30-45% of the total FAME, where C18:1n9c and C18:1n9t made up the majority, for both N sources under 9% CO<sub>2</sub> and flue gas (Figures 26-27, Appendix B, Figures 32-33). Although the cultures grown in sodium nitrate generally had greater monounsaturated fatty acid content under 9% CO<sub>2</sub>, the opposite was seen in flue gas (Figures 26-27). Polyunsaturated fatty acids were in the urea grown cultures under 9% CO<sub>2</sub> and flue gas, although at very low amounts. Polyunsaturated fatty acids decreased in sodium nitrate grown cultures under 9% CO<sub>2</sub> and even more so under flue gas compared to air grown cultures (Figures 26-27). Again, polyunsaturated fatty acids were in the sodium nitrate grown cultures under flue gas on days 3 and 6 but in very low amounts. C18:2n6, C18:3n6, and C22:6n3 were the major polyunsaturated fatty acids in 9% CO<sub>2</sub> (Appendix B, Figure 32), but only C18:3n6 was seen in the flue gas-grown cultures (Appendix B, Figure 33). The average cetane numbers for all tested conditions were high, although cultures grown using urea had slightly greater cetane numbers in all gas compositions (Table 8).

In air, carbohydrate content decreased to about 25% of the total biomass by the final day for both N sources, (Figure 28). Whereas carbohydrates remained relatively constant at around 33% when grown using sodium nitrate in 9% CO<sub>2</sub>, it varied when cultures were grown using urea, with the final

carbohydrate content reaching about 50% of the total biomass. Lastly, in flue gas treatment, the carbohydrate content increased throughout the experiment in sodium nitrate cultures and by day 6 made up the majority of biomass composition at 62%. The carbohydrate content was maintained around 50% in cultures grown using urea, and only decreased to about 45% of the total biomass by the final day.

### **3.4.3 Photochemical Measurements**

In cultures using sodium nitrate, chlorophyll a content increased throughout the experiment under all gases, but with urea it increased by day 3, then decreased by day 6 under all gases (Figure 29A-C). When grown under air, urea cultures had greater chlorophyll a content until day 6 when cultures using sodium nitrate had 5-fold greater chlorophyll a content (Figure 29A). Likewise, in CO<sub>2</sub> and flue gas, the cultures grown using sodium nitrate had 10-fold greater chlorophyll a content than those using urea ( $p < 0.05$ ).

Furthermore, only when the cultures were grown in air using sodium nitrate did the Fv/Fm values increase throughout the experiment, otherwise they generally followed the same pattern of slightly increasing by day 3, and subsequently decreasing by day 6 (Figures 29D-F). Overall Fv/Fm values remained moderately high in all treatments, except on day 6 in the sodium nitrate treatment under 9% CO<sub>2</sub> where they dropped below 0.200.

The pattern of P:R when cultures were grown in air largely agrees with that seen in chlorophyll a (Figure 29G). Notably, there was a clear contrast in the P:R between cultures grown in 9% CO<sub>2</sub> and flue gas, specifically on day 3

(Figure 29H-I). In 9% CO<sub>2</sub> the P:R was significantly greater when cultures were grown using sodium nitrate, whereas in flue gas the opposite was seen.

### 3.5 Discussion

There were not only differences in growth and biochemical composition of *S. acutus* when grown with sodium nitrate or urea as N sources, but the gas composition also influenced how this alga grew with these different nitrogen sources. Urea was clearly the favorable N source in terms of biomass productivity and specific growth rate when grown under air and 9% CO<sub>2</sub>, and in flue gas, biomass productivity was not significantly different between the N sources. Notably, the urea treatment maintained high growth rates despite the considerable decrease in pH when cultures were grown in CO<sub>2</sub> or flue gas. The lack of any change in cultures pH while grown with sodium nitrate under high CO<sub>2</sub> or flue gas was possible due to the fact that assimilation of nitrate generates excess OH<sup>-</sup> that are expelled by the cell and possibly buffered the growth media (Borowitzka, et al., 2016).

Given that urea costs less per metric ton than sodium nitrate, urea would be the best N source for large-scale *S. acutus* cultivation. However, it is important to consider the concentration of the N source since, in certain conditions, relatively low concentrations of nitrate can support faster growth and higher biomass productivity in *Scenedesmus* sp. (Vasileva et al., 2015). Our preliminary data also showed that sodium nitrate supported greater *S. acutus* productivity when grown in 9% CO<sub>2</sub>, even though the nitrogen concentration in that treatment was about 5-fold less than that in the urea treatment (Appendix B,

Table 9, Figure 30). This further emphasizes the need to test the influence of N source and N concentration on the growth of *S. acutus*.

The higher CO<sub>2</sub> concentration in the 9% CO<sub>2</sub> and flue gas promoted greater productivity in both treatments when compared to growth on air alone, thus indicating that air-grown cultures were experiencing some CO<sub>2</sub> limitation, although, in air-grown cultures using sodium nitrate growth was still much slower than those using urea. The increased chlorophyll a content, Fv/Fm, and P:R, together with the low cell density indicate that air grown cultures using sodium nitrate were not photochemically inhibited. Rather, the low protein and high lipid content, despite the high residual nitrogen in the media, suggests that nitrate uptake was inhibited in these cultures.

It is difficult to determine the cause of this inhibition because, at 4.3 mM sodium nitrate, this concentration is much lower than those reported to be inhibitive toward growth. Concentrations of 15 and 20 mM were associated with poor biomass production and considered to be inhibitory in *Scenedesmus bijugatus* and *Neochloris oleoabundans* (Arumugam et al., 2013, Li et al., 2008). The CO<sub>2</sub>-limiting condition could lead to a build-up of intracellular ammonium due to an insufficient amount of carbon skeletons for amino acid synthesis, which could also inhibit nitrate uptake (Grant and Turner, 1969). The high lipid content in these cultures (over 50% of total biomass by day 6) is an indication that there was a sufficient amount of fixed carbon to synthesized these carbon skeletons, although increased lipid content is often a response to N-limitation in many chlorophyte microalgae (Fakhry and El Maghraby 2015, Griffiths and Harrison 2009). Nitrate uptake and assimilation is complex and

there are many factors that regulate it, and thus it could be a combination of factors inhibiting nitrate uptake in this case. On the other hand, urea is not only a source of N, but also a source of carbon. The urea cycle has been identified as a key pathway for anaplerotic C fixation directly into nitrogenous compounds (Dong et al., 2014, Allen et al., 2011). This extra source of carbon could be crucial for *S. acutus* to maintain urea assimilation under the CO<sub>2</sub> limited condition and why these cultures exhibited faster growth.

Although CO<sub>2</sub> was no longer limiting in the cultures grown in 9% CO<sub>2</sub>, growth in cultures using sodium nitrate began to plateau around day 3, despite nitrate concentrations remaining high. This was most likely a result of the high cell density and therefore decreased light availability within the culture. At a dry weight of nearly 1.0 g L<sup>-1</sup> there was minimal, if any, light reaching the middle of the culture. Light availability is an important factor for nitrate uptake and assimilation because it is dependent on photosynthetically derived reducing agents like NAD(P)H (Falkowski and Raven 2007). The decreased Fv/Fm value and P:R on day 6 also support this idea that light was limiting growth in these cultures, even though the increased chlorophyll a content in these cultures indicate that they have photoacclimated as much as possible, more so than the urea-grown cultures. However, the cultures using urea in 9% CO<sub>2</sub> continued growing until the nitrogen was exhausted from the media on the final day. This suggests that urea assimilation is not as directly influenced by the availability of light and products of photosynthesis as nitrate assimilation. However, there are limited studies on urea uptake mechanisms in chlorophytes. Williams and Hodson (1977) found that urea uptake is energy-dependent in *Chlamydomonas*

*reinhardtii*, but whether this energy originates from photosynthesis or respiration has yet to be reported for this alga.

It is apparent that light limitation did not inhibit growth in cultures using sodium nitrate in flue gas as it did in 9% CO<sub>2</sub>, since these cultures continued to grow to a final biomass density of about 2.0 g L<sup>-1</sup>. This could be evidence that the NO may have been utilized as an N source in the sodium nitrate grown cultures. Conversely, there was little indication of this in the urea grown cultures, as growth in flue gas was not markedly different from that in just 9% CO<sub>2</sub>. Dong et al. (2014) reported that the harmful alga *Aureococcus anophagefferens* preferentially depleted urea over nitrate when grown in media that contained both sources. From RNA-seq analysis, they hypothesized that certain enzymes used in inorganic N assimilation may have been inhibited by the presence of urea or its metabolic products. This phenomenon could be at play in these cultures.

Understanding how N source effects the biomass composition of *S. acutus* is critical for optimizing downstream product development. This is particularly important for protein content, not only because N directly influences protein yield, but also because a future application of *S. acutus* grown on flue gas emissions is the production of plastic from its protein. Greater protein content was obtained with urea as the N source, reaching about 30% of the total biomass composition in flue gas. Vasileva et al. (2015), also reported greater protein content when *Scenedesmus* sp. BGP cultures were grown using urea rather than nitrate when aerated in 2-3% CO<sub>2</sub> but only during exponential phase growth.

The final lipid content was between 15-20% for both N sources, which is consistent with that for *Scenedesmus* sp. BGP, *Neochloris oleoabundans*, and *Tetraselmis* sp. (Vasileva et al., 2015, Li et al., 2008, Kim et al., 2016). The significant differences seen in fatty acid composition between N sources were unexpected, although under all tested conditions, *S. acutus* generally contained a larger proportion of saturated and monounsaturated fatty acids than polyunsaturated fatty acids. Duhp et al. (2016) also reported differences in fatty acid composition when *Scenedesmus* sp. was grown using urea or sodium nitrate in air, although much of the literature has emphasized the importance of N concentration, rather than N source, when differences in fatty acid composition were reported (Piorreck et al., 1984, Yongmanitchai and Ward 1991, Xu et al., 2001, Sunja et al., 2011).

Despite differences seen in fatty acid composition between N sources, cetane numbers in all treatments were above the minimum cetane number for biodiesel which is 47 (ASTMD 6751, 2002). Cetane number is used as an indicator for the combustion properties of diesel, including ignition delay time, e.g. the shorter the delay time, the higher the cetane number (Islam et al., 2013). Consequently, the high cetane numbers in all treatments suggest that *S. acutus* is capable of producing high quality biodiesel under all tested conditions. Sarat et al., (2016) found that when cultures were grown in air, only those supplemented with sodium nitrate would yield cetane numbers above 40, but the present study found that urea amended cultures actually yielded cetane numbers slightly greater than that for sodium nitrate amended cultures in all gas compositions.

It is noteworthy that a sizeable fraction of the biomass composition was made up of carbohydrates, particularly in cultures grown in flue gas, regardless of N source. Laurens et al. (2014) demonstrated that carbohydrates from *Scenedesmus* sp. could be converted into soluble sugar for fermentation into biogas, which also allowed greater access to lipids for extraction. This would not only provide a purer fraction of protein for plastic development, but also improve the economics and sustainability of the process of carbon capture and reuse (Laurens et al., 2014).

N source significantly influenced the growth and biochemical composition of *S. acutus* when grown under different gas compositions. Of the two tested N sources, urea supported greater biomass productivity and protein content which is ideal for carbon capture and plastic production, respectively. High cetane numbers were also seen in cultures grown on urea indicating good quality biodiesel could be produced from the algal lipids. Due to the fact that urea was the more favorable N source in this study and that it is cheaper than sodium nitrate, urea is the most appropriate N source for cultivation of *S. acutus* for carbon capture and reuse at a coal-fired power plant.

Table 6. Media components and concentrations (g L<sup>-1</sup>).

Media Component	Urea Media	Nitrate Media
Triple Super Phosphate	0.14	0.14
Pot ash	0.068	0.068
Spring 330	0.026	0.026
Urea	0.13 (4.3 mM N)	-
Sodium nitrate	-	0.365 (4.3 mM N)

Table 7. Biomass productivity and specific growth rate of *S. acutus* cultures grown using sodium nitrate or urea in air, 9% CO<sub>2</sub>, and simulated flue gas flue gas (9% CO<sub>2</sub>, 50 ppm NO, 25 ppm SO<sub>2</sub>). Values are means ± SD. Letters denote significant differences between N treatments (p<0.05).

N source:	Air		9% CO <sub>2</sub>		Flue Gas	
	Nitrate	Urea	Nitrate	Urea	Nitrate	Urea
Productivity (g L <sup>-1</sup> d <sup>-1</sup> )	0.006±0.0018 <sup>B</sup>	0.018±0.006 <sup>A</sup>	0.122±0.010 <sup>B</sup>	0.267±0.016 <sup>A</sup>	0.285±0.015 <sup>A</sup>	0.269±0.039 <sup>A</sup>
Specific growth rate (d <sup>-1</sup> )	0.067±0.016 <sup>B</sup>	0.217±0.087 <sup>A</sup>	0.230±0.023 <sup>B</sup>	0.389±0.021 <sup>A</sup>	0.346±0.021 <sup>B</sup>	0.307±0.020 <sup>A</sup>

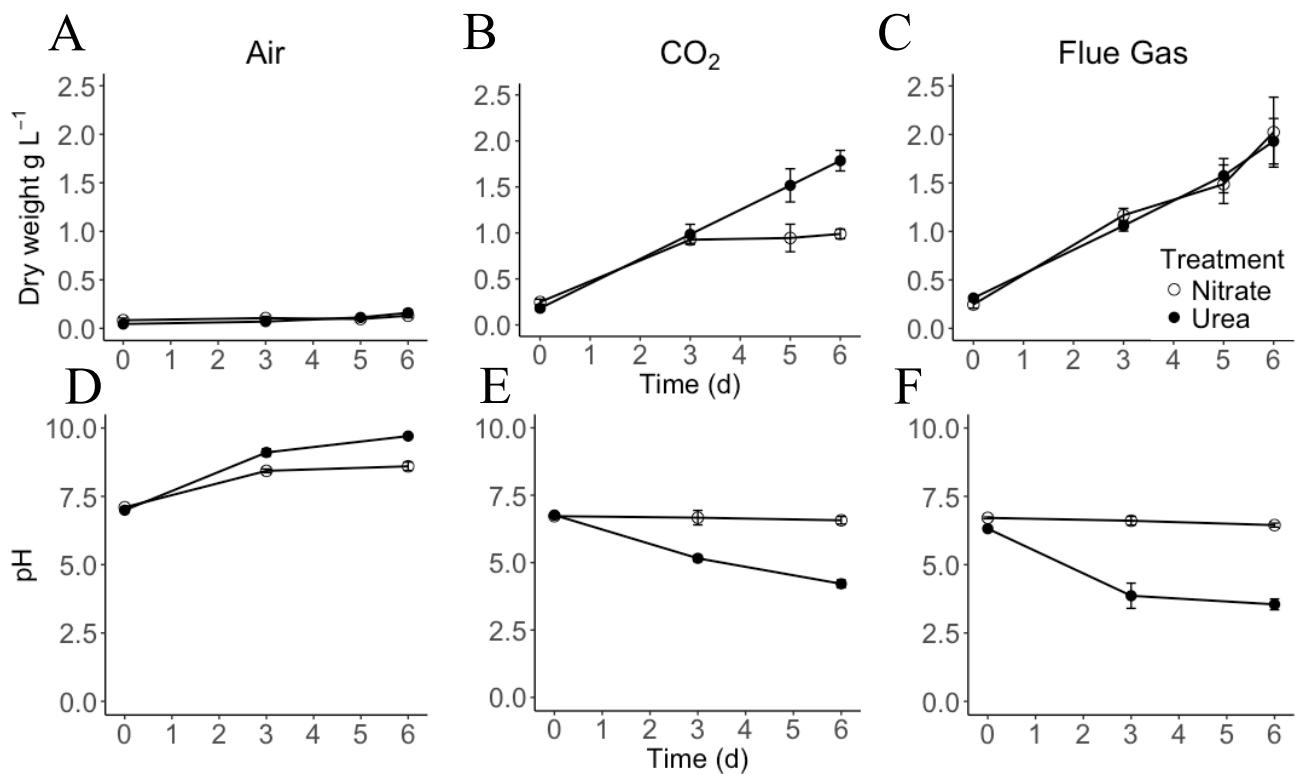


Figure 19. Growth, and pH of *S. acutus* cultures grown using nitrate or urea in air (A, D), 9% CO<sub>2</sub> (B, E) and flue gas (C, F). Values are means  $\pm$  SD.

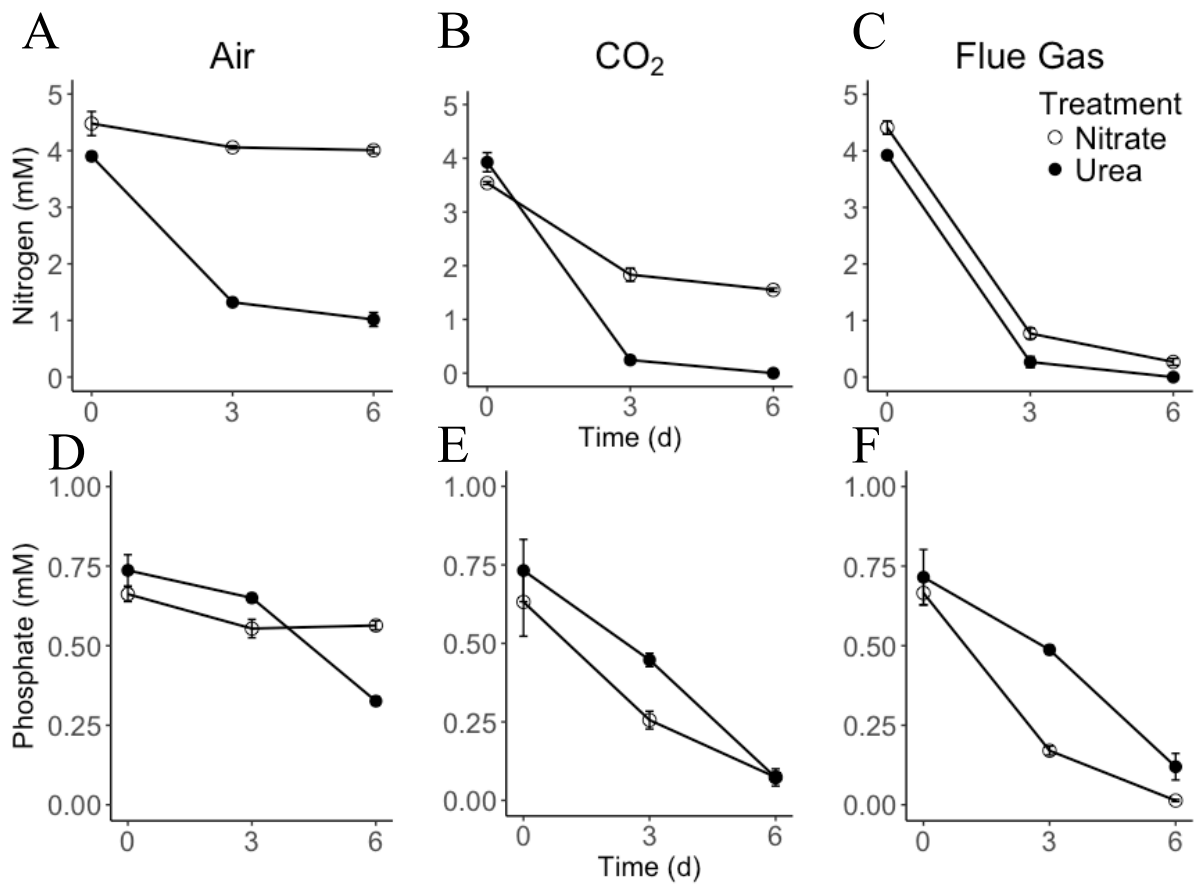


Figure 20. Media concentrations of nitrogen and phosphate in *S. acutus* cultures grown using sodium nitrate or urea in air (A, D), 9% CO<sub>2</sub> (B, E), and simulated flue gas (9% CO<sub>2</sub>, 50 ppm NO, 25 ppm SO<sub>2</sub>) (C, F). Values are means ± SD.

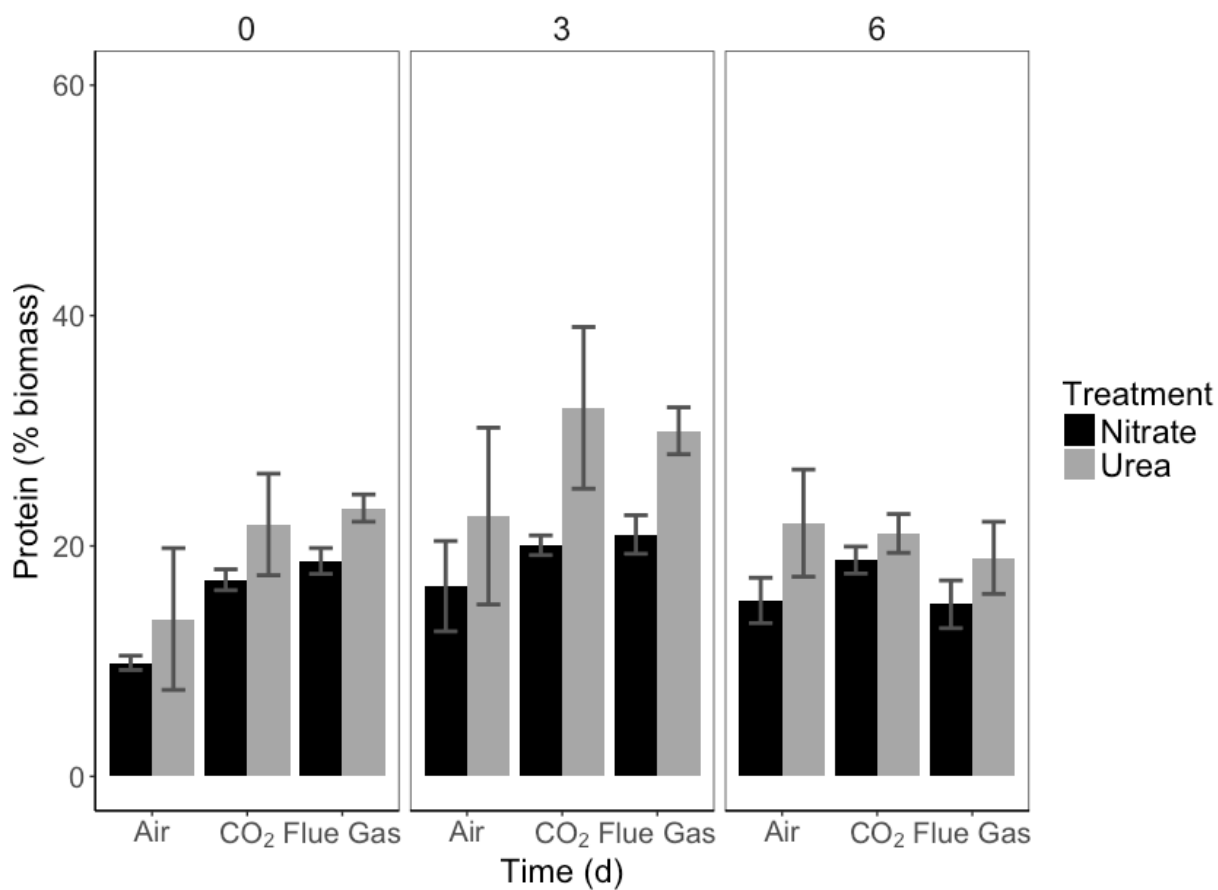


Figure 21. Protein content (% of total biomass) in *S. acutus* cultures grown using sodium nitrate or urea in air, 9% CO<sub>2</sub>, and simulated flue gas (9% CO<sub>2</sub>, 50 ppm NO, 25 ppm SO<sub>2</sub>). Values are means ± SD.

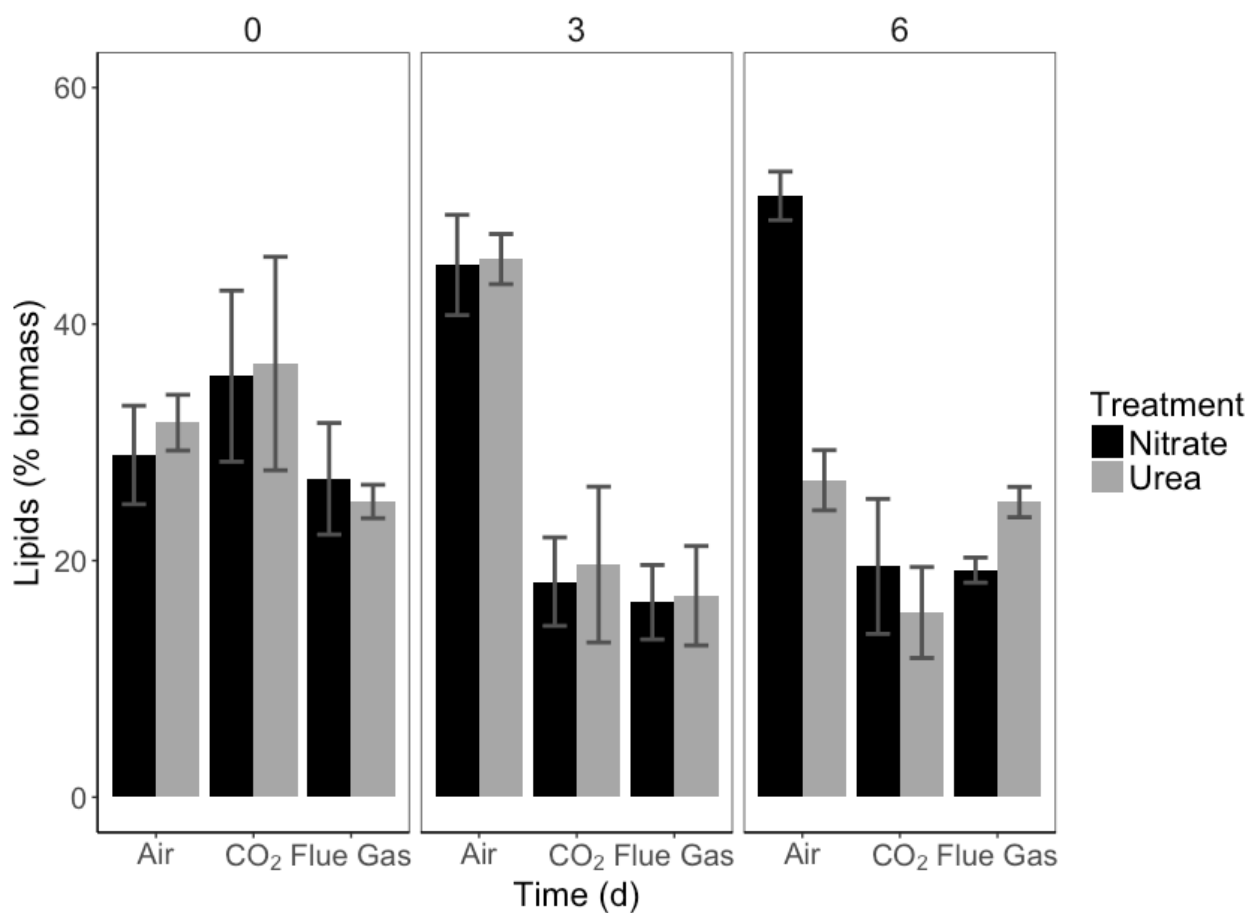


Figure 22. Total lipid content (% of total biomass) in *S. acutus* cultures grown using sodium nitrate or urea in air, 9% CO<sub>2</sub>, and simulated flue gas flue gas (9% CO<sub>2</sub>, 50 ppm NO, 25 ppm SO<sub>2</sub>). Values are means ± SD.

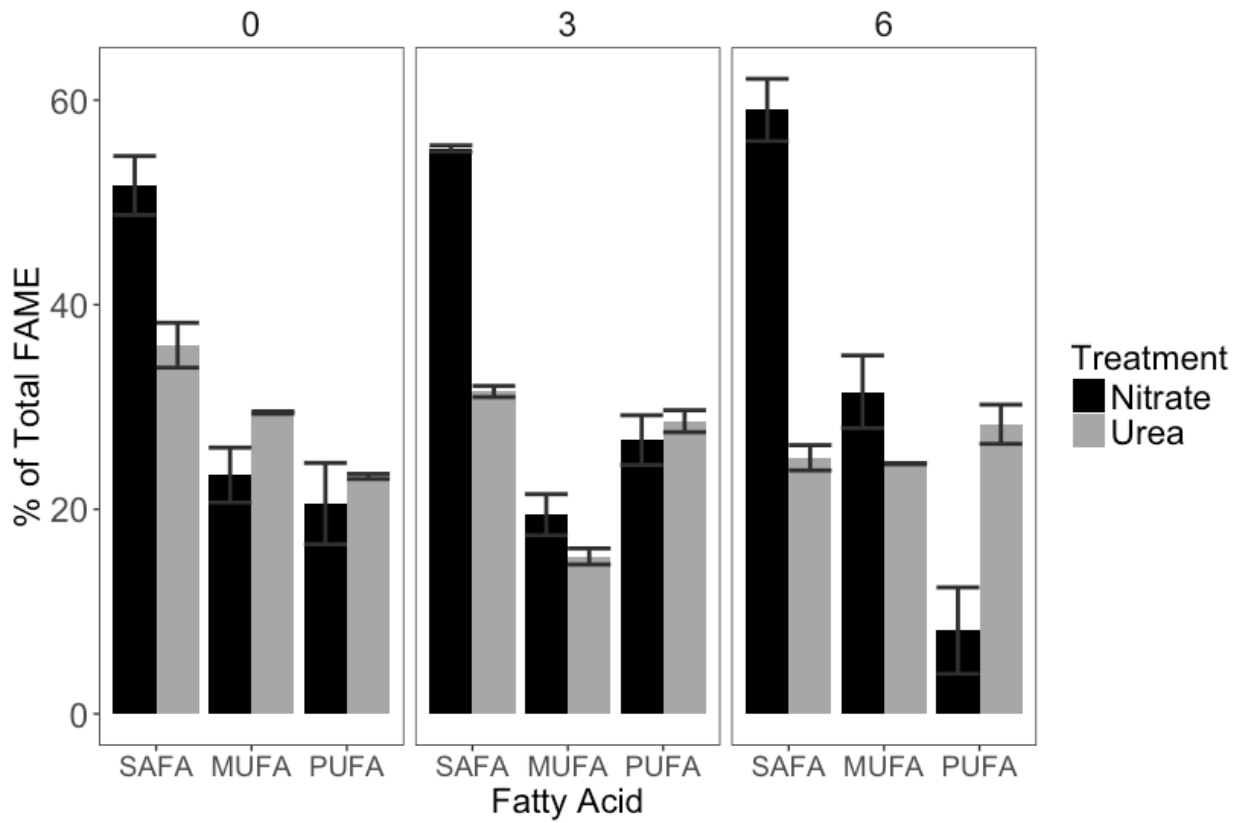


Figure 23. Saturated (SAFA), monounsaturated (MUFA), and polyunsaturated (PUFA) fatty acid content for *S. acutus* grown using sodium nitrate or urea in air (0.04% CO<sub>2</sub>). Values are percent means ± SD of the total fatty acid methyl ester (FAME) content. Only fatty acids that contributed to 2% or more of the total FAME composition were included in the calculation of each fatty acid.

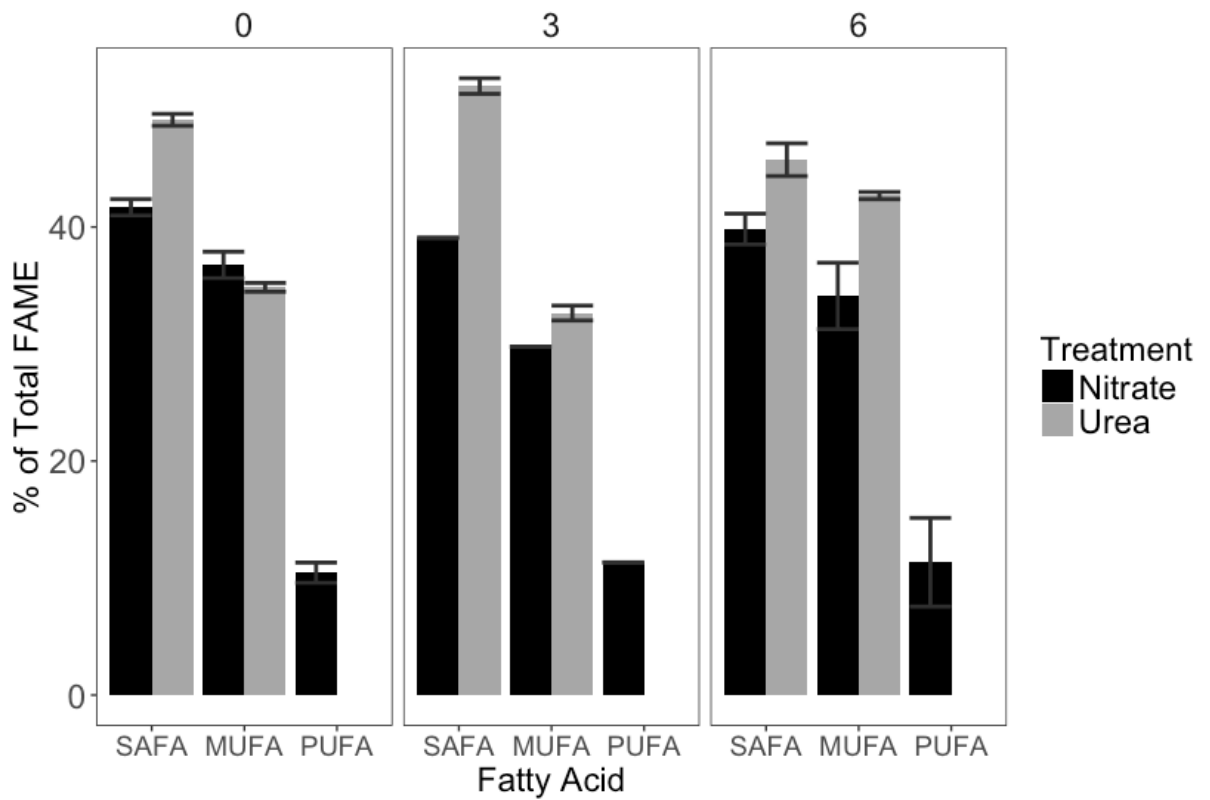


Figure 24. Saturated (SAFA), monounsaturated (MUFA), and polyunsaturated (PUFA) fatty acid content for *S. acutus* grown using sodium nitrate or urea in 9% CO<sub>2</sub>. Values are percent means  $\pm$  SD of the total fatty acid methyl ester (FAME) content. Only fatty acids that contributed to 2% or more of the total FAME composition were included in the calculation of each fatty acid.

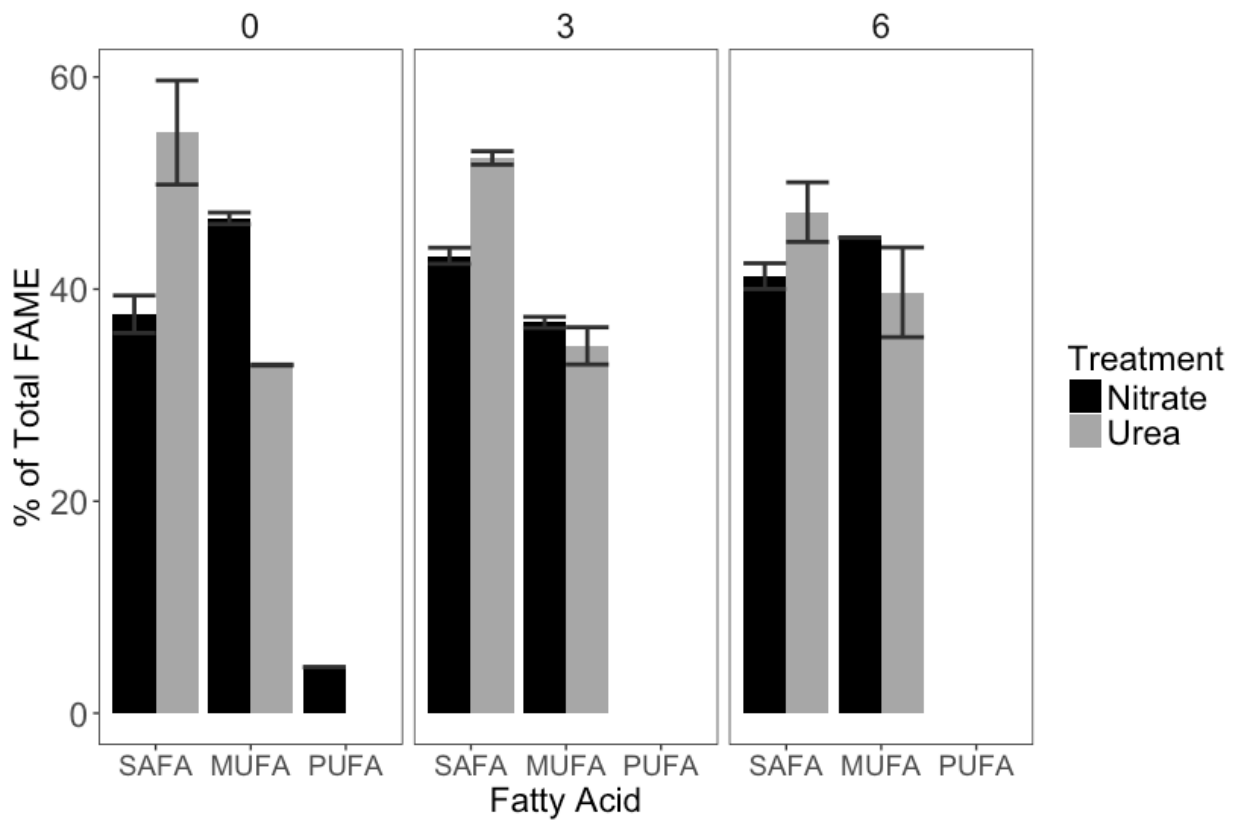


Figure 25. Saturated (SAFA), monounsaturated (MUFA), and polyunsaturated (PUFA) fatty acid content for *S. acutus* grown using sodium nitrate or urea in simulated flue (9% CO<sub>2</sub>, 55pm NO, 25 ppm SO<sub>2</sub>). Values are percent means  $\pm$  SD of the total fatty acid methyl ester (FAME) content. Only fatty acids that contributed to 2% or more of the total FAME composition were included in the calculation of each fatty acid.

Table 8. Average cetane number for *S. acutus* FAME content grown using sodium nitrate or urea in air, 9% CO<sub>2</sub>, and simulated flue gas flue gas (9% CO<sub>2</sub>, 50 ppm NO, 25 ppm SO<sub>2</sub>).

	Air			
	Day 0	Day 3	Day 6	Overall
Nitrate	55	53	60	56
Urea	58	59	59	58
	9% CO <sub>2</sub>			
Nitrate	64	63	61	62
Urea	65	68	65	66
	Flue gas			
Nitrate	60	65	62	62
Urea	65	68	66	66

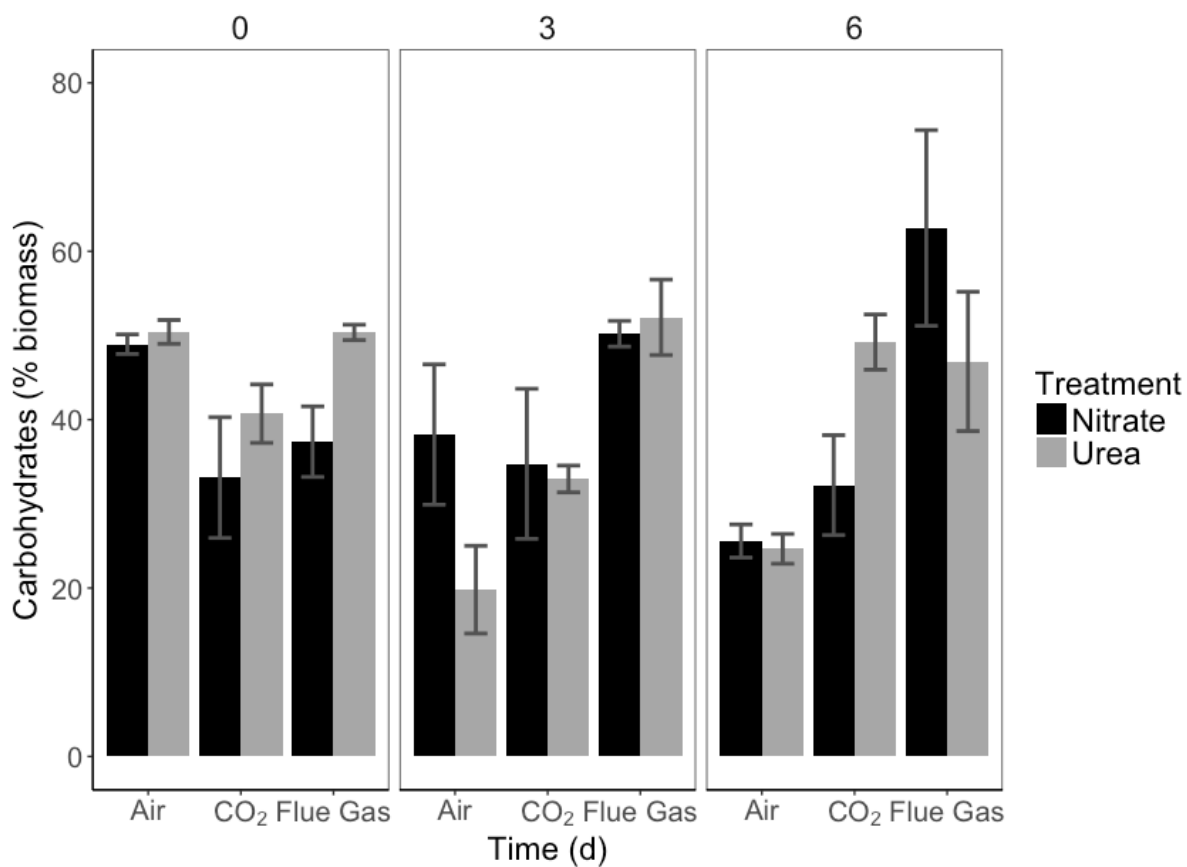


Figure 26. Total carbohydrate content (% of total biomass) in *S. acutus* cultures grown using sodium nitrate or urea in air, 9% CO<sub>2</sub>, and simulated flue gas (9% CO<sub>2</sub>, 50 ppm NO, 25 ppm SO<sub>2</sub>). Values are means ± SD.

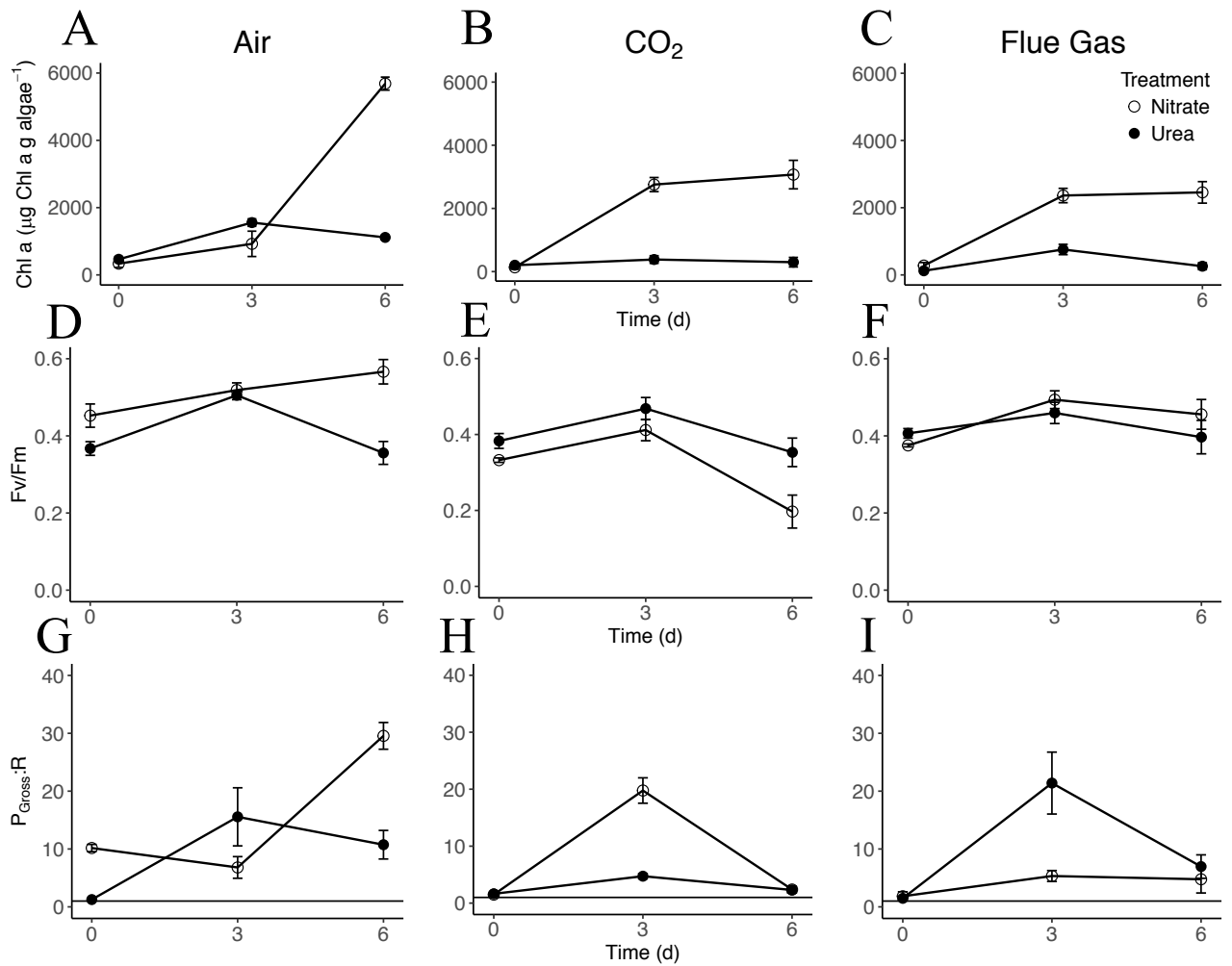


Figure 27. Chlorophyll a content, Fv/Fm value, and gross photosynthesis to respiration ratios for *S. acutus* cultures grown using sodium nitrate or urea in air (A, D, G), 9% CO<sub>2</sub> (B, E, H), and simulated flue gas (9% CO<sub>2</sub>, 50 ppm NO, 25 ppm SO<sub>2</sub>) (C, F, I). Values are means  $\pm$  SD.

## REFERENCES

- Allen AE, Dupont CL, Obornik M, Horak A, Nunes-Nesi A, McCrow JP, Zheng H, Johnson DA, Fernie AR, Bowler C. 2011. Evolution and metabolic significance of the urea cycle in photosynthetic diatoms. *Nature*. 473(7346): 203-207.
- Arumugam M, Agarwal A, Arya MC, Ahmed Z. 2013. Influence of nitrogen sources on biomass productivity of microalgae *Scenedesmus bijugatus*. *Bioresource Technology*. 131: 246-249.
- ASTM. 2002. D 6751-Standard Specification for Biodiesel Fuel (B100) Blend Stock for Distillate Fuels. American Society for Testing and Materials International, West Conshohocken, Penn.
- Borowitzka, M, Beardall J, Raven JA. *The Physiology of Microalgae*. Springer International Publishing. 2016.
- Cheng Y, Zheng Y, VanderGheynst J. 2011. Rapid quantitative analysis of lipids using a colorimetric method in a microplate format. *Lipids* 46: 95-103
- Crofcheck C, E X, Shea A, Montross M, Crocker M, Andrews R. 2012. Influence of media composition on the growth rate of *Chlorella vulgaris* and *Scenedesmus acutus* utilized for CO<sub>2</sub> mitigation. *J Biochem Tech*. 4(2): 589-594.
- Dong H, Huang K, Wang H, Lu S, Cen J, Dong Y. 2014. Understanding strategy of nitrate and urea assimilation in a Chinese strain of *Aurococcus anophagefferens* through RNA-seq analysis. *PLoS One*. 9(10): e111069.
- Dhup S, Kannan DC, Dhawan V. 2016. Understanding urea assimilation and its effect on lipid production and fatty acid composition of *Scenedesmus* sp. *SOJ Biochem* 2(1): 1-7.
- Falkowski PG, Raven JA. *Aquatic Photosynthesis*. Princeton University Press. 2007.
- Fakhry EM, El Maghraby DM. 2015. Lipid accumulation in response to nitrogen limitation and variation of temperatures in *Nannochloropsis salina*. *Botanical Studies*. 56(6): 1-8

- Folch J, Lees M, Sloane Stanley GH. 1957. A simple method for the isolation and purification of total lipids from animal tissues. *J Biol Chem.* 226(1): 497-509.
- Grant BR, Turner IM. 1969. Light-stimulated nitrate and nitrite assimilation in several species of algae. *Comp. Biochem. Physiol.* 29: 995-1004.
- Griffiths MJ, Harrison STL. 2009. Lipid productivity as a key characteristic for choosing algal species for biodiesel production. *J Appl Phycol.* 21: 493-507.
- Islam MA, Magnusson M, Brown RJ, Ayoko GA, Nabi MN, Heimann K. 2013. Microalgal species selection for biodiesel production based on fuel properties derived from fatty acid profiles. *Energies.* 6: 5676-5702.
- Kim G, Mujtaba G, Lee K. 2016. Effects of nitrogen sources on cell growth and biochemical composition of marine chlorophyte *Tetraselmis* sp. for lipid production. *Algae* 31(3): 257-266.
- Laurens LML, Nagle N, Davis R, Sweeney N, Van Wycken S, Lowell A, Pienkos P T. 2015. Acid-catalyzed algal biomass pretreatment for integrated lipid and carbohydrate-based biofuels production. *Green Chemistry.* 17: 1145.
- Leftley JW, Syrett PJ. 1973. Urease and ATP:Urea amidolyase activity in unicellular algae. *J. gen. Microbiol.* 77: 109-115.
- Li Y, Horsman M, Wang B, Wu N, Lan C. 2008. Effects of nitrogen sources on cell growth and lipid accumulation of green alga *Neochloris oleoabundans*. *Appl Microbiol Biotechnol.* 81: 629-636.
- Lin Q, Lin J. 2011. Effects of nitrogen source and concentration on biomass and oil production of a *Scenedesmus rubescens* like microalga. *Bioresource Technology.* 102: 1615-1621.
- Piorreck M, Baasch KH, Poiil P. Biomass production, total protein, chlorophylls, lipids and fatty acids of freshwater green and blue-green algae under different nitrogen regimes. *Phytochemistry.* 23(2): 207-216.
- Sarat CT, Deepak RS, Kumar MM, Mukherji S, Chauhan VS, Sarada R, Mudliar SN. 2016. Evaluation of indigenous fresh water microalga *Scenedesmus*

*obtusus* for feed and fuel applications: Effect of carbon dioxide, light and nutrient sources on growth and biochemical characteristics.

Solomon CM, Collier JL, Berg GM, Glibert PM. 2010. Role of urea in microbial metabolism in aquatic systems: a biochemical and molecular review. *Aquat Microb Ecol* 59:67–88

Sunja, C, Lee D, Luong TT, Park S, Oh YK, Lee T. 2011. Effects of carbon and nitrogen sources on fatty acid contents and composition in green microalgae, *Chlorella* sp. 227.

Templeton D W, Laurens LML. 2015. Nitrogen-to-protein conversion factors revisited for applications of microalgal biomass conversion to food, feed and fuel. *Algal Research*. 11: 359-367.

Van Wychen S, Laurens LML. 2015. Determination of Total Carbohydrates in Algal Biomass. NREL/TP-5100-60957. Golden, CO: National Renewable Energy Laboratory.

Van Wychen S, Ramirez K, Laurens LML. 2015. Determination of Total Lipids as Fatty Acid Methyl Esters (FAME) by in situ Transesterification. NREL/TP-5100- 60958. Golden, CO: National Renewable Energy Laboratory.

Vasileva I, Marinova G, Gigova L. 2015. Effect of nitrogen source on the growth and biochemical composition of a new Bulgarian isolate of *Scenedesmus* sp. *J BioSci. Biotechnol.* 125-129

Williams II SK, Hodson RC. 1977. Transport of urea at low concentrations in *Chlamydomonas reinhardtii*. *J Bacteriol.* 130(1): 266-273.

Wilson MH, Groppo J, Placido A, Graham S, Morton III S A, Santillan-Jimenez E, Shea A, Crocker M, Crofcheck C, Andrews R. 2014. CO<sub>2</sub> recycling using microalgae for the production of fuels. *Applied Petrochemical Research*. 4(1): 41-53.

Wilson MH, Mohler DT, Groppo JG, Grubbs T, Kesner S, Frazar EM, Shea A, Crofcheck C, Crocker M. 2016. Capture and recycle of industrial CO<sub>2</sub> emissions using microalgae. *Applied Petrochemical Research*. 6(3): 279-293.

- Xu N, Zhang X, Fan X, Han L, Zeng C. 2001. Effects of nitrogen source and concentration on growth rate and fatty acid composition of *Ellipsoidion* sp. (Eustigmatophyta). *J of Appl Phycol.* 12: 463-469.
- Yongmanitchai W, Ward OP. 1991. Growth of and omega-3 fatty acid production by *Phaeodactylum tricornutum* under different culture conditions. *Applied and Environmental microbiology.* 57(2): 419-425.
- Zawada RJ, Kwan P, Olszewski KL, Llinas M, Huang SG. 2009. Quantitative determination of urea concentrations in cell culture medium. *Biochem. Cell Biol.* 87: 541-544.

## Chapter 4

### SURVERY OF CONTAMINATION IN A PILOT-SCALE PBR SYSTEM

#### 4.1 Abstract

Contamination by invading organisms is one of the largest limitations of large-scale microalgae cultivation. Instances of contamination causing culture crashes have occurred in outdoor cultures of the green alga, *Scenedesmus acutus*, which is currently being studied for carbon capture and reuse at Duke Energy's East Bend Station located in Boone County, Kentucky. However, these organisms had yet to be identified through molecular methods. Over the 2016 harvest season samples were taken periodically from the outdoor cultures and the DNA was extracted and sequenced. Throughout the season the culture experienced several severe contamination events that often went unnoticed for a considerable amount of time and caused culture death. Several contaminants were identified, including other species of green algae, fungi and fungi-like organisms, as well as many different types of bacteria. Two sources were the seed cultures, in which many of the prominent contaminants were also found, as well as the residual biofilms on the inside of the tubes of the cultivation system that were not effectively killed during sterilization. Identifying these invading organisms and the potential sources of contamination are crucial for the development of procedures to prevent or treat contamination in large-scale microalgae cultivations.

## 4.2 Introduction

One of the largest limitations of large-scale microalgae cultivation is contaminating organisms that often negatively impact algal growth and harvesting conditions (Prokop et al., 2015). Contamination by invading organisms is the leading cause of decreased biomass yield in mass outdoor microalgae cultures (Gong et al., 2015). Contaminants can be other microalgae or bacteria that compete for nutrients, parasites such as viruses or fungi, or predators that graze directly on the microalgae (Hannon et al., 2012). They can be introduced to the culture via the water used for the culture media, or any exposure of the culture to air. Closed photobioreactors (PBRs hereafter) decrease the risk of contamination, but the initial construction and maintenance of sterility comes at a much higher cost than open pond systems (Hannon et al., 2012).

Contamination events have occurred in outdoor cultures of the freshwater chlorophyte, *Scenedesmus acutus*, currently being studied in a PBR for carbon capture and reuse at Duke Energy's East Bend Station located in Boone County, Kentucky. In 2013, a filamentous cyanobacterium-like organism was identified via microscopy, but its identity has yet to be resolved at the species level. In 2014, this cyanobacterium-like organism was seen again, as well as a red alga, *Coelastrella saipanesis*, that was subsequently identified by DNA sequencing of the 18S rRNA gene (Stewart and Gerken, unpublished). It was evident that this red alga was capable of growing on flue gas, and under certain conditions it actually outcompeted *S. acutus* (Wilson, personal communication). Not much is known about this organism, but the fact that it is a native species to the area and capable of such growth makes it worth

investigating further. In 2015, very little contamination was seen until the last few weeks of operation, in which both of these organisms were also detected (Wilson, personal communication).

Contamination in this system may decrease the overall carbon capture efficiency, compromise the composition of the biomass for downstream processing, and ultimately cause culture death. In the event of culture death, closed PBRs need to be flushed out and sterilized. Biofouling on the interior of the tubes by invading species is an additional limitation of these closed systems, as it inhibits light penetration and may also compromise the structural integrity of the tubes (Prokop et al., 2015). This would substantially add to operational costs with little to no economic benefit depending on if any of the biomass was salvageable.

The development of effective measures for prevention or treatment of contamination is critical for the successful of outdoor mass cultivation of algae for carbon capture and reuse (Letcher et al., 2013). However, in order to do so, identifying the contaminating organisms must be the first step. The present study used next generation DNA sequencing to identify organisms that contaminated an outdoor PBR growing *S. acutus* on flue gas emissions over the entire harvest season in 2016. From this analysis, we were able to gain a comprehensive idea of the scale of contamination that occurs in this system and also identified two potential sources of contamination.

## **4.3 Methods**

### **4.3.1 Overview of *S. acutus* Cultivation in Pilot-Scale PBR**

*S. acutus* UTEX B72 was obtained from the Culture Collection of Algae at the University of Texas at Austin. *S. acutus* was cultivated in an outdoor 1200 L vertical tube PBR for CO<sub>2</sub> capture from flue gas emissions at Duke Energy's East Bend Station located in Boone County, Kentucky. Stock cultures of *S. acutus* were grown using a urea media previously described in Crofcheck et al., 2012, and maintained in 10 L airlift reactors in a greenhouse at the University of Kentucky's Center for Applied Energy Research. The water used to fill the reactor was from wells located on site, and it passed through a UV sterilizer before entering the PBR. The PBR was initially inoculated on June 14<sup>th</sup>, 2016 at a biomass density of about 0.05 g L<sup>-1</sup>. Growth was monitored using dry weight and qualitative observations of the culture were recorded. Additional details about the demonstration facility can be found in Wilson et al., 2014 and Wilson et al., 2016.

### **4.3.2 Sample Collection, DNA Extraction, and Sequencing**

Samples were periodically collected from the PBR from June 14<sup>th</sup> to October 18<sup>th</sup>, 2016, and preserved in DMSO buffer at -20°C until the DNA could be extracted. A method combining the Promega Wizard Genomic Purification protocol (Promega Corporation, Madison, WI, USA) and the Doyle and Doyle (1987) CTAB based method was used to extract the DNA. Briefly, samples were centrifuged at 12,000 rpm for 3 min, and the DMSO buffer was decanted. The cell pellet was first washed with DI water then lysed by bead beating for 100 s in nuclei lysis buffer (0.2 M TRIS, 2mM EDTA, 0.7% SDS,

pH 7.6). Proteins were digested by adding Proteinase K ( $20 \text{ mg mL}^{-1}$ ) and incubating samples at  $56^\circ\text{C}$  for 1 h, vortex mixing every 15 min. To degrade RNA, RNase ( $4 \text{ mg mL}^{-1}$ ) was added, then samples incubated at  $37^\circ\text{C}$  for 20 min. Proteins were precipitated using 9 M ammonium acetate, samples were placed on ice for 1 h, then centrifuged at 12,000 rpm for 5 min. This step was repeated on dense samples until the supernatant was translucent. The supernatant was transferred to a new 1.5 mL tube, then a 24:1 chloroform:isoamyl alcohol solution was added and the tubes were gently inverted for 20 min. After centrifuging at 12,500 rpm for 15 min the supernatant was transferred to a new 1.5 mL tube. The DNA was precipitated using 3 M sodium acetate and 100% ethanol, incubated at  $-20^\circ\text{C}$  for 15 min, then centrifuged at 12,500 rpm for 15 min. The DNA pellet was rinsed twice with 70% ethanol, dried, and resuspended in elution buffer (Promega Corporation, Madison, WI, USA).

Amplicon sequencing of the 18S rRNA gene using primer pair Euk7F – 530R, and the 16S rRNA gene using primer pair 799F-1293R, was performed to identify eukaryotes and bacteria in the samples, respectively. Additional sequencing of the internal transcribed spacer region using primer pair ITS1-ITS2 of the rRNA operon was used to more accurately identify the fungi present in the samples. Sequencing was performed using Illumina MiSeq at Mr. DNA Lab, Shallowater, TX, USA. Sequence processing was also performed at Mr. DNA Lab. This included joining sequences, removing sequences with greater than 150 bp and those with ambiguous base calls, and generating operational taxonomic units by clustering at 3% divergence (mrdnalab.com). Taxonomy was assigned

using the NCBI BLASTn tool against GreenGenes, RDPII, and NCBI databases. Relative abundances of eukaryotes, bacteria, and fungi were determined. Bacteria and fungi were identified to taxonomic class level, whereas eukaryotes were identified to the genus level, and for clarity purposes, only organisms that contributed to 5% or more of the composition in any sample were included in the figures.

#### 4.4 Results

Samples were taken for DNA sequencing of *S. acutus* cultures grown on flue gas in an outdoor PBR from June to October 2016. Adequate biomass densities of 0.80-1.0 g L<sup>-1</sup> were reached throughout the season (Figure 34). However, it is evident from the composition of eukaryotes that the culture was not predominantly *Scenedesmus* for a good portion of the season (Figure 35). It is apparent that there were also shifts in the bacterial and fungal communities over time (Figure 36 and 37, respectively). Some species of fungi were identified using the general primers, for the 18S rRNA gene, but the ITS primers were employed because they have been shown to better distinguish between closely related species of fungi than general 18S rRNA primers (Op De Beeck et al., 2014).

There were four instances where the PBR had to be re-inoculated with new seed cultures of *S. acutus*: July 6, July 18, August 17, and September 15. The first instance was due to a power outage at the plant, during which time the culture was switched to bottled CO<sub>2</sub> until harvest on June 27. Upon harvest, the composition of eukaryote community was still about 80% *Scenedesmus* (Figure 35). However, there was low gas flow in the PBR and the culture began to turn

yellow, indicating that it was dying. The system was subsequently drained and re-inoculated with culture at a biomass density of  $0.10 \text{ g L}^{-1}$  on July 6. The first harvest of viable biomass took place on July 11, with a biomass density of  $1.15 \text{ g L}^{-1}$  and about 80% of the composition was identified as *Scenedesmus*, although three days later it was clear that the culture had died (Figure 35). No samples were taken at this time to know if the eukaryotic community had changed significantly at the time of the culture crash, but some of the equipment was destroyed, possibly due to a weather event, which could have also caused the culture to die.

The PBR was bleached and rinsed prior to re-inoculating on July 18. However, it was reported that there was residual biofilm on the inside of the tubes. The eukaryotic community remained greater than 95% *Scenedesmus* for one week after inoculation, but the pre-harvest sample taken on July 25 indicated that the culture had been compromised by a *Chlorococcum* species, another green chlorophyte (Figure 35). The culture did appear to be dying at this time, so fresh culture from the greenhouse was added to the reactor post-harvest in hopes that it would recover. From visual inspection on July 27, the culture seemed to recover as it had maintained its signature green color it is evident that *Chlorococcum* sp. actually made up a majority of the composition (Figure 35). From July 29 until the culture death on August 11, *Scenedesmus* only made up 10-35% of the eukaryotic composition, with the exception of the post-harvest sample on August 4, where it made up 60%. Notable contaminating eukaryotes that were identified during this time were organisms of the Ichthyophonida family, and *Pseudorhizidium* sp. The presence of contaminating organisms was

not evident from visual inspection, but signs of declining culture health were reported on August 9, two days prior to the culture death. After the PBR was bleached, residual biofilm still appeared to be growing in it and 85% of the eukaryotic composition of this biofilm was made up of *Pseudorhizidium* sp., the bacteria were largely from the Alpha- and Betaproteobacteria classes, and 86% of the fungi composition was of the Agaricomycetes class (Figures 36-37).

The third re-inoculation of the PBR took place on August 17. The initial culture density was about  $0.2 \text{ g L}^{-1}$ . *Scenedesmus* made up the majority of the composition for a week following inoculation, but it was reported that the culture turned a yellow-green color on harvest days August 25 and August 29. At this time, the population of *Scenedesmus* declined to about 40% of the composition. By September 2, the green color returned, although large flocs of cells were observed in the culture which was a visual indication that there was contamination and the results from sequencing agreed. Thus, the PBR was drained, rinsed, and bleached.

*Scenedesmus* also made up the majority of the composition for a week after the last inoculation of the season on September 15. The pre-harvest sample on September 23 indicated that about half of the eukaryotic community was *Scenedesmus*, but upon harvest the *Scenedesmus* population rebounded and made up 80% of the composition. However, a severe decline followed shortly thereafter and lasted until the final harvest on October 18. During that time, *Scenedesmus* only made up 10% or less of the eukaryotic community, and this was not recognized by visual observations.

The bacterial populations largely varied over time and between seed cultures. Alpha-, Beta- and Gammaproteobacteria made up a vast majority of the composition throughout the entire season, but no obvious trends in populations were detected (Figure 36). The fungi composition was largely dominated by the Agaricomycetes class, especially from mid-July to mid-September (Figure 37). While ITS primers are often utilized to distinguish between fungal species, other protozoa and metazoans were identified by this method, including Cryptomycotes and Enopleans.

Lastly, DNA was extracted from a stock culture of *S. acutus* to use as a representative sample to compare against the compositions of the 5 seed cultures (Figures 38-40). While over 95% of the composition of the stock and most seed cultures was *Scenedesmus*, it is apparent that they were not axenic. Furthermore, the compositions of bacteria and fungi varied between these cultures.

#### **4.5 Discussion**

One of the primary advantages of using a closed PBR system for large scale cultivation of microalgae is that it prevents the large contamination events that are often seen in open pond systems (Hannon et al., 2011). However, this survey not only provides evidence that these large events occur in closed PBRs, but also that they can go unnoticed for a considerable amount of time and ultimately cause culture death. Over the 2016 season, the target alga, *Scenedesmus acutus*, would remain the dominant organism for about a week after inoculation, then the culture either died soon after or it was compromised by other organisms. Among these invading organisms were other species of green algae that were most likely directly competing with *S. acutus* for light and

nutrients. *Chlorococcum* sp. and *Choricystis* sp. are notable organisms that invaded at the end of July and end of September, respectively.

Invasion by other microalgae could be detrimental to the health of the target alga, but if the overall carbon capture efficiency does not significantly decline, and the biochemical composition are not markedly different, the harvested biomass may still be viable for downstream processing.

*Chlorococcum* sp. has been described as a high CO<sub>2</sub> tolerant alga, that can grow in a pH range of 6.5-9 (Ota et al., 2009, Harwati et al. 2012). The total fatty acid content for *Chlorococcum* grown under 6% CO<sub>2</sub> reached about 15% of the total biomass composition, which is comparable to that reported for *S. acutus* under 9% CO<sub>2</sub> (Ota et al., 2009, see section 3.3.2). Furthermore, Chen et al. (2017) found that *Choricystis* sp., isolated from wastewater, grew well in an outdoor PBR and had a total lipid content of 25-30% of the total biomass. The biodiesel properties calculated for this alga also met the standard requirements of the US and Europe (Chen et al., 2017). While the lipid content of these organisms could make it a good feedstock for biodiesel, more tests would be necessary to determine how their presence influences the overall biochemical composition of the biomass. The presence of these two organisms in this system indicates that they are robust to the flue gas and the fluctuations in other environmental parameters, which could make them ideal candidates for polyculture studies.

Other notable eukaryotes included organisms of the Ichthyophonida family that were present at the end of July and in October, as well as *Pseudorhizidium* species that proliferated after the Ichthyophonida in August. Ichthyophonida is a group of protozoa, some of which are known fish parasites,

and others are saprotrophic microbes (Mendoza et al., 2002). *Pseudorhizidium* sp. are chytrid fungi, which are a group known to parasitize microalgae in freshwater environments (Carney and Lane, 2014). Chytrid fungi have caused production losses of microalgae in commercial settings, including loss of *Scenedesmus* in open pond systems (Ilkov 1975). Other fungi, in particular those of the classes agaricomycetes and cryptomycota, were also identified by sequencing the ITS region of the rRNA operon. Of the cryptomycota, aphelids were a prominent taxon and are known to be intracellular parasites of microalgae (Karpov et al., 2013). A species of aphelid was identified in commercial ponds growing *Scenedesmus dimorphus* (Letcher et al., 2013). Many fungi and fungi-like organisms are known to produce spores that may be able to withstand sterilization of the PBR using bleach, allowing them to infect subsequent cultures (Carney and Lane 2014). The biofilm sample taken from the inside of the PBR after it was bleached corroborates this idea. Of the organisms identified by sequencing of the 18S rRNA gene in this sample, 85% was identified as a *Pseudorhizidium* species, and 86% of the organisms identified by ITS sequencing were agaricomycetes. Quantitative PCR would be necessary to determine how these organisms contribute to the overall composition of this sample, but it is clear that fungi are dominant in the residual biofilm.

Alpha-, Beta-, and Bammaproteobacteria, as well as Flavobacteria, made up a large portion of the bacterial composition in the stock and seed cultures that were all healthy upon inoculating the PBR. Although, the large variability seen in the bacterial composition, and the broad level of identification make it difficult to hypothesize how these bacteria influence the growth of *S. acutus*. It

is known that certain bacteria can promote microalgal growth by releasing vitamins or growth factors (Schwenk et al., 2014). Gonzalez and Bashan (2000) saw a significant increase in growth of the commercially important chlorophyte, *Chlorella vulgaris*, when grown with the bacterium *Azospirillum brasilense*, possibly from the production of phytohormones like indole-3-acetic acid by the bacterium. Schwenk et al. (2014) found several strains of bacteria in laboratory cultures of *Scenedesmus obliquus* from the *Rhodobacteraceae* and *Rhizobiaceae* families (both Alphaproteobacteria). These bacteria had coexisted with the algae for several years of culturing in an artificial medium, indicating that there could be a symbiosis between the algae and bacteria (Schwenk et al., 2014). Algae-bacteria interactions are complex, can be species-specific, and have yet to be widely investigated, especially in commercial settings (Schwenk et al., 2014). Future studies should focus on identifying these bacteria at the genus or species level, and if they are cultivable, growth experiments should be performed to see how they influence the overall growth of *S. acutus*.

Lastly, there can be numerous sources of contamination with any outdoor large-scale algae cultivation (Wang et al., 2008). Exposure of the culture to air for any amount of time poses the risk of introducing a contaminating organism. This study provided some insight on two potential sources of contamination in this system. It was apparent that many of the invading organisms seen throughout the season were actually identified in the seed cultures. Although these organisms were only present in small numbers, the variability in the outdoor environment could have been detrimental to the health of *S. acutus*, thereby allowing a contaminant to take over, or provided favorable

conditions that directly allowed a contaminant to proliferate. Another source of contamination was the residual biofilm on the tubes of the PBR due to ineffective sterilization after draining the system.

Through DNA sequencing, several contaminants were identified in the outdoor cultivation of *S. acutus* growing on flue gas in a closed PBR systems. The present study raises many more questions for future directions of research. These include investigating polycultures of *S. acutus* with the other green algae found in the PBR to increase overall resiliency of the mass culture, identifying any growth promoting bacteria, and finding more effective sterilization techniques. However, identifying the invading organisms and potential sources of contamination are crucial first steps in developing procedures to prevent and/or treat contamination.

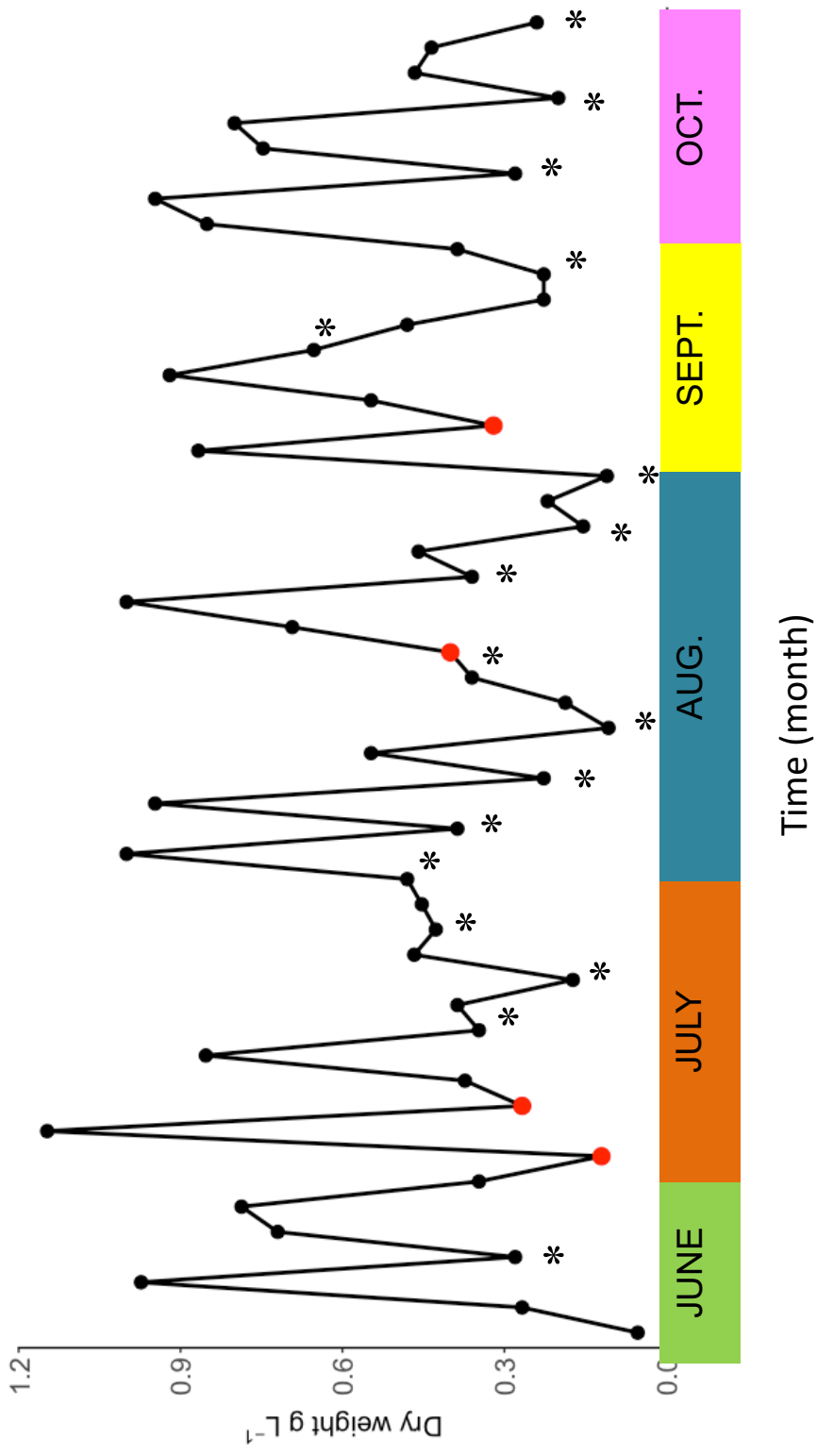


Figure 28. Dry weights for *S. acutus* grown on flue gas emissions in a 1200 L outdoor PBR from June to October 2016. Seed cultures are represented by the red points and biomass harvests are indicated with asterisks.

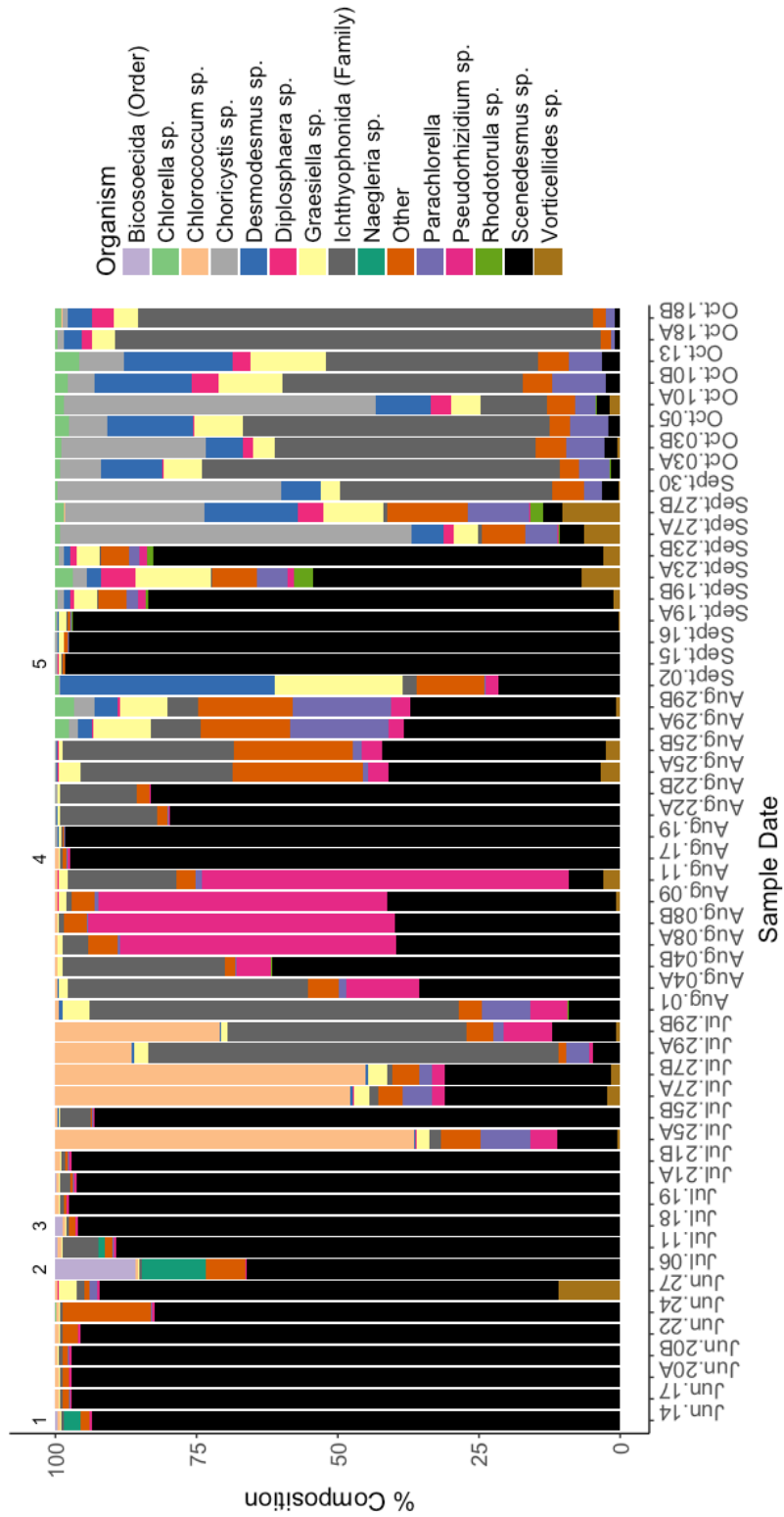


Figure 29. Composition of eukaryotic organisms in the outdoor PBR from June to October 2016, identified by sequencing the 18S rRNA gene.

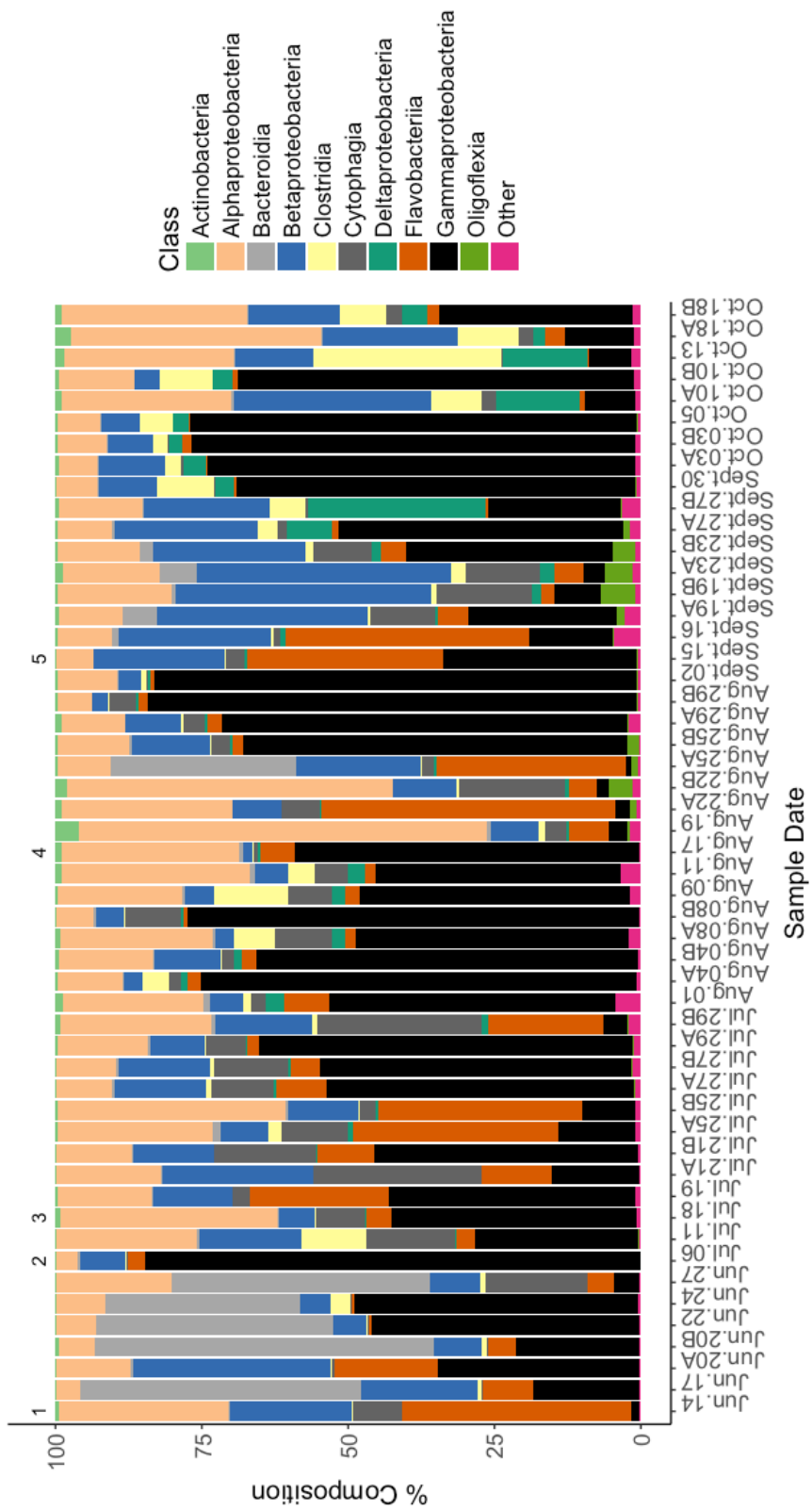


Figure 30. Composition of bacteria in the outdoor PBR from June to October 2016, identified by sequencing the 16S rRNA gene.

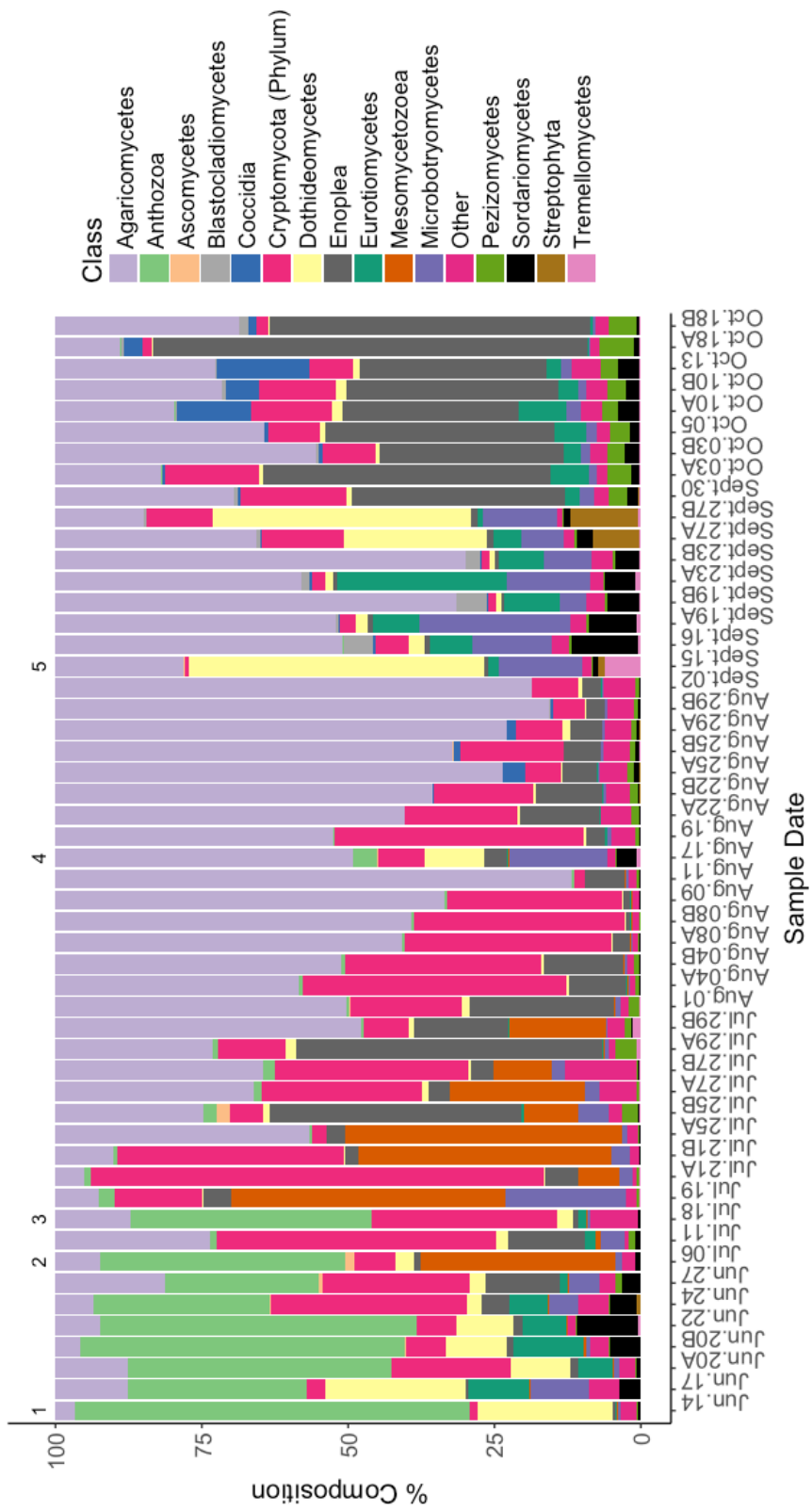


Figure 31. Composition of fungi in the outdoor PBR from June to October 2016, identified by sequencing the ITS region in the rRNA opero

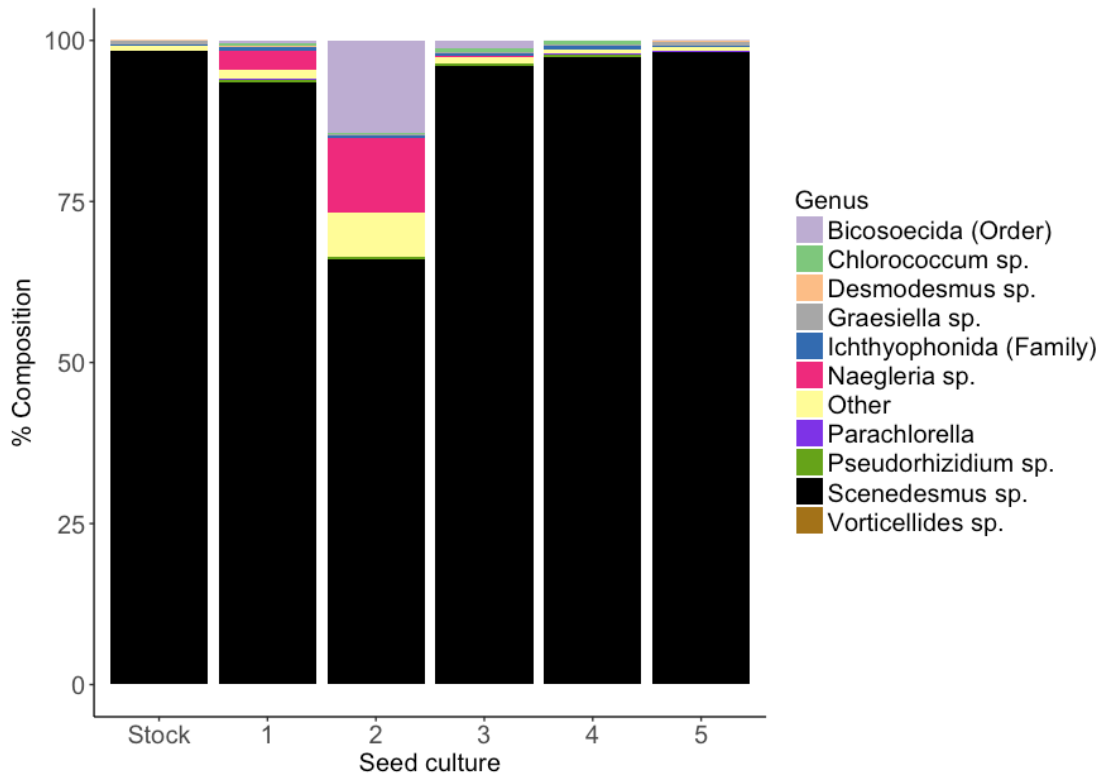


Figure 32. Composition of eukaryotes in a stock culture of *S. acutus* compared to the five seed cultures used to inoculate the PBR

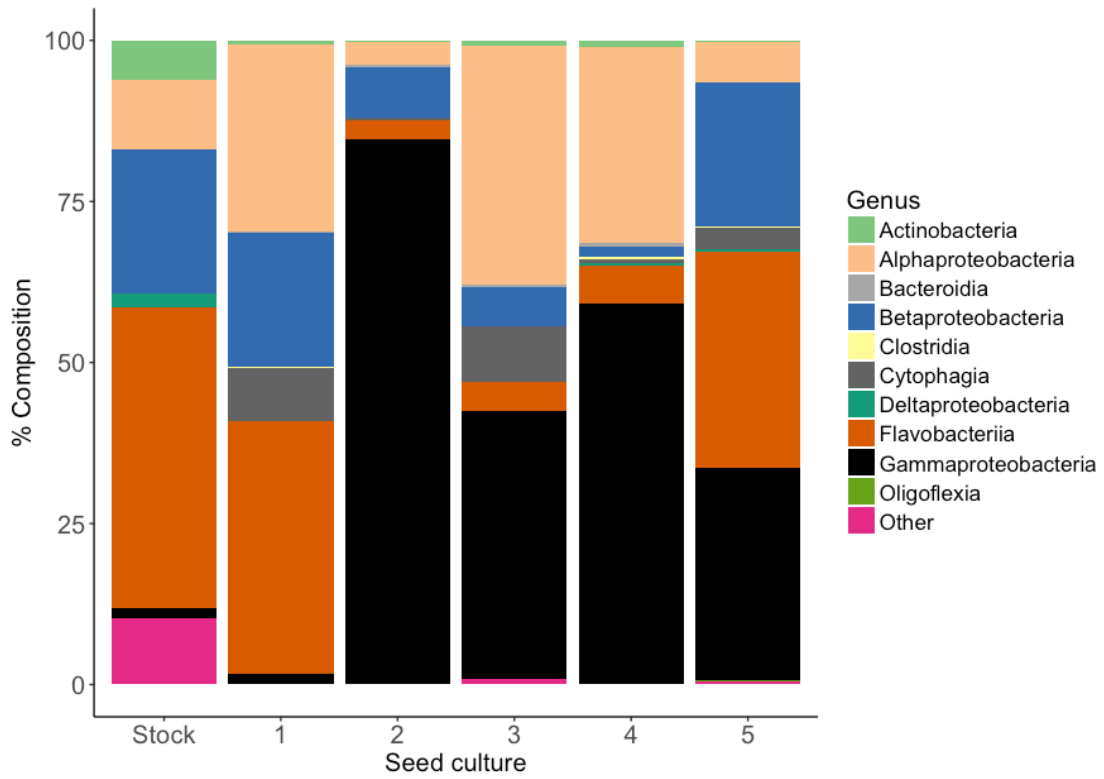


Figure 33. Composition of bacteria in a stock culture of *S. acutus* compared to the five seed cultures used to inoculate the PBR.

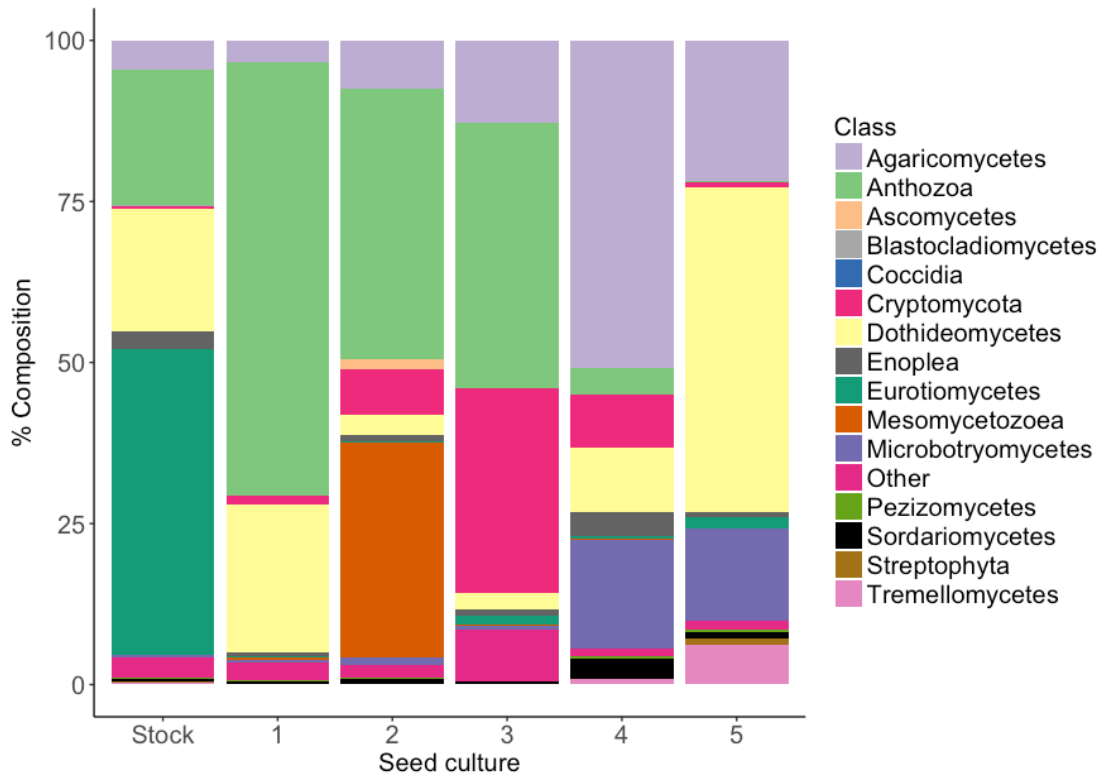


Figure 34. Composition of fungi in a stock culture of *S. acutus* compared to the five seed cultures used to inoculate the PBR.

## REFERENCES

- Carney L T, Lane T W. 2014. Parasites in algae mass culture. *Front Microbiol.* 5: 278
- Chen, Y, Li X, Sun Z, Zhou Z. 2017. Isolation and identification of *Choricystis minor* Fott and mass cultivation for oil production. *Algal Research.* 25: 142-148
- Crofcheck, C. 2012. Influence of media composition on the growth rate of *Chlorella vulgaris* and *Scenedesmus acutus* utilized for CO<sub>2</sub> mitigation. *Journal of Biochemical Technology.* 4(2): 589-594.
- Gong, Yingchun, et al. 2014. *Vernalophrys algivore* gen. nov., sp. nov. (Rhizaria: Cercozoae: Vampyrellida), a New Algal Predator Isolated from Outdoor Mass Culture of *Scenedesmus dimorphus*. *Applied and Environmental Microbiology.* 81(12): 3900-3913.
- Gonzalez L E, Bashan Y. 2000. Increased growth of the microalga *Chlorella vulgaris* when coimmobilized and cocultured in alginate beads with the plant-growth-promoting bacterium *Azospirillum brasilense*. *Appl. Environ. Microbiol.* 66(4): 1527-1531.
- Hannon M, Gimpel J, Miller T, Rasala B, Mayfield S. 2011. Biofuels from algae: challenges and potential. *Biofuels.* 1(5): 763-784.
- Hawarti T U, Willke T, Vorlop K D. Characterization of the lipid accumulation in a tropical freshwater microalgae *Chlorococcum* sp. *Bioresource Technology.* 121: 54-60.
- Ilkov G. 1975. Population dynamic relationships during *Phlyctidium scenedesmi* development in *Scenedesmus acutus* cultures. *Appl. Microbiol.* 6: 104-110.
- Karpov S A, Mamkaeva M A, Aleoshin V V, Nassonova E, Lilije O, Gleason F H. Morphology, phylogeny, and ecology of the aphelids (Aphelidea, Opisthokonta) and proposal for the new superphylum Opisthosporidia. *Front Microbiol.* 5: 112.
- Letcher, P.M. et al. 2013. Characterization of *Amoebophilidium protococcarum*, an algal Parasite New to the Cryptomycota Isolated from an Outdoor Algal Pond used for the Production of Biofuel. *PLoS One.* 8(2): e56232.

- Mendoza L, Taylor J W, Ajello L. 2002. The class mesomycetozoea: A heterogeneous group of microorganisms at the animal-fungal boundary. *Annual Review of Microbiology*. 56: 315-344.
- Op De Beeck M, Lievens B, Busschaert P, Declerck S, Vangronsveld J, Colpaert J V. 2014. Comparison and validation of some ITS primer pairs useful for fungal metabarcoding studies. *PLoS One*. 9(6): e97629.
- Ota M, Kato Y, Watanage H, Watanabe M, Sato Y, Smith RL Jr, Inomata H. 2009. Effect of inorganic carbon on photoautotrophic growth of microalga *Chlorococcum littorale*. 25(2): 492-498.
- Prokop, A. et al. 2015. *Algal Biorefineries: Volume 2: Products and Refinery Design*. Springer.
- Schwenk D, Nohynek L, Rischer H. 2014. Algae-bacteria association inferred by 16S rDNA similarity in established microalgae cultures. *Microbiology Open*. 3(3): 356-368
- Wang B, Li Y, Wu N, Lan CQ. 2008. CO<sub>2</sub> bio-mitigation using microalgae. *Appl Microbiol Biotechnol*. 79(5):707-718.
- Wilson M H, Groppo J, Placido A, Graham S, Morton III S A, Santillan-Jimenez E, Shea A, Crocker M, Crofcheck C, Andrews R. 2014. CO<sub>2</sub> recycling using microalgae for the production of fuels. *Applied Petrochemical Research*. 4(1): 41-53.
- Wilson M H, Mohler D T, Groppo J G, Grubbs T, Kesner S, Frazar E M, Shea A, Crofcheck C, Crocker M. 2016. Capture and recycle of industrial CO<sub>2</sub> emissions using microalgae. *Applied Petrochemical Research*. 6(3): 279-293.

## Appendix A

### CHAPTER 2 SUPPLEMENTAL FIGURES

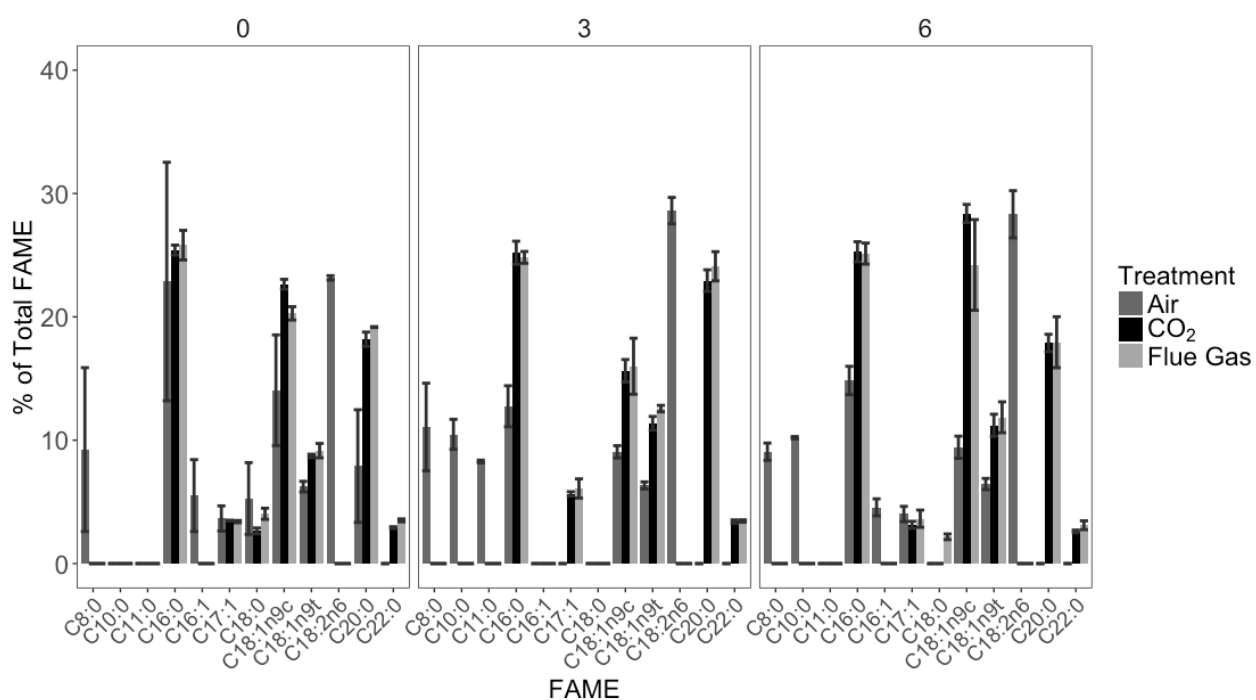


Figure 35. Fatty acid methyl ester (FAME) profiles of *S. acutus* when grown under air (0.04% CO<sub>2</sub>), 9% CO<sub>2</sub>, and simulated flue gas (9% CO<sub>2</sub>, 55 ppm NO, 25 ppm SO<sub>2</sub>). Values are means  $\pm$  SD.

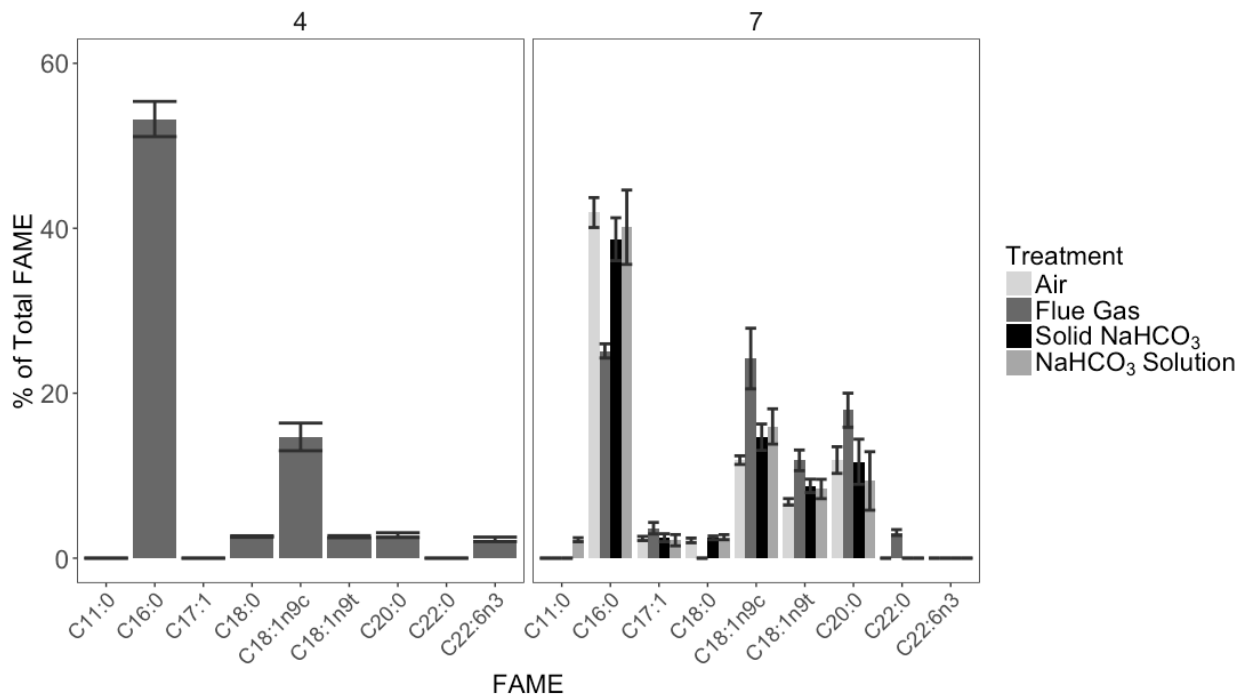


Figure 36. Fatty acid methyl ester (FAME) profiles of *S. acutus* before and after flue gas was shut off and cultures were supplemented with bicarbonate or air. Values are mean  $\pm$  SD.

## Appendix B

### CHAPTER 3 SUPPLEMENTAL FIGURES

Table 9. Productivity, specific growth rate, and final biomass yield of *S. acutus* grown using media amended with 0.94 mM sodium nitrate or 4.3 mM urea in 9% CO<sub>2</sub>. Values are means ± SD.

	Nitrate	Urea
Productivity (g L <sup>-1</sup> d <sup>-1</sup> )	0.17 ± 0.03	0.10 ± 0.02
Specific growth rate (μ)	0.42 ± .08	0.31 ± 0.09
Final biomass yield (g L <sup>-1</sup> )	0.96 ± 0.05	0.70 ± 0.08

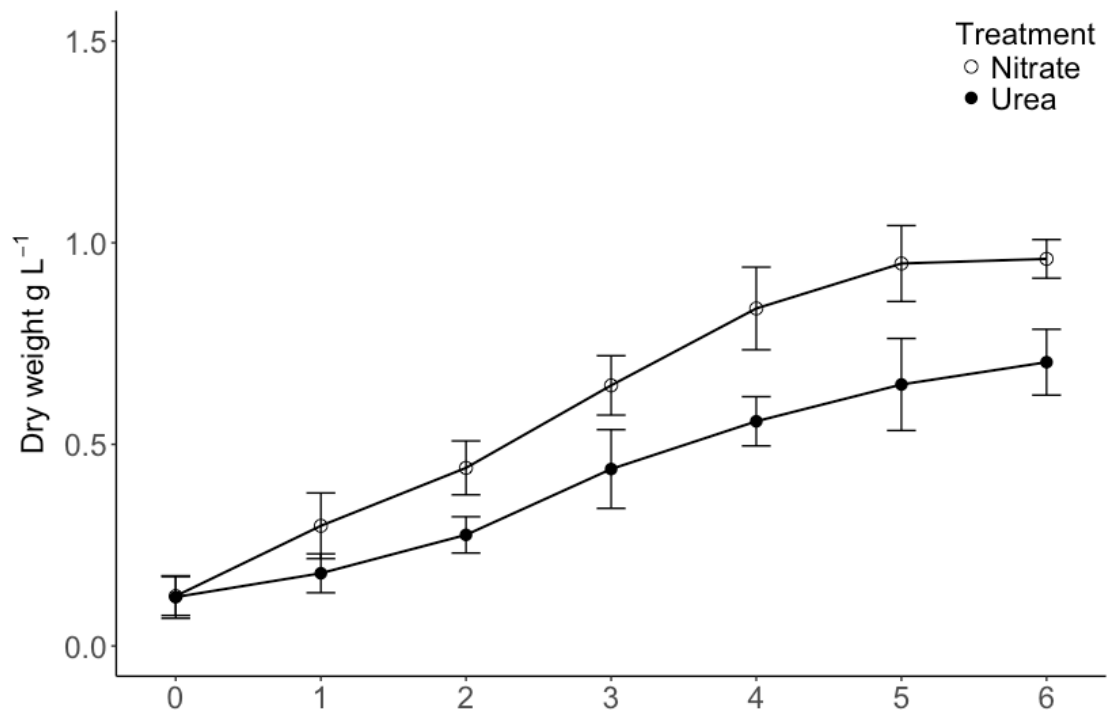


Figure 37. Growth of *S. acutus* grown using media amended with 0.94 mM sodium nitrate or 4.3 mM urea in 9% CO<sub>2</sub>. Values are means ± SD

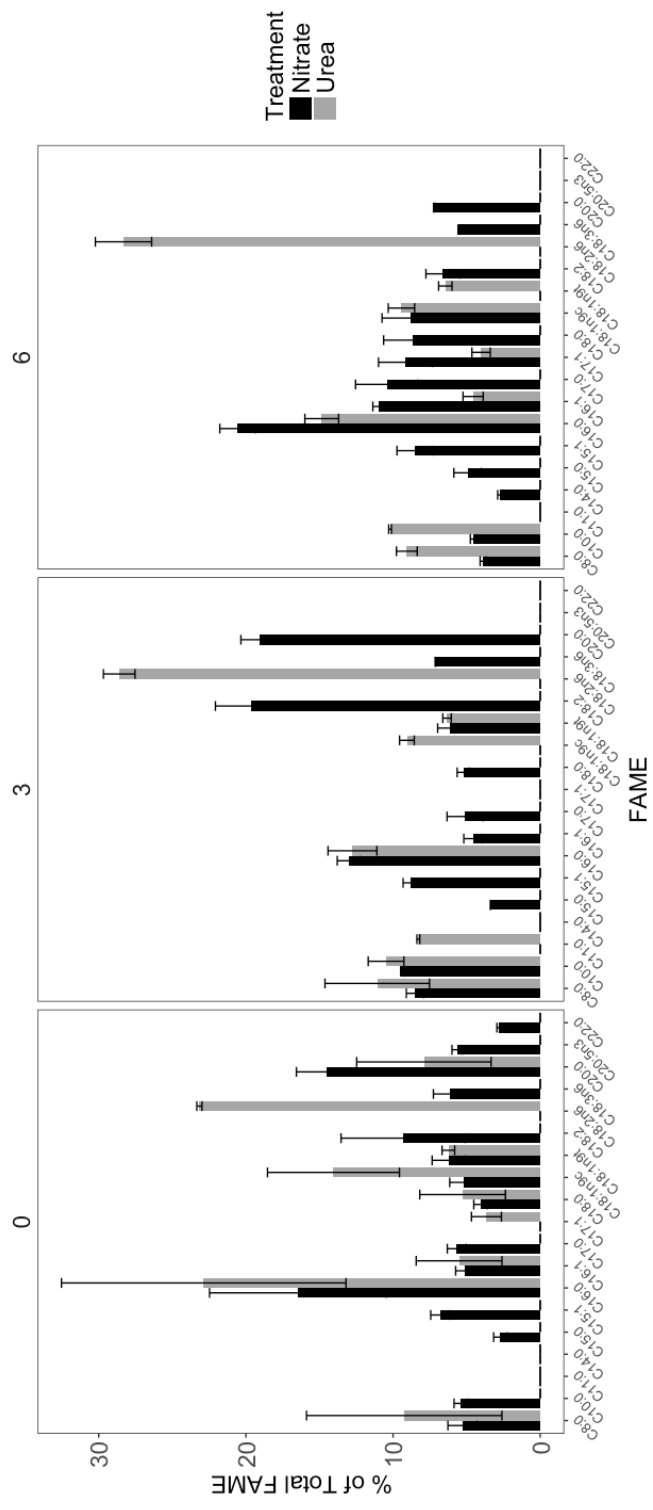


Figure 38. Fatty acid methyl ester (FAME) profile of *S. acutus* cultures grown using sodium nitrate or urea in air. Values are means  $\pm$  SD.

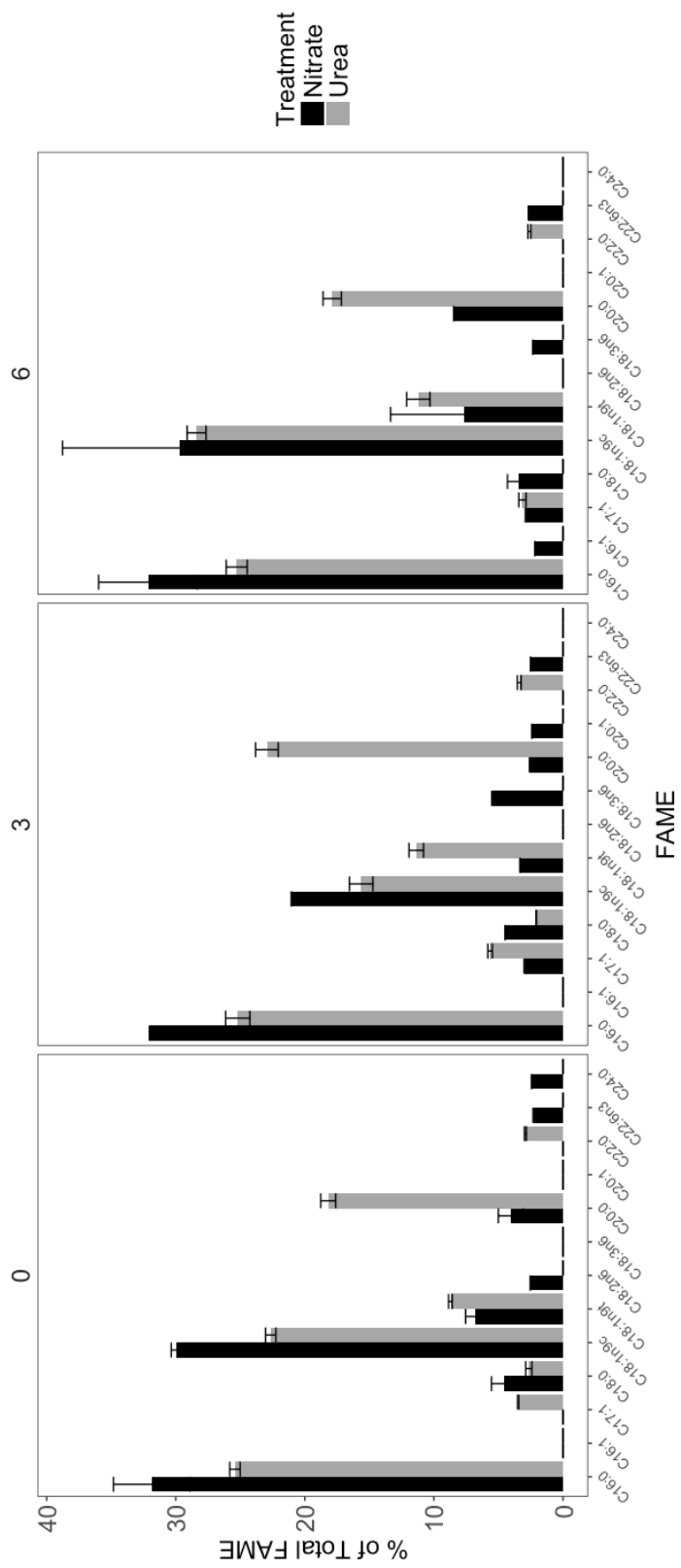


Figure 39. Fatty acid methyl ester (FAME) profile of *S. acutus* cultures grown using sodium nitrate or urea in 9% CO<sub>2</sub>. Values are means  $\pm$  SD.

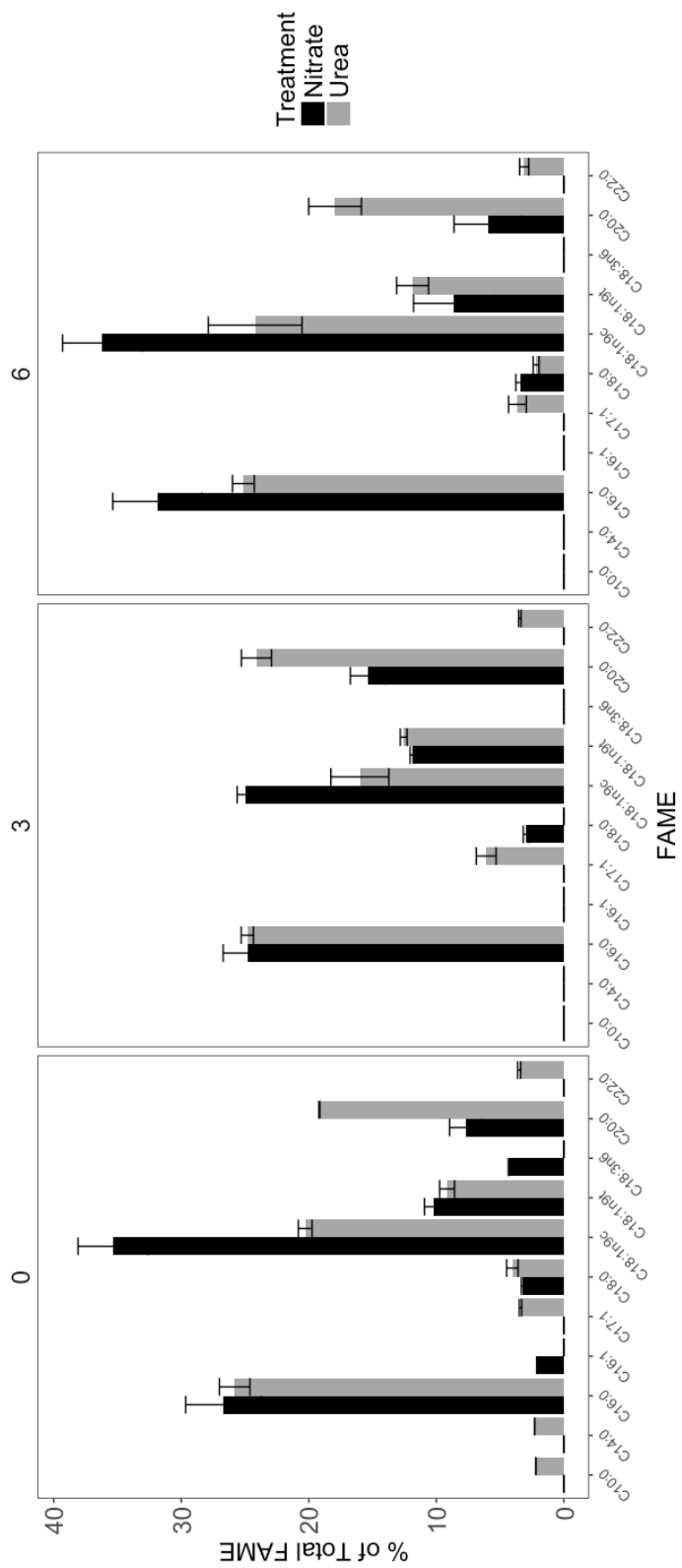


Figure 40. Fatty acid methyl ester (FAME) profile of *S. acutus* cultures grown using sodium nitrate or urea in simulated flue gas flue gas (9% CO<sub>2</sub>, 50 ppm NO, 25 ppm SO<sub>2</sub>). Values are means ± SD.